

Electronic Theses and Dissertations, 2004-2019

2015

Tidal hydrodynamic response to sea level rise and coastal geomorphology in the Northern Gulf of Mexico

Davina Passeri
University of Central Florida

 Part of the [Civil Engineering Commons](#)
Find similar works at: <https://stars.library.ucf.edu/etd>
University of Central Florida Libraries <http://library.ucf.edu>

This Doctoral Dissertation (Open Access) is brought to you for free and open access by STARS. It has been accepted for inclusion in Electronic Theses and Dissertations, 2004-2019 by an authorized administrator of STARS. For more information, please contact STARS@ucf.edu.

STARS Citation

Passeri, Davina, "Tidal hydrodynamic response to sea level rise and coastal geomorphology in the Northern Gulf of Mexico" (2015). *Electronic Theses and Dissertations, 2004-2019*. 1429.
<https://stars.library.ucf.edu/etd/1429>

**TIDAL HYDRODYNAMIC RESPONSE TO SEA LEVEL RISE AND COASTAL
GEOMORPHOLOGY IN THE NORTHERN GULF OF MEXICO**

by

DAVINA LISA PASSERI
B.S. University of Notre Dame, 2010

A thesis submitted in partial fulfillment of the requirements
for the degree of Doctor of Philosophy
in the Department of Civil, Environmental, and Construction Engineering
in the College of Engineering and Computer Science
at the University of Central Florida
Orlando, Florida

Spring Term
2015

Major Professor: Scott C. Hagen

© 2015 Davina Lisa Passeri

ABSTRACT

Sea level rise (SLR) has the potential to affect coastal environments in a multitude of ways, including submergence, increased flooding, and increased shoreline erosion. Low-lying coastal environments such as the Northern Gulf of Mexico (NGOM) are particularly vulnerable to the effects of SLR, which may have serious consequences for coastal communities as well as ecologically and economically significant estuaries. Evaluating potential changes in tidal hydrodynamics under SLR is essential for understanding impacts to navigation, ecological habitats, infrastructure and the morphologic evolution of the coastline. The intent of this research is to evaluate the dynamic effects of SLR and coastal geomorphology on tidal hydrodynamics along the NGOM and within three National Estuarine Research Reserves (NERRs), namely Grand Bay, MS, Weeks Bay, AL, and Apalachicola, FL.

An extensive literature review examined the integrated dynamic effects of SLR on low gradient coastal landscapes, primarily in the context of hydrodynamics, coastal morphology, and marsh ecology. Despite knowledge of the dynamic nature of coastal systems, many studies have neglected to consider the nonlinear effects of SLR and employed a simplistic “bathtub” approach in SLR assessments. More recent efforts have begun to consider the dynamic effects of SLR (e.g., the nonlinear response of hydrodynamics under SLR); however, little research has considered the integrated feedback mechanisms and co-evolution of multiple interdependent systems (e.g., the nonlinear responses and interactions of hydrodynamics and coastal morphology under SLR). Synergetic approaches that integrate the dynamic interactions between physical and ecological

environments will allow for more comprehensive evaluations of the impacts of SLR on coastal systems.

Projecting future morphology is a challenging task; various conceptual models and statistical methods have been employed to project future shoreline positions. Projected shoreline change rates from a conceptual model were compared with historic shoreline change rates from two databases along sandy shorelines of the South Atlantic Bight and NGOM coasts. The intent was not to regard one method as superior to another, but rather to explore similarities and differences between the methods and offer suggestions for projecting shoreline changes in SLR assessments.

The influence of incorporating future shoreline changes into hydrodynamic modeling assessments of SLR was evaluated for the NGOM coast. Astronomic tides and hurricane storm surge were simulated under present conditions, the projected 2050 sea level with present-day shorelines, and the projected 2050 sea level with projected 2050 shorelines. Results demonstrated that incorporating shoreline changes had variable impacts on the hydrodynamics; storm surge was more sensitive to the shoreline changes than astronomic tides. It was concluded that estimates of shoreline change should be included in hydrodynamic assessments of SLR along the NGOM.

Evaluating how hydrodynamics have been altered historically under a changing landscape in conjunction with SLR can provide insight to future changes. The Grand Bay estuary has undergone significant landscape changes historically. Tidal hydrodynamics were simulated for present and historic conditions (dating back to 1848) using a hydrodynamic model modified with unique sea levels, bathymetry, topography, and shorelines representative of each time period. Changes in tidal

amplitudes varied across the domain. Harmonic constituent phases sped up from historic conditions. Tidal velocities in the estuary were stronger historically, and reversed from being flood dominant in 1848 to ebb dominant in 2005.

To project how tidal hydrodynamics may be altered under future scenarios along the NGOM and within the three NERRs, a hydrodynamic model was used to simulate present (circa 2005) and future (circa 2050 and 2100) astronomic tides. The model was modified with projections of future sea levels as well as shoreline positions and dune elevations obtained from a Bayesian network (BN) model. Tidal amplitudes within some of the embayments increased under the higher SLR scenarios; there was a high correlation between the change in the inlet cross-sectional area under SLR and the change in the tidal amplitude within each bay. Changes in harmonic constituent phases indicated faster tidal propagation in the future scenarios within most of the bays. Tidal velocities increased in all of the NERRs which altered flood and ebb current strengths.

The work presented herein improves the understanding of the response of tidal hydrodynamics to morphology and SLR. This is beneficial not only to the scientific community, but also to the management and policy community. These findings will have synergistic effects with a variety of coastal studies including storm surge and biological assessments of SLR. In addition, findings can benefit monitoring and restoration activities in the NERRs. Ultimately, outcomes will allow coastal managers and policy makers to make more informed decisions that address specific needs and vulnerabilities of each particular estuary, the NGOM coastal system, and estuaries elsewhere with similar conditions.

ACKNOWLEDGMENTS

This research was funded in part under Award No. NA10NOS4780146 from the National Oceanic and Atmospheric Administration (NOAA) Center for Sponsored Coastal Ocean Research (CSCOR) and the Louisiana Sea Grant Laborde Chair endowment. The STOKES Advanced Research Computing Center (ARCC) (webstokes.ist.ucf.edu) and Extreme Science and Engineering Discover Environment (XSEDE) which is supported by the National Science Foundation grant number ACI-1053575, provided the computational resources for the simulations. The statements, findings, conclusions and recommendations expressed herein are those of the authors and do not necessarily reflect the views of NOAA-CSCOR, Louisiana Sea Grant, STOKES ARCC, XSEDE, or their affiliates.

I am deeply grateful to Dr. Scott Hagen for providing me with the opportunity to be a part of the CHAMPS Lab. His guidance and continuous support have enriched my development and leadership as a young engineer. He exemplifies the university's academic mission and motto, "UCF stands for opportunity". The numerous opportunities with which he has provided me, whether attending international conferences, publishing journal articles, or tutoring freshman engineering students have prepared me for my future endeavors beyond UCF. It has been a pleasure working with you these past five years, and I sincerely hope we will continue to collaborate in the future.

I would also like to thank Dr. Stephen Medeiros, Dr. Dingbao Wang, and Dr. John Weishampel for providing insight on this research as well as for serving on my committee. Thank you to Dr.

Nathaniel Plant at the USGS Coastal and Marine Science Center for collaborating with me on a portion of this dissertation. I look forward to continuing this research together.

The CHAMPS Lab is more than a group of researchers, it is a family. A special thank you to Matthew Bilskie, Dr. Stephen Medeiros and Karim Alizad, with whom I have closely worked over the past five years. You have each taught me invaluable skills and I am fortunate to not only call you my colleagues, but more importantly, my friends. I hope we will continue to work together after my departure. Thank you to former CHAMPS Lab members Dr. Pete Bacopoulos, Daina Smar, Lillie Thomas and Dr. Ammarin Daranpob for their guidance, especially when I was just starting at UCF. Best of luck to Milad Hooshyar, Paige Hovenga, Aaron Thomas, Megan Leslie, Amanda Tritinger and Erin Ward. I know you will all find success in your future careers.

I would also like to thank Stephanie Garvis and Melinda Donnelly (UCF Biology Department), as well as Dr. Jim Morris (University of South Carolina). They have been instrumental in helping me gain a better understanding of the interconnectivity between engineering and biology. I also wish to thank Dave Kidwell (EESLR-NGOM Project Manager) and the Apalachicola, Grand Bay and Weeks Bay NERRs. Lastly, I am especially grateful to Dr. Joannes Westerink (University of Notre Dame) who introduced me to hydrodynamic modeling and inspired me to attend graduate school.

During my time at UCF, I had the opportunity to be a part of the NSF funded UCF EXCEL program led by Dr. Cynthia Young and Dr. Michael Georgiopoulos. Through this opportunity, I was able to be involved in inspiring the next generation to pursue careers in science and engineering. This was a rewarding experience that I will carry forward.

Most importantly, I am thankful for the unconditional love and support from my parents, David and Lisa Passeri. They have provided me with the best education possible for which I am eternally grateful. Without their perpetual encouragement, advice and assistance, I would not have the success I have experienced today. I am proud to be the second Dr. D. Passeri in the family.

TABLE OF CONTENTS

LIST OF FIGURES	xiv
LIST OF TABLES	xvii
CHAPTER 1. INTRODUCTION	1
1.1 Hypothesis and Research Objective	2
1.2 Dynamic Effects of Sea Level Rise on Coastal Landscapes	3
1.3 Shoreline Change Rate Comparison	4
1.4 Sensitivity Analysis of a Hydrodynamic Model to Projected Shoreline Changes	4
1.5 Historic Changes in Tidal Hydrodynamics	5
1.6 Comparison of Present and Future Hydrodynamics	6
1.7 References	6
CHAPTER 2. THE DYNAMIC EFFECTS OF SEA LEVEL RISE ON LOW GRADIENT COASTAL LANDSCAPES: A REVIEW	8
2.1 Introduction	8
2.2 Coastal Hydrodynamics	13
2.2.1 Background	13
2.2.2 Hydrodynamic Response to Sea Level Rise	17
2.2.3 Hydrodynamic Modeling of Sea Level Rise	19
2.3 Coastal Morphology	23
2.3.1 Background	23
2.3.2 Coastal Morphologic Response to Sea Level Rise	25

2.3.3	Coastal Morphologic Modeling of Sea Level Rise.....	28
2.4	Marsh Ecology	34
2.4.1	Background.....	34
2.4.2	Marsh Response to Sea Level Rise.....	37
2.4.3	Marsh Modeling of Sea Level Rise	39
2.5	Synergetic Studies of Sea Level Rise.....	43
2.6	Additional Considerations.....	47
2.6.1	Additional Coastal Dynamics	47
2.6.2	Socioeconomic Considerations.....	49
2.6.3	Managing Future Risk.....	50
2.7	Conclusions	52
2.8	Acknowledgments.....	54
2.9	References	54
CHAPTER 3. COMPARISON OF SHORELINE CHANGE RATES ALONG THE SOUTH ATLANTIC BIGHT AND NORTHERN GULF OF MEXICO COASTS FOR BETTER EVALUATION OF FUTURE SHORELINE POSITIONS UNDER SEA LEVEL RISE.....		
3.1	Introduction	71
3.2	Study Area.....	74
3.3	Methodology	76
3.4	Results	81

3.4.1	Coastal Vulnerability Index vs. Long-Term Rates	82
3.4.2	Bruun Rule vs. Coastal Vulnerability Index and Long-Term Rates	82
3.4.3	Effect of Beach Nourishment.....	83
3.5	Discussion	86
3.6	Summary and Recommendations.....	87
3.7	Acknowledgments.....	88
3.8	References	89
CHAPTER 4. ON THE SIGNIFICANCE OF INCORPORATING SHORELINE CHANGES FOR EVALUATING COASTAL HYDRODYNAMICS UNDER SEA LEVEL RISE		92
4.1	Introduction	92
4.2	Methods.....	96
4.2.1	Projected 2050 Shoreline and Nearshore Morphology.....	96
4.2.2	Projected 2050 Sea Level.....	100
4.2.3	Hydrodynamic Model and Simulations	100
4.3	Results	104
4.3.1	Astronomic Tides.....	104
4.3.2	Hurricane Storm Surge	108
4.4	Discussion	117
4.5	Conclusions	118
4.6	Acknowledgments.....	120

4.7	References	120
CHAPTER 5. IMPACTS OF HISTORIC MORPHOLOGY AND SEA LEVEL RISE ON TIDAL HYDRODYNAMICS		126
5.1	Introduction	126
5.2	Study Domain.....	127
5.3	Methodology	131
5.3.1	Hydrodynamic Model	131
5.3.2	Historic Simulations.....	132
5.4	Results	136
5.4.1	Water Levels	136
5.4.2	Currents.....	143
5.5	Implications.....	147
5.6	Conclusions	150
5.7	Acknowledgments.....	151
5.8	References	152
CHAPTER 6. TIDAL HYDRODYNAMICS UNDER FUTURE SEA LEVEL RISE AND COASTAL MORPHOLOGY ALONG THE NORTHERN GULF OF MEXICO		155
6.1	Introduction	155
6.2	Study Domain.....	156
6.3	Methodology	159
6.3.1	Hydrodynamic Model	159

6.3.2	Future SLR and Morphology	160
6.3.3	Modeling Approach	163
6.4	Results	168
6.4.1	Validation.....	168
6.4.2	Water Levels	171
6.4.3	Currents.....	177
6.4.4	Inundation	184
6.5	Implications	185
6.6	Conclusions	187
6.7	Acknowledgments	188
6.8	References	189
CHAPTER 7. CONCLUSION.....		194
7.1	Implications	197

LIST OF FIGURES

Figure 2.1: Coastal dynamics of SLR along sandy shorelines: (a) existing mean sea level, (b) a static rise on sea level simply elevates existing mean sea level by the amount of SLR, resulting in inundation of the coast, (c) a dynamic rise in sea level accounts for the nonlinear response of the tides, (d) higher water levels allow wave energy to act higher on the beach profile, resulting in erosion, (e) the eroded beach profile results in further inundation under SLR, (f) rising seas have the potential to exacerbate coastal flooding during storm events. 12

Figure 2.2: Coastal dynamics of SLR along sandy shorelines: (a) existing mean sea level, (b) a static rise on sea level simply elevates existing mean sea level by the amount of SLR, resulting in inundation of the coast, (c) a dynamic rise in sea level accounts for the nonlinear response of the tides, (d) higher water levels allow wave energy to act higher on the beach profile, resulting in erosion, (e) the eroded beach profile results in further inundation under SLR, (f) rising seas have the potential to exacerbate coastal flooding during storm events. 13

Figure 3.1: NGOM and SAB study area where the Bruun Rule, CVI and LT rates are compared. 76

Figure 3.2: Example of historic mean SLR at NOS station in Mayport, FL. 79

Figure 3.3: DOC estimates along the SAB derived from Dean and Grant (1989), Nicholls et al. (1996) and wave data at NDBC buoy 41008. 80

Figure 3.4: Average DOC value is assigned along SAB span where wave climate does not change using the linear regression equation; contours running parallel with the coast indicate unchanging wave climate. 81

Figure 4.1: Top: Study area with projected erosion and accretion along Gulf and non-hardened bay shorelines from CVI database Bottom: 2050 shoreline change along Gulf shoreline estimated with CVI erosion and accretion rates. 96

Figure 4.2: Comparison of measured and modeled high water mark (HWM) data for (a) Hurricane Ivan, (b) Hurricane Dennis and (c) Hurricane Katrina. 103

Figure 4.3: Difference in maximum elevations of water for 2050-S and 2050 simulations of (a) Hurricane Ivan (b) Hurricane Dennis and (c) Hurricane Katrina, solid black line represents hurricane track; color scale bar changes in each plot. 113

Figure 4.4: Maximum elevations of water for Hurricane Dennis (a) 2005, (b) 2050 (c) 2050-S simulations, illustrating extent of overtopping of Santa Rosa Island; dotted ovals indicate notable regions of increased inundation. 114

Figure 5.1: Mississippi Sound study area (a) with zoomed in inset of Grand Bay estuary (b) for present day conditions..... 130

Figure 5.2 Model elevations circa (a) 1848, (b) 1917, (c) 1960 and (d) 2005 using historic bathymetry and shoreline positions in the Mississippi Sound; notable changes include gains and losses of land along the offshore MSAL barrier islands, presence and size of inlets, the existence of the dredged shipping channels, and the submergence of the Grand Batture Island in the Grand Bay estuary..... 135

Figure 5.3: Percent change in total tidal amplitude from (a) 1848 to 2005, (b) 1917 to 2005 and (c) 1960 to 2005. The black line represents the 2005 shoreline; differences greater than 0 indicate percent increases in tidal amplitude from the historic condition to 2005, differences less than 0 indicate percent decreases in the tidal amplitude from the historic condition to 2005. The dots in (a) represent locations where constituent amplitudes are measured in Table 1..... 139

Figure 5.4: Phase differences of the K1 constituent from (a) 1848 to 2005, (b) 1917 to 2005 and (c) 1960 to 2005. The black line represents the 2005 shoreline; differences equal to 0 indicate the constituent phase is unchanged from the historic scenario, differences greater than 0 indicate the constituent phase is slower in 2005 than the historic scenario, and differences less than 0 indicate the constituent phase is faster in 2005 than the historic scenario. 142

Figure 5.5: Differences in maximum tidal velocities from (a) 1848 to 2005 (b) 1917 to 2005 (c) 1960 to 2005 (d) 2005 to 2005-GBI. The black line represents the 2005 shoreline; differences greater than 0 indicate maximum tidal velocities have increased from the historic condition, differences less than 0 indicate maximum tidal velocities have decreased from the historic condition, differences equal to 0 indicate maximum velocities have not changed..... 145

Figure 5.6: Flood-ebb ratios for (a) 1848, (b) 1917, (c) 1960, and (d) 2005. The black line represents the 2005 shoreline; flood-ebb ratios greater than 1 indicate stronger flood currents; ratios less than 1 indicate stronger ebb currents. 146

Figure 5.7: Percent change in flood-ebb ratio from (a) 1848 to 2005, (b) 1917 to 2005 and (c) 1960 to 2005. 147

Figure 6.1: Hydrodynamic model elevations of the NGOM study area with insets of the Grand Bay, Weeks Bay and Apalachicola NERRs..... 159

Figure 6.2: 50th percentile of probability projections of shoreline change and dune height for the year 2100 under low, intermediate-low, intermediate-high and high SLR across the NGOM domain. In the plot of shoreline change, positive numbers indicate accretion, negative numbers indicate erosion. 163

Figure 6.3: Decision making flow chart for how to implement projected shoreline changes and dune heights from BN into hydrodynamic model..... 167

Figure 6.4: Comparison of amplitudes (top) and phases (bottom) measured by NOAA and predicted by the hydrodynamic model. Difference bands are located at 0.025 m and 0.05 m in the amplitude plot, and 10° and 20° in the phase plot. 170

Figure 6.5: (a) Total tidal amplitudes across the NGOM for the 2005 scenario; (b) percent change in tidal amplitude from 2005 to 2050-high scenario; (c) percent change in tidal amplitude from 2005 to 2100-high scenario..... 174

Figure 6.6: Percent change in inlet cross-sectional area versus SLR for each bay; data is fitted with trend equations. 175

Figure 6.7: Changes in tidal velocities from the 2005 scenario for (a) the 2050-high scenario and (b) the 2100-high scenario; warm colors indicate tidal velocities have increased from the 2005 scenario, cool colors indicate tidal velocities have decreased from the 2005 scenario. 179

Figure 6.8: Flood-ebb ratios for the 2005 scenario in (a) Grand Bay, (b) Weeks Bay and (c) Apalachicola; at the locations marked with the black dot, flood-ebb ratios are (a) 0.75, (b) 1.10 and (c) 1.35. 182

LIST OF TABLES

Table 3.1: Percent differences across the NGOM and SAB between CVI, CVI erosion rates (CVI-E), LT, LT erosion rates (LT-E), the Bruun Rule (BR), and pre-nourished rates (PN).....	84
Table 3.2: Absolute differences across the NGOM and SAB between CVI erosion rates (CVI-E), LT erosion rates (LT-E), the Bruun Rule (BR), and pre-nourished rates (PN)	85
Table 4.1: Calculated tidal ranges and tidal prisms for each bay under 2005, 2050 and 2050-S scenarios.....	107
Table 4.2: Difference between low tide and high tide wetted area and volume of bay systems, and percent increase in tidal range and tidal prisms under 2005, 2050 and 2050-S scenarios.....	108
Table 4.3: Peak surge values and location for Hurricanes Ivan, Dennis and Katrina under 2005, 2050 and 2050-S scenarios	115
Table 4.4: Dry area and inundation index for barrier islands under 2005, 2050 and 2050-S scenarios for Hurricanes Ivan, Dennis and Katrina	115
Table 4.5: Volumes of surge and percent increases for bay systems under 2005, 2050 and 2050-S scenarios for Hurricanes Ivan, Dennis and Katrina	116
Table 5.1: Percent change in constituent amplitudes from 1848 to 2005, 1917 to 2005 and 1960 to 2005 at locations 1-4, illustrated in Figure 5.3.	140
Table 6.1: Trend equations, correlation coefficient (R) and coefficient of determination (R^2) between the ratio of the future to present tidal amplitude ($\text{Amplitude}_{\text{future}}/\text{Amplitude}_{\text{present}}$) versus the ratio of the future to present inlet cross-sectional area ($\text{Area}_{\text{future}}/\text{Area}_{\text{present}}$) for each future scenario.	175
Table 6.2: Dominant harmonic constituent amplitudes for the 2005 scenario and changes in constituent amplitudes and phases from the 2005 scenario to the 2100-high scenario within each bay system in the NGOM.	177
Table 6.3: Change in flood-ebb ratio from 2005 to future scenarios in the three NERRs. The top number is the flood-ebb ratio for the given scenario, the number in parentheses is the percent change in the flood-ebb ratio from the 2005 scenario to the given future scenario.....	183

CHAPTER 1. INTRODUCTION

Coasts contain interrelated dynamic systems that continuously transform over different temporal and spatial scales as a result of geomorphic and oceanographic changes. Long-term tide gauge data indicates a global average rate of SLR over the past century of approximately 1.7 mm/year (Church and White, 2006), whereas global satellite altimetry suggests a recent acceleration, with rates as high as 3.3 mm/year between 1993 and 2007 (Cazenave and Llovel, 2010). SLR has the potential to affect coastal environments in a multitude of ways, including submergence, increased flooding, and increased shoreline erosion. Effects will be felt along coastal beaches and estuaries with consequences to barrier islands, submerged aquatic vegetation (SAV) beds, sand and mud flats, oyster reefs, and tidal and freshwater wetlands. Low-lying coastal environments such as the NGOM are particularly vulnerable to SLR, which may have serious consequences for coastal communities as well as ecologically and economically significant estuaries.

The future of the NGOM coastal environment relies on information regarding risks such as SLR to make informed decisions for managing human and natural communities. The Ecological Effects of Sea Level Rise in the Northern Gulf of Mexico (EESLR-NGOM) is a five-year interdisciplinary effort funded by the National Oceanic and Atmospheric Administration (NOAA) to assess the physical and biological responses of the NGOM coast to future SLR scenarios with particular focus on three NERRs. NERRs are designated by NOAA as protected regions with the mission of allowing for long-term research and monitoring, estuarine education, and resource management to provide a basis for more informed coastal management decisions (Edmiston et al., 2008a). The three NERRs, namely Apalachicola, FL, Grand Bay, MS, and Weeks Bay, AL represent a variety

of estuarine types and contain an array of plant and animal species that support commercial fisheries. In addition, the coast attracts millions of residents, visitors and businesses. Evaluating potential changes in tidal hydrodynamics under SLR is essential for understanding impacts to navigation, ecological habitats, infrastructure and the morphologic evolution of the coastline as tidal hydrodynamics influence major physical processes such as inundation, circulation and sediment transport. Due to unique morphology and hydrodynamic influences in each NERR, it is likely that each basin will respond differently to SLR, with various effects to the coastal wetlands and organisms within them.

1.1 Hypothesis and Research Objective

The intent of this research is to evaluate the dynamic effects of SLR and coastal morphology on tidal hydrodynamics along the NGOM coast and within the three NERRs. This dissertation seeks to test the following hypothesis:

Tidal hydrodynamic response to SLR is nonlinear and dependent on local estuarine conditions, e.g., morphology, geometry, friction, exposure, etc. Therefore, incorporating estimates of future morphology into the model will alter hydrodynamic parameters such as inundation, tidal prisms and current velocities.

Examination of the hypothesis leads to two scientific research questions that will also be addressed:

How will SLR and morphology alter tidal hydrodynamics?

Is one estuary more vulnerable to SLR than the others? If so, what factors influence the vulnerability of an estuary to SLR (e.g., morphology, tidal range, shoreline change rates, shoreline exposure, circulation patterns)?

Ultimately, this research provides a more integrated, holistic understanding of the NGOM system that will support restoration efforts and adaptation strategies. This allows coastal managers and policy makers to make more informed decisions that address specific needs and vulnerabilities of each estuary, and similar estuaries elsewhere.

1.2 Dynamic Effects of Sea Level Rise on Coastal Landscapes

Coastal responses to SLR include inundation of wetlands, increased shoreline erosion, and increased flooding during storm events. Hydrodynamic parameters such as tidal ranges, tidal prisms, tidal asymmetries, increased flooding depths and inundation extents during storm events respond non-additively to SLR. Coastal morphology continually adapts towards equilibrium as sea levels rise, inducing changes in the landscape. Marshes may struggle to keep pace with SLR and rely on sediment and organic accumulation and the availability of suitable uplands for migration. Whether hydrodynamic, morphologic or ecologic, the impacts of SLR are inter-related. Chapter 2 examines previous studies that have accounted for the dynamic, integrated responses of hydrodynamics, coastal morphology and marsh ecology to SLR by implementing more complex approaches rather than the simplistic so-called “bathtub” approach. These studies provide an improved understanding of the dynamic effects of SLR on coastal environments and contribute to an overall paradigm shift in how coastal scientists and engineers approach modeling the effects of SLR.

1.3 Shoreline Change Rate Comparison

Projecting long-term changes in coastal morphology is challenging due to the stochastic nature of the processes as well as a lack of understanding in the dynamic interactions and feedback mechanisms (Sampath et al., 2011). As a result, coastal scientists do not have a reliable, universal model to accurately predict the impacts of SLR along a variety of coastlines (Fitzgerald et al., 2008). Various conceptual models and statistical methods have been employed to project future shoreline position. Chapter 3 compares shoreline change rates established by the USGS Coastal Vulnerability Index (CVI) (Thieler and Hammar-Klose, 1999; Thieler and Hammar-Klose, 2000) and the USGS National Assessment of Shoreline Change (Morton et al., 2004; Morton and Miller, 2005) as well as erosion rates estimated using the Bruun Rule (Bruun, 1962) conceptual model along sandy shorelines of the U.S. South Atlantic Bight and Northern Gulf of Mexico Coasts. The intent is not to regard one method as superior to the others, but rather to explore similarities and differences between the methods and present recommendations for quantifying future shoreline positions in SLR assessments.

1.4 Sensitivity Analysis of a Hydrodynamic Model to Projected Shoreline Changes

When conducting hydrodynamic evaluations of the effects of SLR, it is necessary to properly represent the dynamics in the physical system. Chapter 4 presents a sensitivity analysis in which the influence of incorporating future shoreline changes associated with SLR into hydrodynamic modeling is evaluated for the NGOM coast. A two-dimensional, depth integrated hydrodynamic model forced by astronomic tides and hurricane winds and pressures representative of Hurricanes Ivan (2004), Dennis (2005) and Katrina (2005) is used to simulate present conditions, 2050

projected sea level with present-day shorelines, and 2050 sea level with projected 2050 shorelines. The 2050 shoreline and nearshore morphology are projected using CVI shoreline change rates to determine the position of the new Gulf and bay shorelines, while the active beach profile is shifted horizontally according to the amount of erosion or accretion, and vertically to keep pace with rising seas. Results further demonstrate the necessity of taking a dynamic approach to modeling SLR, as opposed to a static, or “bathtub” approach.

1.5 Historic Changes in Tidal Hydrodynamics

The complexities in coastal processes make determining the future impacts of SLR a difficult task. Evaluating how hydrodynamics have been altered historically under a changing landscape in conjunction with SLR can provide insight as to how water levels and currents may change in the future. Out of the three NERRs, Grand Bay has had undergone the most significant landscape changes historically. Chapter 5 evaluates the combined effects of historic SLR and morphology on tidal hydrodynamics within Grand Bay. A large-domain hydrodynamic model is used to simulate present (circa 2005) and past conditions (circa 1848, 1917, and 1960) with unique sea levels, bathymetry, topography and shorelines representative of each time period. Comparison of tidal parameters illustrates the hydrodynamic response of the system to SLR and the changing landscape, and provides insight into potential future changes under SLR and further morphologic evolution.

1.6 Comparison of Present and Future Hydrodynamics

Evaluating potential future changes in tidal hydrodynamics under SLR is essential for understanding impacts to navigation, ecological habitats, infrastructure and the morphologic evolution of the coastline; tidal hydrodynamics govern inundation, circulation and sediment transport processes. Chapter 6 examines the integrated dynamic effects of SLR and projected morphology on tidal hydrodynamics along the NGOM coast with particular focus on the Apalachicola, FL, Grand Bay, MS and Weeks Bay, AL NERRs. A large-domain hydrodynamic model is used to simulate astronomic tides for present (circa 2005) and future conditions (circa 2050 and 2100). The model is modified with projections of future sea levels as well as future shoreline positions and dune elevations obtained from a BN model that represents the relationships between driving forces and geological constraints to produce probabilistic projections of morphology. Changes in harmonic constituent amplitudes and phases, current velocities and inundation are examined. Findings can be used in storm surge and biological assessments of SLR, as well as management decision making and adaption planning.

1.7 References

- Bruun, P. (1962). "Sea-level rise as a cause of shore erosion." *Proceedings of the American Society of Civil Engineers, Journal of the Waterways and Harbors Division* 88: 117-130.
- Cazenave, A. and Llovel, W. (2010). "Contemporary Sea Level Rise." *Annual Review of Marine Science* 2: 145-173.
- Church, J. A. and White, N. J. (2006). "A 20th century acceleration in global sea-level rise." *Geophys. Res. Lett.* 33(1): L01602.

- Edmiston, H. L., Calliston, T., Fahrny, S. A., Lamb, M. A., Levi, L. K., Putland, J. and Wanat, J. M. (2008a). "A River Meets the Bay: A Characterization of the Apalachicola River and Bay System", Apalachicola National Estuarine Research Reserve.
- Fitzgerald, D. M., Fenster, M. S., Argow, B. A. and Buynevich, I. V. (2008). "Coastal Impacts Due to Sea Level Rise." *Annual Review Earth Planet Science* 36: 601-647.
- Morton, R. A. and Miller, T. L. (2005). "National Assessment of Shoreline Change: Part 2, Historical Shoreline Changes and Associated Coastal Land Loss Along the U.S. Southeast Atlantic Coast", USGS: 40p.
- Morton, R. A., Miller, T. L. and Moore, L. J. (2004). "National assessment of shoreline change: Part 1: Historical shoreline changes and associated coastal land loss along the U.S. Gulf of Mexico". Open-file Report 2004-1043. St. Petersburg, Florida, U.S. Geological Survey: 45p.
- Sampath, D. M. R., Boski, T., Silva, P. and Martins, F. A. (2011). "Morphological evolution of the Guadiana estuary and intertidal zone in response to projected sea level rise and sediment supply scenarios." *Journal of Quaternary Science* 26(2): 156-170.
- Thieler, E. R. and Hammar-Klose, E. S. (1999). "National Assessment of Coastal Vulnerability to Sea Level rise: Preliminary Results for the U.S. Atlantic Coast". Woods Hole, Massachusetts, U.S. Geological Survey.
- Thieler, E. R. and Hammar-Klose, E. S. (2000). "National Assessment of Coastal Vulnerability to Sea-Level Rise: Preliminary Results for the U.S. Gulf of Mexico Coast". Woods Hole, MA, U.S. Geological Survey.

CHAPTER 2. THE DYNAMIC EFFECTS OF SEA LEVEL RISE ON LOW GRADIENT COASTAL LANDSCAPES: A REVIEW

The content in this chapter is under review as: Passeri, D.L., Hagen, S.C., Medeiros, S.C., Bilskie, M.V., Alizad, K., Wang, D. 2015. The dynamic effects of sea level rise on low gradient coastal landscapes: a review. *Earth's Future, Under Review*.

2.1 Introduction

Direct observations from long-term tide gauges and global satellite altimetry show that sea level is rising. Analyses of tide gauge records indicate a global mean SLR between 1.6 mm/year and 1.8 mm/year over the 20th century (Church and White, 2006; Jevrejeva et al., 2006; Jevrejeva et al., 2008; Church and White, 2011). High-precision satellite altimetry suggest a recent acceleration with rates as high as 3.4 mm/year between 1993 and 2009 (Nerem et al., 2010; Hay et al., 2015). Unlike infrequent large magnitude storms that can reshape the coast within hours, the impacts attributed solely to SLR are typically slow, repetitive and cumulative (Fitzgerald et al., 2008). Immediate effects include submergence, increased flooding and saltwater intrusion into surface water, whereas long-term effects will increase shoreline erosion and induce saltwater intrusion into groundwater as the coast adjusts. In addition, coastal wetlands will struggle to keep pace with SLR if sediment supplies are not sufficient (Nicholls and Cazenave, 2010). The effects of SLR have significant socioeconomic consequences for the vast number of coastal communities worldwide. In 2003, it was estimated that 1.2 billion people (23% of the world's population) lived within 100 km of a shoreline and 100 m in elevation of sea level (Small and Nicholls, 2003). Beaches are a key element of the travel and tourism industry, which is becoming increasingly prevalent in global economies (Houston, 2013). In addition to human communities, coastal areas contain ecologically and economically significant estuaries. Coastal wetlands and marshes provide food, shelter and

nursery areas for commercially harvested fish and shellfish. Wetlands also help protect coastal communities by mitigating the impacts of storm surge and erosion (NOAA, 2011). Increased shoreline erosion under accelerated SLR poses a serious threat to economies worldwide. As populations increase, coastal areas are also susceptible to additional stresses due to land-use and hydrological changes (Nicholls et al., 2007).

Projecting future SLR is complex due to uncertainty in modeling the various contributory processes, including thermal expansion of ocean water, land ice loss, and changes in land water storage (Church and White, 2006; Jevrejeva et al., 2006). Although historic sea level trends provide valuable information for preparing for future changes, they are insufficient for assessing risk under future uncertainties (Parris et al., 2012). The Intergovernmental Panel on Climate Change (IPCC) Fifth Assessment Report projects a global mean SLR between 52 cm and 98 cm by the year 2100 under the highest emissions scenario, and 28 cm to 61 cm under the lowest emissions scenario (Church et al., 2013). Alternatively, scenarios of future global mean SLR are a common way to consider multiple future conditions and develop response options, given the range of uncertainty (Parris et al., 2012). To plan for changes under future sea levels at a local scale, it is necessary to have local projections of SLR that accommodate various risk tolerances and cover a range of timescales relevant for planning purposes (Kopp et al., 2014).

Additionally, coastal managers need scientific data regarding the potential impacts of SLR to make informed decisions for managing human and natural communities. Therefore, developing integrated, multidisciplinary studies that incorporate the various factors that impact coastal systems at local scales should be given high priority, as they will benefit coastal scientists and

stakeholders (Cazenave and Le Cozannet, 2013). However, the complexities associated with coastal systems make determining the future impacts of SLR a difficult process. SLR induces nonlinear changes in hydrodynamics, which influences sediment transport and ecological processes. Although coastal systems are known to be dynamic, many studies have employed a simplistic static or “bathtub” approach when modeling the effects of SLR. More recent efforts have begun to consider the dynamic effects associated with SLR (e.g., the nonlinear response of hydrodynamics under SLR), but little research has considered the integrated feedback mechanisms and co-evolution of multiple interdependent systems (e.g., the nonlinear responses and interactions of hydrodynamics, morphology and ecology under SLR) (Figure 2.1, Figure 2.2).

This review examines the dynamic effects of SLR on low gradient coastal landscapes, primarily in the context of hydrodynamics, coastal morphology, and marsh ecology, which can ultimately lead to alterations of natural and built communities. The highlighted processes were selected due to their interdependence and integrated feedback mechanisms. Determining future changes in coastal processes under SLR is a complicated task, and coastal dynamics are not limited to those discussed herein; many other ecological habitats and organisms may experience dynamic alterations in response to rising seas. However, the purpose of this review is to provide a basis for establishing many of the prominent dynamic effects associated with SLR, as well as identifying future research needs. Sections 2.2, 2.3 and 2.4 parallel one another with discussions of hydrodynamics, coastal morphology and marsh ecology, respectively. Sections 2.2.1, 2.3.1 and 2.4.1 review the physical processes and interactions of these systems to establish a basis for assessing their integrated, dynamic responses to SLR (Sections 2.2.2, 2.3.2 and 2.4.2). Sections 2.2.3, 2.3.3 and 2.4.3 discuss physics and process-based models and methodologies that have been

developed to project the response of these processes to SLR, as well as findings from recent modeling and observational studies. By moving beyond the “bathtub” model and employing more complex approaches, these studies aid in understanding the dynamic responses of these processes under SLR scenarios. Although these studies provide insight to potential future conditions, an integrated approach is necessary to fully understand the response of coastal systems to SLR; Section 2.5 contrasts the previous sections by describing synergetic studies that consider multiple dynamics in coastal systems. Section 2.6 summarizes additional considerations for coastal dynamics, as well as potential socioeconomic and management implications. The review concludes with a summary of future research needs.

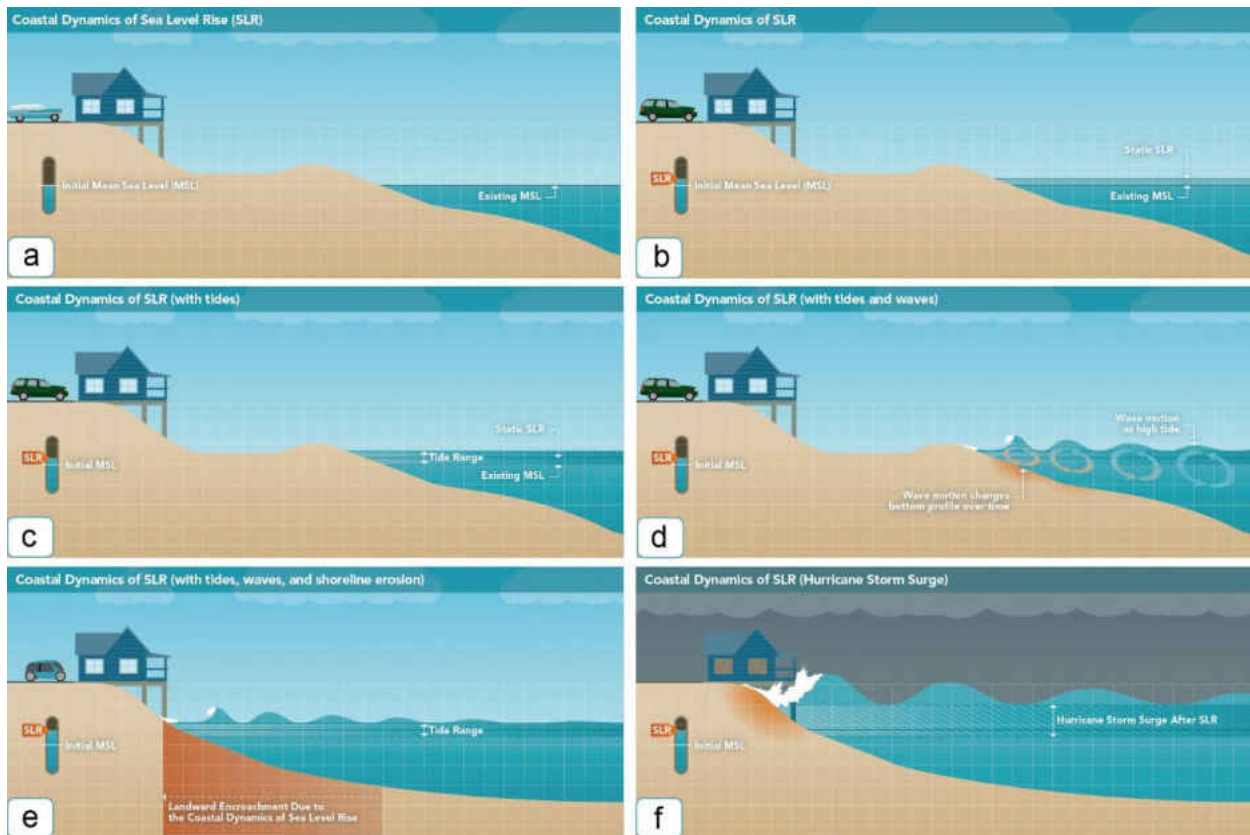


Figure 2.1: Coastal dynamics of SLR along sandy shorelines: (a) existing mean sea level, (b) a static rise on sea level simply elevates existing mean sea level by the amount of SLR, resulting in inundation of the coast, (c) a dynamic rise in sea level accounts for the nonlinear response of the tides, (d) higher water levels allow wave energy to act higher on the beach profile, resulting in erosion, (e) the eroded beach profile results in further inundation under SLR, (f) rising seas have the potential to exacerbate coastal flooding during storm events.

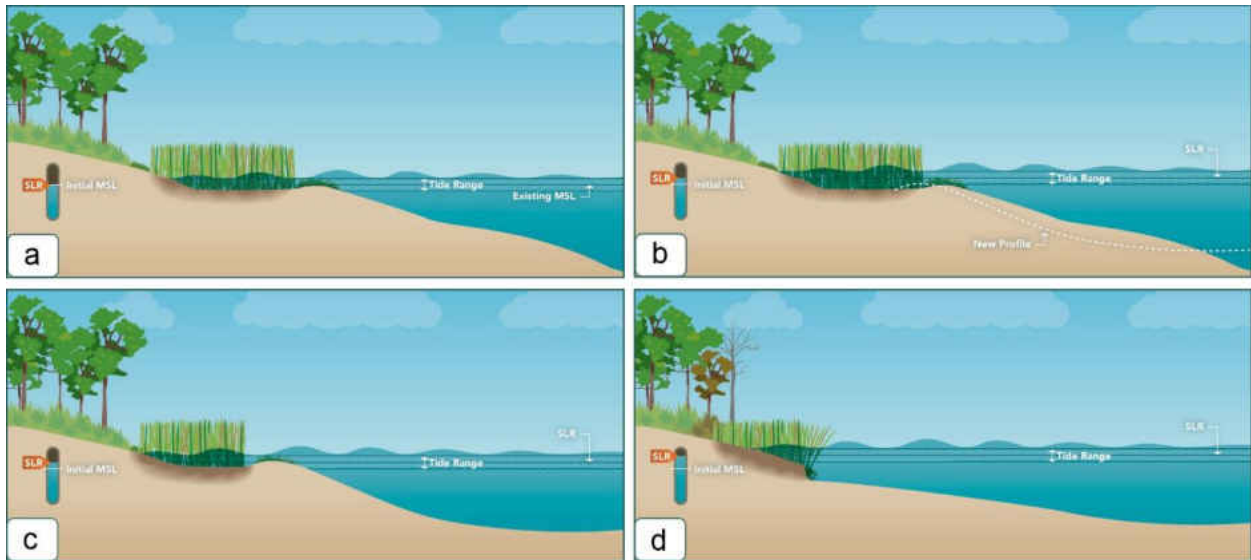


Figure 2.2: Coastal dynamics of SLR along sandy shorelines: (a) existing mean sea level, (b) a static rise on sea level simply elevates existing mean sea level by the amount of SLR, resulting in inundation of the coast, (c) a dynamic rise in sea level accounts for the nonlinear response of the tides, (d) higher water levels allow wave energy to act higher on the beach profile, resulting in erosion, (e) the eroded beach profile results in further inundation under SLR, (f) rising seas have the potential to exacerbate coastal flooding during storm events.

2.2 Coastal Hydrodynamics

2.2.1 Background

Hydrodynamics influences processes in estuaries such as inundation, circulation patterns, and sediment transport. In estuaries, tidal range (the maximum vertical difference between the high and subsequent low tide during a spring tidal cycle) is a significant parameter in determining the strength of tidal currents and their ability to transport and redistribute sediment (Stevens, 2010). Coastal systems and estuaries can be classified based on tidal ranges. Macrotidal coasts exceed 5 m (e.g., the Bay of Fundy), low-macrotidal coasts are between 3.5 m and 5.0 m (e.g., the German Bight in the North Sea), high-mesotidal are between 2.0 m and 3.5 m (e.g., the Georgia and South

Carolina coasts), low-mesotidal are between 1.0 m and 2.0 m (e.g., the New Jersey coast), and microtidal are less than 1 m (e.g., the Florida Gulf coast) (Hayes, 1979). For coasts that experience minimal tides, Tagliapietra et al. (2009) proposed the nanotidal class for ranges less than 0.5 m (e.g., the Mediterranean Sea). When the tide outside of an estuary rises and becomes higher than the water within the estuary, the water surface gradient drives water into the estuary; similarly, when the tide outside of the estuary is falling and becomes lower than the water surface within the estuary, the water surface gradient drives water out of the estuary (Masselink et al., 2011). The total volume of water entering the bay on the flooding tide is referred to as the tidal prism (Dean and Dalrymple, 2002). Tidal prisms influence estuarine flushing, mixing and residence time (Sheldon and Alber, 2006).

Tidal asymmetry occurs when the offshore tide becomes distorted as it propagates into shallow estuaries. Generally, tidal asymmetry can be characterized by the duration of the flood/ebb tide and the corresponding velocity; if the duration of the flood tide is longer, leading to a strong peak ebb velocity, then the system will be ebb-dominant. Likewise, if the duration of the ebb tide is longer, leading to a stronger peak flood velocity, then the system is flood-dominant. A flood-dominant system typically has a net sediment transport shoreward (into the estuary), whereas an ebb-dominant system typically has a net sediment transport seaward (out of the estuary) (Aubrey and Speer, 1985). A distinction can be made between vertical (i.e., water level) and horizontal (i.e., flow velocity) asymmetries. A vertical asymmetry is generated if the period of the flood tide is unequal to ebb, whereas a horizontal asymmetry occurs if a residual transport is generated. This may occur if a difference in the magnitude between maximum ebb and flood velocities exists. Horizontal asymmetry may lead to a residual transport of bed and suspended sediment loads; if

the maximum flood velocity exceeds the ebb velocity, a residual transport in the flood direction is likely to result. Another type of asymmetry that exists is the difference in the duration of slack water, which affects residual transport of fine suspended sediment. If the duration of slack water before the ebb tide exceeds the duration of slack water before the flood tide, a residual sediment transport in the flood direction is likely (Wang et al., 1999).

In semidiurnal regions, oceanic tides generate higher frequency overtides as they enter the estuary's shallow waters (Aubrey and Speer, 1985). These overtides result from the nonlinear physical processes associated with friction and continuity (Speer and Aubrey, 1985). The overtides grow nonlinearly as they propagate through the estuary, which causes the sinusoidal form of the tides to become distorted (Friedrichs and Aubrey, 1988; Blanton et al., 2002). Therefore, asymmetry can be characterized by the M2 (principal lunar semidiurnal) constituent and its overtides M4 and M6 (Blanton et al., 2002). Speer and Aubrey (1985) developed relationships to classify if an estuary is flood or ebb-dominant by determining the relative M2-M4 phase, equal to twice the M2 phase minus the M4 phase ($2M_2 - M_4$). Blanton et al. (2002) adapted this concept to include the M6 overtide, yielding a relative phase calculated as $3M_2 - M_6$. The magnitude of asymmetry may also vary throughout the estuary, and can be measured using the ratio of the amplitudes of M4 to M2 (the M_4/M_2 ratio) (Aubrey and Speer, 1985).

Although tidal asymmetry is not unique to semidiurnal systems, studies in diurnal regions are less common. Unlike semidiurnal regions, shallow water modifications are not required to generate asymmetry in diurnal regions. Flow asymmetry in diurnal regions is attributed to the interaction of the O1 (principal lunar diurnal), K1 (lunar-solar diurnal) and M2 tidal constituents; phase-angle

relationships between these constituents create a cyclic asymmetry with maximum spring tide velocities persistently in the same direction (Hoitink et al., 2003). The phase-angle relationship varies spatially and therefore the magnitude and direction of the tidal asymmetry may also vary (van Maren et al., 2004). Bathymetry may also have indirect effects on tidal asymmetry, resulting from flow acceleration or divergent propagation of the semidiurnal and diurnal tidal waves (Pugh, 1987; Jewell et al., 2012). Fluctuations in flood or ebb dominance may occur throughout the annual cycle, as opposed to fixed asymmetry seen in semidiurnal regions (Ranasinghe and Pattiaratchi, 2000; van Maren et al., 2004; O'Callaghan et al., 2010; Jewell et al., 2012). Tidal asymmetry is equally important in comparison with residual flow (long-term averaged flow) for sediment transport; fine sediment is likely dominated by residual flow whereas coarser sediment may be more influenced by tidal asymmetry (van Maren et al., 2004).

Waves also have significant influences on suspended sediment concentrations in estuaries, especially at times near low tide (Green and Coco, 2014); wave suspended sediments have been found to exceed tidal suspended sediments by a factor of 3 to 5 (Sanford, 1994). Similarly, wave energy during storm events can cause macrotidal estuaries to become wave-dominant, which may increase suspended sediment concentrations by an order of magnitude (Christie et al., 1999). In mesotidal estuaries, re-suspension of sediments can be completely controlled by episodic waves (Green et al., 1997). In microtidal estuaries, suspended sediment concentrations may decrease as waves subside (Ralston and Stacey, 2007). In some estuaries, tidal current strength (flood and ebb dominance) is not the sole force influencing net sediment transport; wave action has the potential to alter ebb and flood dominance in channels (Green et al., 1997).

2.2.2 *Hydrodynamic Response to Sea Level Rise*

SLR can influence tidal hydrodynamics through increased tidal ranges, tidal prisms, surge heights, and inundation of present day shorelines (National Research Council, 1987) (Figure 1). In addition, it has the potential to change circulation and sediment transport patterns, which may result in changes to habitats and their organisms (Nichols, 1989). Increased tidal ranges have the potential to increase tidal current velocities; if the increase is significant, additional shorelines may undergo erosion (Stevens, 2010). The magnitude of change in a bay's tidal prism under SLR is dependent on the morphology of the bay's shorelines. Bays surrounded by Pleistocene uplands typically have steep slopes which mitigate the extent-driven impacts of SLR. Shallow bays surrounded with wetlands broaden under SLR due to their gently sloping shoreline; this may be further increased if the marshes drown and transition to open water (National Research Council, 1987). An increase in the tidal prism under SLR is reflected in stronger tidal flows (Boon and Byrne, 1981). In addition, SLR can alter tidal asymmetries (Speer and Aubrey, 1985); understanding tidal asymmetry and its influence on residual sediment transport is necessary to determine if an estuary will keep pace or drown under SLR (Wang et al., 1999). Changes in tidal propagation (which is strongly influenced by morphology) can influence sediment balance in systems, and may modify the potential of the system to export sediment and consequently alter morphology (Dias and Picado, 2011).

Estuaries are especially sensitive to SLR since they undergo different reactions to forcing factors depending on their ecological systems (Rilo et al., 2013). The hydrodynamics of estuaries have important implications for navigation, fisheries, flooding, water quality and the geological

evolution of the coastline. If rising seas increase channel depths or alter the volume of water stored in the intertidal zone, tidal asymmetries and resulting sediment transport patterns in estuaries may be fundamentally altered (Friedrichs et al., 1990). Residual transport and circulation are typically dominated by tidal asymmetries and river inflow; understanding changes to residual circulation under SLR is crucial for understanding the impact to a coastal system and its ecosystems (Valentim et al., 2013). In addition, coastal topography will affect how estuaries respond to future accelerated rates of SLR (Church, 2001).

Rising seas also have the potential to increase coastal flooding caused by storm surges. For a storm of a given magnitude, the surge will be elevated and potentially produce more areas of inundation. In addition, storm surges of a given height are expected to occur more frequently (Fitzgerald et al., 2008). Although there is evidence that tropical cyclones will intensify in the future, SLR is expected to become a dominant driver in increased tropical cyclone flooding. SLR is considered to be a competing, if not more significant factor in increasing the frequency of extreme coastal flooding due to tropical cyclones (Woodruff et al., 2013). SLR may also cause future changes in wind-wave climates. Wave height is limited by available water depth; therefore deeper water in nearshore environments will cause wave heights to increase (Smith et al., 2010). Inshore wave heights in shallow areas may increase with SLR in some coastal areas, which can affect nearshore sediment transport processes (Chini et al., 2010). As SLR rates increase, extreme flooding from tropical cyclones will also increase. It is expected that resulting storm damage will be the most severe where morphology along populated shorelines heighten storm impacts, as opposed to where tropical cyclone activity is the highest (Woodruff et al., 2013).

2.2.3 Hydrodynamic Modeling of Sea Level Rise

Many numerical models have been developed to simulate hydrodynamic and transport processes including currents, waves and sediment transport within coastal systems. One-dimensional (1D) hydrodynamic models can be used to model flood flows. Flow in a channel is calculated by average equations over a cross-section, providing an average flow velocity for each section (Kilanehei et al., 2011). These models are computationally efficient and can be used for large hydrologic systems and complex river/channel systems. However, using a 1D approach is not appropriate for modeling floodplain flows. Two-dimensional (2D) depth-integrated hydrodynamic models have been used for predicting free surface flows, although they can be computationally expensive and less flexible for including complex channel networks (Lin et al., 2006). These models typically simulate flow by integrating governing equations over depth, which results in horizontal velocity and water depth components in each element (Kilanehei et al., 2011). Because these models are depth-integrated, they are unable to simulate vertical components of currents or density variations in the water column. Three-dimensional (3D) models are able to simulate horizontal and vertical currents as well as transport of suspended matter. These models can be useful for simulating hydrodynamics as well as morphology.

Wave-current interactions can be captured with one- or two-way coupling of wave and hydrodynamic models. In the one-way coupling approach, wave radiation stresses are computed in the wave model and provided to the hydrodynamic model to be implemented as surface stress; the hydrodynamic model does not feedback any information to the wave model. In a two-way coupling approach, wave radiation stresses are calculated, then passed to the hydrodynamic model

which calculates currents and water surface elevations, which are fed back to the wave model to calculate the new wave radiation stress. For both approaches, feedback does not occur at every time step.

Integrated coastal/ocean processes models can aid in dynamic assessments of local impacts of SLR to better assess coastal vulnerability and coastal hazard management (Ding et al., 2013). The coastal flooding response under SLR can have be either linear or nonlinear. A linear response, or static response, occurs when the existing dynamics are simply elevated by the amount of SLR. For example, if the present flooding extent is located at the 10 m topographic contour, then the future flooding extent under 0.5 m of SLR would be located at the 10.5 m topographic contour. A nonlinear response, or dynamic response, accounts for nonlinear effects in the system; the 0.5 m of SLR may lead to a greater or lesser flooding extent than the 10.5 m topographic contour (Hagen and Bacopoulos, 2012). Two-dimensional and three-dimensional hydrodynamic models have been widely applied to simulate the dynamic responses to SLR scenarios (e.g., Mousavi et al. (2011); Hagen and Bacopoulos (2012); Atkinson et al. (2013); Ding et al. (2013); Bilskie et al. (2014); Passeri et al. (2015)). However, there is neither a vetted framework for incorporating SLR into hydrodynamics, nor critical reviews comparing various methodologies and outcomes.

Hydrodynamic assessments of SLR have shown changes in tidal parameters including constituents, tidal range, tidal prisms, flow velocities, residual currents, and tidal datums. French (2008) used a two-dimensional model to simulate hydrodynamics in a mesotidal, barrier-enclosed estuary in England under SLR. Tidal hydrodynamics were simulated under a rise of 0.30 m with present day bathymetric conditions. Tidal prisms increased by 28% in the estuary, which

significantly increased peak flood tidal flows and slightly increased peak ebb flows. The M2 tidal constituent amplitude decreased by approximately 5%, whereas the M4 amplitude was reduced by 20% to 40%. Overall, SLR significantly reduced the ebb dominance of the estuary (French, 2008). SLR has also been shown to reduce residual circulation. Under 0.42 m of SLR in a mesotidal estuary in Portugal, residual circulation was reduced by almost 30% under normal river discharge conditions, and 10% under maximum discharge conditions (Valentim et al., 2013). Inundation extent may also be altered under SLR, although quantification may vary depending on whether a static or dynamic approach is taken. Using a two-dimensional model to simulate astronomic tides under various SLR scenarios in the Florida Panhandle, U.S., Hagen and Bacopoulos (2012) found that a static approach underestimated the amount of the inundated floodplain area by a ratio as low as 2:3 in comparison with the dynamic approach. The authors concluded that SLR should be assessed using a dynamic approach to capture future dynamic interactions that may otherwise be missed with a static approach (Hagen and Bacopoulos, 2012). Hindcast studies can also be beneficial for studying the effects of SLR on hydrodynamics. Leorri et al. (2011) employed a three-dimensional hydrodynamic model to simulate water levels and currents in response to SLR over the Holocene period in the mesotidal Delaware Bay, U.S. The sea level was lowered corresponding to 4000 years ago although bathymetry was not altered from present day conditions. Lowering the water level changed the geometry of the bay from a funnel-shape to an elongated wide type, which in turn altered the hydrodynamic behavior. The tidal range increased in the shallower section of the bay near the mouth, and decreased upstream. The reduction in the elevation of high tide and mean tide was nonlinearly related to the amount of sea level fall. In addition, tidal currents became asymmetrical with longer ebb durations. (Leorri et al., 2011).

In addition to tidal hydrodynamics, SLR has the potential to alter storm surge dynamics with increased flooding and wave heights. Using a two-dimensional hydrodynamic model coupled with a wave model, Smith et al. (2010) simulated hypothetical hurricanes that produced 100 year water levels in Southeast Louisiana, U.S., under future SLR scenarios. The authors found that the response of the surge to SLR was nonlinear, and that the long return period water levels could modestly increase above the SLR, whereas shorter return period water levels could significantly increase. In addition, wave heights significantly increased in previously shallow areas as a result of the larger depths (Smith et al., 2010). Similarly, Mousavi et al. (2011) demonstrated the nonlinear effects of storm surge along the Texas Coast, U.S., under SLR scenarios, with some areas experiencing reductions in peak surge, and others experiencing increases in peak surge. The effects of SLR on storm surge vary depending on the geographic region and storm scenario. Atkinson et al. (2013) used a coupled wave and hydrodynamic model to simulate storms along the Texas Coast, U.S., with similar meteorological characteristics but various landfall locations to examine how coastal features influenced storm surge under SLR. Topography controlled increased flooding, although regions were not equally at risk. In addition, SLR increased wave heights in the nearshore and inland areas (Atkinson et al., 2013). It is also important to note that implementing a dynamic approach when quantifying storm surge flooding under SLR may result in the same depth of floodplain inundation as a static approach, however, the spatial distribution of flooding may differ (Hagen and Bacopoulos, 2012).

2.3 Coastal Morphology

2.3.1 Background

Coasts are dynamic systems that are continuously transforming over different temporal and spatial scales as a result of geomorphological and oceanographical changes (Cowell et al., 2003a; Cowell et al., 2003b). Shorelines assume a specific maintained state that can often be distinguished by a characteristic morphology. The state is sustained by negative feedbacks, but may be altered as a result of short-term perturbations, the system exceeding an inherent threshold, or a change in boundary conditions (e.g., sea level). Shorelines can adopt different types of equilibrium. If the processes are balanced, the shoreline will remain constant in a static equilibrium. If the boundary conditions do not change and the average state of the shoreline is unchanged over time, a steady-state equilibrium occurs. If the boundary conditions change and the landscape continuously evolves to adjust to the new conditions, a dynamic equilibrium occurs (Woodroffe, 2003; Woodroffe, 2007).

Coastal environments can be generally characterized as wave dominated, tide dominated or mixed (a balance between wave and tide forces), depending on the predominate force for sediment transport. Microtidal coasts are often wave dominant. Low-mesotidal coasts have mixed wave and tidal energy but are more wave dominant. High-mesotidal coasts also have mixed wave and tidal energy, but are more tide dominant. Low-macrotidal and macrotidal coasts are tidal dominant (Hayes, 1979). Coastal morphology is often influenced by tidal range, except along coastlines with high wave energy and high tidal range (e.g., the Bay of Fundy), as well as low wave energy and low tidal range (e.g., the Gulf of Mexico). In high energy regions, high wave energy controls

coastal morphology rather than tidal range. In low energy regions, there is a delicate balance between wave and tidal processes that allow tide dominant, wave dominant, or mixed energy morphology to develop with little variation in wave and tidal parameters; a low energy region may transition from wave dominant to mixed energy or tide dominant with a small increase in tidal range (Davis and Hayes, 1984). Additionally, because morphological response times in low energy regions are long, morphology is often dominated by high energy processes such as storms (Masselink et al., 2011).

Storm surge has a significant impact on morphology in locations that are sheltered from waves and tides (e.g., near the heads of estuaries and landward sides of barrier islands), as well as low energy regions, especially when surge levels exceed tidal ranges. Surge allows wave processes to operate on the upper foreshore of beaches, which are typically only affected by Aeolian processes (Jackson et al., 2002). Storm inundation processes are nonlinear; inundation is gradual until a threshold is reached, followed by rapid inundation due to local topography (Zhang, 2011). Barrier islands are especially susceptible to impacts from storms, depending not only on the magnitude of the storm, but also characteristics such as surge, waves, wave runup, and the geometry of the island. Barrier island impact from tropical and extra-tropical storms are typically characterized by the following four regimes: (1) the swash regime (2) the collision regime (3) the overwash regime and (4) the inundation regime. In the swash regime, runup is confined to the foreshore, which typically erodes during the storm but recovers post-storm; therefore, there is no net change. The collision regime occurs when wave runup exceeds the base of the foredune ridge and impacts the dune with net erosion. In the overwash regime, wave runup overtops the berm or foredune ridge. This causes net landward transport which contributes to the net migration of the barrier island landward. In the

inundation regime, storm surge completely and continuously submerges the island, which initiates net landward sediment transport (Sallenger, 2000). However, these regimes do not consider the influence of storm surge ebb flows, which can transport sediment seaward across the shoreface, resulting in net losses. Although this phenomenon has been studied less, it has been well documented as a dominant erosive force during hurricanes including Hugo (1989) (Hall et al., 1990), Andrew (1992) (Davis, 1995), and Ike (2008) (Goff et al., 2010) along the U.S. coasts. Although storms have the ability to reshape beach profiles from equilibrium conditions over a relatively short period of time (Walton and Dean, 2007), shorelines and nearshore bathymetry tend to recover to the pre-storm equilibrium conditions (Leadon, 1999; Wang et al., 2006).

2.3.2 Coastal Morphologic Response to Sea Level Rise

The most simplistic approach to assess the physical response of shorelines to SLR is to consider inundation under a static rise (or fall) in sea level, often referred to as the “drowned valley concept” (Leatherman, 1990). Under this approach, the shoreline migrates landward according to the slope of the coast as the sea level rises. The shore becomes submerged, but otherwise unaltered (Leatherman, 1990). Areas with mild slopes will experience more inundation for a given rise in sea level than areas with steep slopes (Zhang et al., 2004). This concept is suitable for regions with rocky or armored shorelines, or even where the wave climate is subdued (Leatherman, 1990). Along sandy shorelines and coastal marshes, shoreline retreat has a more dynamic effect than just inundation, including permanent or long-term erosion of sand from beaches as a result of complex, feedback-dependent processes that occur within the littoral zone, as well as migration and loss of marshes (Fitzgerald et al., 2008) (Figure 1, 2). Unlike inundation, erosion is a physical process in

which sand is removed from the shoreface and deposited elsewhere, typically offshore. Long-term, gradual shoreline recession is believed to be mainly a result of low energy processes such as SLR, as well as variations in sediment supplies (Zhang et al., 2002). The relatively moderate era of SLR that shorelines have experienced in the recent past has concluded, and shorelines are beginning to adjust to new boundary conditions (Woodruff et al., 2013). As SLR continues to accelerate, long-term erosion rates are also expected to increase (Zhang et al., 2004), which may have significant consequences for barrier islands and coastal embayments.

Barrier islands are often considered to be either transgressive (consistently migrating landward) or regressive (consistently building seaward), depending on the rate of SLR and sand supply along a particular coast (Curry, 1964). A low sand supply and/or high SLR rate will cause barriers to migrate landward. Likewise, a high sand supply and/or low SLR rate will allow for seaward migration. Tidal prisms control the cross-sectional area of inlets and ebb-tidal delta volumes. Increases in bay tidal prisms as a result of SLR can increase the dimensions of tidal inlets. This allows for sand to be transferred from the adjacent barriers, which increases the volume of sand contained in the ebb-tidal deltas. Ultimately, this may cause barrier segmentation and landward migration (Hayes and Fitzgerald, 2013). Barriers may experience one of three responses to high rates of SLR: erosion, translation or overstepping. Barrier erosion occurs when the shoreface geometry is maintained but decreases over time as the entire profile migrates landward with SLR. Barrier translation or “roll over” entails the entire barrier migrating landward without loss of material as a result of erosion from the shoreface being deposited behind the barrier as washover fans. Overstepping occurs when SLR is too high and the barrier cannot respond, resulting in drowning. Determining the response of barriers to SLR depends on the SLR rate, the gradient of

the underlying substrate, longshore transport, and sedimentation in back-bays (Masselink et al., 2011).

Shoreline changes under SLR are not limited to beaches; SLR can be a major factor in estuarine shoreline changes resulting in the loss of inter-tidal areas, erosion of shorelines and increased flooding of low lying areas (Rossington, 2008). Estuarine shorelines are often comprised of both sandy and marsh shorelines that interact with physical processes including waves, winds, tides and currents, which dictate erosion, transport and deposition processes (Riggs and Ames, 2003). Estuarine shoreline response to SLR is dependent upon the amount of energy acting on the shoreline (Stevens, 2010); if the energy is high enough, the shoreline will erode, whereas if the energy is low, the shoreline will be inundated (Department of Environmental and Heritage Protection, 2013). The eroded material becomes part of the estuary's sediment budget and is deposited along other shorelines within the basin (Stevens, 2010). Inundated marsh shorelines in estuaries experience an increase in wave energy, which may erode the marsh platform and accelerate marsh loss (Fitzgerald et al., 2008).

Under some circumstances, changes in wave climates may cause shoreline recession to be an order of magnitude greater than recession due to SLR alone (Cowell and Thom, 1994). Changes in littoral transport budgets as well as changes in storm intensity and recurrence intervals will influence wave climates and alter episodic erosion and nearshore recovery (Cowell and Kench, 2001). For example, shifts in hurricane-generated wave climates since the 1970's have already begun to reshape large-scale, coastal cusped features in North Carolina, U.S., by making them more asymmetrical (Moore et al., 2013). SLR will likely contribute to changes in wave directions

as a result of changes in water depths influencing nearshore wave refraction patterns (Cowell and Kench, 2001).

2.3.3 Coastal Morphologic Modeling of Sea Level Rise

Projecting long-term morphology is difficult due to the stochastic nature of the processes as well as a lack of understanding in the dynamic interactions and feedback that cause changes (Sampath et al., 2011). As a result, coastal scientists do not have a reliable, universal model to accurately predict the impacts of SLR along a variety of coastlines (Fitzgerald et al., 2008). Observations of beach profiles led to the characterization of the equilibrium beach profile concept, which assumes that the beach profile maintains an average, constant shape (aside from periods of storm induced changes) as the profile moves parallel to itself seasonally (Bruun, 1954). Assuming conditions other than sea level remain unchanged, the active beach profile extending from the shoreline to a seaward boundary denoted as the depth of closure will translate upward and landward to keep pace with rising seas, while maintaining shape (equilibrium) (Bruun, 1962). This concept, known as the Bruun Rule, can be used to predict shoreline recession (R) under a rise in mean sea level, given as

$$R = S \frac{L^*}{b+h^*} \quad (1)$$

where S is the rise in mean sea level, b is the elevation of the berm, h^* is the depth of closure, and L^* is the width of the active beach profile (Bruun, 1962). The depth of closure delineates the nearshore (landward of the closure depth to the shoreline) from the offshore (seaward of the closure depth), and represents the threshold where bed sediments are no longer significantly transported by waves. Therefore, it is assumed that all sediment erosion, transportation and deposition occurs

landward of the closure depth (Fitzgerald et al., 2008). The Bruun Rule is considered a coarse, first-approximation approach, as it is a theoretical model and does not take into account the effects of longshore transport, coastal inlets or structures, or Aeolian transport (DECCW, 2010). The legitimacy of the assumptions behind the Bruun Rule such as the existence of an equilibrium profile, and/or uniform alongshore transport have been questioned (Thieler et al., 2000; Cooper and Pilkey, 2004), and numerous studies that have applied the Bruun Rule have come to conflicting conclusions about its validity (Schwartz, 1967; Rosen, 1978; Hands, 1983; Schwartz, 1987; List et al., 1997; Leatherman et al., 2000; Zhang et al., 2004). However, the underlying concept remains a central assumption in many coastal response models (Hanson, 1989; Dean, 1991; Patterson, 2009; Ranasinghe et al., 2012). In addition, various models have modified the Bruun Rule to incorporate factors such as barrier translation (Dean and Maurmeyer, 1983), landward transport (Rosati et al., 2013), the dune sediment budget (Davidson-Arnott, 2005), and variations in rainfall/runoff (Ranasinghe et al., 2012).

Statistical methods such as extrapolation of historical trends have also been applied to predict future shoreline positions (Fenster et al., 1993; Crowell et al., 1997; Crowell and Leatherman, 1999; Galgano and Douglas, 2000). This involves determining the location of new shorelines based on trends established from historical shoreline positions. Various methods have been used to compute shoreline change rates including linear regression, end point and minimum description length criterion (Crowell et al., 1997). The advantage of using historical trend analysis is that it takes into account the variability in shoreline response based on local coastal processes, sedimentary environments and coastline exposures, under the assumption that shorelines in the future will respond in a similar way as in the past (with a secondary assumption that SLR is the

prominent function and all other parameters remain relatively constant) (Leatherman, 1990). Passeri et al. (2014) compared erosion rates predicted by the Bruun Rule with historic shoreline erosion rates provided by the USGS Coastal Vulnerability Index (CVI) (Thieler and Hammar-Klose, 1999; Thieler and Hammar-Klose, 2000) and the USGS National Assessment of Shoreline Change (Morton et al., 2004; Morton and Miller, 2005) along the U.S. South Atlantic Bight and Northern Gulf of Mexico coasts. The authors found that erosion rates predicted by the Bruun Rule matched long-term erosion rates in parts of northeast Florida (e.g., Melbourne, FL) and concluded the Bruun Rule could be used at these locations to predict future recession, under the assumption that historic erosion is completely attributed to the forces related to SLR. The CVI shoreline change rates were typically much larger than those provided by the National Assessment of Shoreline Change; therefore, the authors advise that care should be taken when extrapolating historical shoreline change rates to predict future shoreline positions (Passeri et al., 2014).

More recently, researchers have implemented probabilistic approaches to manage uncertainty associated with long-term shoreline predictions (Cowell and Zeng, 2003; Cowell et al., 2006). Statistical approaches using Bayesian networks have been applied to project long-term shoreline changes under SLR (Hapke and Plant, 2010; Gutierrez et al., 2011; Yates and Le Cozannet, 2012). The Bayesian network, based on the application of Bayes' theorem, is used to define relationships between driving forces, geological constraints and coastal responses to make probabilistic predictions of shoreline changes under future SLR scenarios (Gutierrez et al., 2011). Considering observations of local rates of RSLR, wave height, tidal range, geomorphic classification, coastal slope and shoreline change rates, Gutierrez et al. (2011) developed a Bayesian network to predict long-term shoreline changes. The Bayesian network was used to make probabilistic predictions of

shoreline changes along the U.S. Atlantic coast under different SLR scenarios. Results indicated the probability of shoreline retreat increased with higher SLR rates. The accuracy of the model was assessed with a hindcast evaluation, in which the network correctly predicted 71% of the cases (Gutierrez et al., 2011). Following this methodology, Yates and Le Cozannet (2012) created a Bayesian network to make statistical predictions of shoreline evolution along European coastlines. The output was compared with historic shoreline evolution trends and was found to accurately reproduce more than 65% of the trends. The authors concluded that the development of Bayesian networks is a useful tool for estimating future coastal evolution under changes in wave regimes or SLR (Yates and Le Cozannet, 2012). Bayesian networks have also been applied to project retreat along coastal cliffs, which are typically more complex due to the need to model both sandy beaches in conjunction with the coastal cliff system. Hindcast evaluation accurately predicted 70% to 90% of the modeled transects, indicating that the approach could be used to predict cliff erosion on time scales ranging from days (storm events) to centuries (SLR) (Hapke and Plant, 2010).

Since changes in coastal morphology occur at time scales that are an order to two orders of magnitude greater than hydrodynamic time scales (Stive et al., 1990), conventional morphodynamic simulations using numerical models have been inefficient and lengthy (Dissanayake et al., 2012). However in more recent years, progress in process-based models has allowed the simulation of multi-scale hydrodynamic and morphology to be feasible. These simulations can be accomplished using numerical modeling in which the wave field, current field and bathymetric changes are computed sequentially under the specified boundary conditions and sea level changes. The following are practical numerical models for simulating hydrodynamic and morphodynamic processes in coasts and estuaries: (1) one-dimensional longshore coastline models

that describe longshore sediment transport and shoreline evolution using the sand budget approach (2) two-dimensional cross-shore profile models that predict variations in coastal profiles but don't consider longshore transport (3) two-dimensional horizontal coastal/estuarine/oceanic process models that simulate hydrologic and morphologic variations with a wide range of spatial scales but no considerations of variations in waves and currents (4) three-dimensional models that take into account vertical and horizontal variations in waves and currents, but are generally restricted to predicting changes on small scales and in short durations (Ding, 2012).

Behavior-oriented models based on empirical rules and analysis can be more effective for simulating long-term shoreline evolution in comparison with numerical models, which are unable to account for variability in wave and current conditions on longer timescales. In the 1990s, large scale morphological-behavior models were developed to simulate future changes in coastal morphology under SLR and variations in sediment supply. Many of these models are centered on the equilibrium profile translation principle, but incorporate additional drivers to predict shoreline evolution. However, validation of these models is difficult and can only be accomplished through inverse modeling, in which the model is calibrated with stratigraphic data and sea level history for specific areas and shoreline translation is recreated on geological time scales.

Early behavior-oriented models include The Shoreface-Translation Model (STM) (Cowell et al., 1995), and those of Stive and De Vriend (1995) and Niedoroda et al. (1995). The coast-basin interaction model ASMITA (Aggregated Scale Morphological Interaction between a Tidal basin and the Adjacent coast) was developed to describe the morphological interactions between tidal basins and the adjacent coast at various spatial and temporal scales in response to external forcing

factors. This behavior-oriented model is based on the assumption that a tidal basin can reach an equilibrium volume relative to mean sea level, at which point the accommodation space is equal to zero. A morphological equilibrium can be obtained for each element in the tidal system (e.g., ebb-tidal delta, intertidal flats, etc.) depending on its hydrodynamic and morphometric conditions (Stive et al., 1998). Van Goor et al. (2003) employed this model to examine if the geomorphology of tidal inlets in the Dutch Wadden Sea could maintain equilibrium under rising sea levels. The authors found that if the rate of sediment import matched the rate of SLR, a new state of dynamic equilibrium was achieved, whereas if the import rate was less than SLR, the morphological state would deviate from equilibrium and the system would eventually drown. GEOMBEST (Geomorphic Model of Barrier, Estuarine, and Shoreface Translations) was developed to simulate the evolution of coastal morphology under changes in sea level and variations in sediment volume. The model is able to simulate the effects of geological framework on shoreline migration by defining the substrate with stratigraphic units characterized by erodibility and sediment composition. Unlike the Bruun Rule, changes in morphology are controlled by disequilibrium stress caused by changes in sea level, which vertically displace the equilibrium profile. This may result in net loss or gain of sediment volume as the profile tries to attain equilibrium. Applying GEOMBEST to simulate coastal stratigraphy in Washington, U.S., and North Carolina, U.S., indicated that the model could be used as a quantitative tool for coastal evolution assessments on geological time scales (Stolper et al., 2005). Following the approach of Storms et al. (2002), BIT (Barrier Island Translation) was developed to simulate the evolution of a sand barrier using simplified equations and taking into consideration the effects of various processes such as wind waves, storm surge and sea level oscillations. The model is based on the assumptions of

conservation of mass, and conservation of the equilibrium profile. It is capable of simulating the processes of sediment redistribution by waves in the shoreface, sediment diffusion by waves in the inner shelf, overwash during storms and lagoonal deposition in the back-barrier. The model used to simulate the dynamics and evolution of a barrier island in Sand Key, Florida U.S. during the last 8000 years. Results indicated that the rate of overwash and lagoonal deposition was crucial for the survival for the barrier island under the historic sea level changes (Masetti et al., 2008). Sampath et al. (2011) used a simplified behavior-oriented model to predict long-term morphological evolution in the Guadiana estuary, Portugal in response to SLR based on historic sedimentation rates and tidal inundation frequency. The model calculated the increased tidal inundation frequency under SLR using an empirical formula based on tidal range, determined from historic tide gauge data. However, the model did not take into account potential changes to tidal ranges or inundation areas under SLR. Ranasinghe et al. (2012) developed a physically based, scale-aggregate model to estimate changes in coastlines due to SLR and variations in rainfall-runoff in Vietnam. Results indicated changes can be very significant along shorelines adjacent to small inlet-basin systems; these areas cannot be neglected in coastal management and planning decisions.

2.4 Marsh Ecology

2.4.1 Background

Tidal marshes are dynamic systems governed by tidal inundation, hydroperiod, sediment supply and biological dynamics (Stralberg et al., 2011). Areas with limited tidal prisms create smaller inlet/marsh systems with shallow channels (Friedrichs and Madsen, 1992), which dictate tidal

propagation and asymmetry (Townend et al., 2011). Vegetation on the marsh platform is crucial for damping the flow of water and waves. Energy is reduced exponentially with distance from tidal creek edges due to a decrease in flow speed (Leonard and Luther, 1995). Flow damping allows particles to settle within the marsh, limits erosion on the marsh surface and can increase accretion (Townend et al., 2011); this interconnection works as a hydrologic system (Leonard and Luther, 1995). In addition, dissipation of wave energy protects nearby shorelines from erosion (Möller et al., 1999). Moreover, transported and deposited sediments near rivers and creeks play a key role in sustaining marsh habitats in river deltas (Martin et al., 2002).

The governing parameters for biomass productivity in salt marshes are the elevation of the marsh table, mean low water (MLW), and mean high water (MHW), which determine the relative depth of the salt marsh (Morris et al., 2002). The elevation of the marsh table progresses through sedimentation and accretion; deposition is controlled by tidal inundation and direct deposition of organic matter from root growth. The capturing of particles during inundation periods is dictated by flow velocities; at high tidal flows greater than 0.4 m/s, particle capture can account for over 70% of the sediment delivered to the marsh (Mudd et al., 2010). In addition, hydroperiod is an influencing factor on vertical marsh accretion. Hydroperiod depends on tidal range, which also dictates sediment transport potential (Reed, 1990). In general, an increased hydroperiod will increase the accretion rate of inorganic sediments until the accreted platform eventually decreases the hydroperiod. For organic sediments, an increased hydroperiod induces stress on the vegetation, which lowers the production of organic matter, decreases accretion and increases the hydroperiod as a positive feedback (Friedrichs and Perry, 2001). In conjunction with hydroperiod, an optimal

level between mean sea level and mean high water exists where plant productivity is at a maximum (McKee and Patrick Jr., 1988).

Processes that increase sediment concentration in tidal creeks adjacent to marshes can also increase the marsh accretion rate. These processes include local suspension of sediments through increased tidal velocity, wind waves, proximity to estuarine turbidity and an increase in background concentration due to offshore erosion (Friedrichs and Perry, 2001). Distance from creeks is also crucial, since areas near the banks of the creeks tend to accrete faster than inner marsh (Townend et al., 2011). Tidal asymmetries affect sediment transport in marsh tidal creeks, which can also dictate marsh sediment supply. Flood dominant tides in salt marsh creeks move sediment landward whereas ebb dominant tides tend to move sediment seaward. Flood dominant currents increase the suspended sediment concentration at the creek/marsh boundary, which supplies more marine sediment to the marsh. This causes accretion on the platform until the decreased inundation frequency reduces net deposition. Similarly, ebb dominant currents reduce the supply of the sediment to the marsh. An additional parameter that influences net sediment transport in tidal creeks is the difference in the rate of current change near high water slack compared to low water slack. If high water slack duration is longer than that of low water slack, more sediment will fall out of suspension after the flood tide relative to the ebb tide; this enhances landward sediment transport and increases the sediment supply to the marsh (Friedrichs and Perry, 2001). Sediment movement onto the marsh can also occur regardless of tidal asymmetry, due to settling lag (Postma, 1967) as well as higher sediment concentrations moving landward during flood tides in comparison to those moving seaward during ebb tides (Krone, 1987).

Since marsh vegetation considerably dampens the flow across the marsh, waves typically do not cause long-term erosion of the marsh platform (Townend et al., 2011). Although particle erosion may occur if stress is exerted on the marsh platform by hydrodynamic forces (Francalanci et al., 2013), eroded areas are typically restored with regular tidal inundation (Pethick, 1992). However, waves can influence edge erosion, bank failure and retreat. Wave impact may undermine the residual cohesion in the marsh platform due to normal and shear stresses occurring on the soil that connects the platform to the bank (Pethick, 1992). The integrated influences of tidal range, waves and storms provide insight to distinctions in marsh morphology and response. Unlike mesotidal and macrotidal estuarine marshes which depend on recurrent tidal action for sediment distribution (Stumpf, 1983; French and Spencer, 1993), marshes in microtidal estuaries depend upon storms for sediment supply and respond with rapid vertical accretion and horizontal expansion (Townend et al., 2011). For example, in Louisiana, U.S., Hurricane Andrew increased vertical accretion and surface elevation on the order of what typically occurs over semi-annual and annual time scales; the storm generated between 2 cm and 6 cm more vertical accretion than the accumulation in the marsh during the year before and the year after the storm (Cahoon et al., 1995). Erosion during storm events occurs as the marsh adjusts to maximize cross-shore dissipation of wave energy and increase resiliency (Townend et al., 2011).

2.4.2 Marsh Response to Sea Level Rise

Marsh response to increased rates of SLR is dependent on factors such as sediment supply, vegetation productivity, rates of subsidence or uplift, changes in storm frequency and intensity and availability of inland areas for migration (Stralberg et al., 2011). Under a given sediment supply,

a marsh can prograde or erode as a function of SLR (Mariotti and Fagherazzi, 2010). For a marsh to maintain its present form and withstand SLR, sedimentation must keep pace with the rate of rise. A slight increase in sea level may advance biomass production and increase the amount of settling on the marsh surface (Reed, 1990; Nyman et al., 2006). However, if the rate of SLR exceeds the rate of accretion, the marsh will drown (Reed, 1990). SLR may cause marshes to migrate landward at a rate almost equal to the seaward erosion; this can be especially detrimental if the marsh is backed by seawalls or bulkheads (Friedrichs and Perry, 2001). A low rate of SLR can reduce depths on adjacent tidal flats, increasing wave dissipation and sediment deposition; this leads to the marsh boundary prograding. However, a high rate of SLR deepens the tidal flats and allows higher waves to erode the marsh boundary (Figure 2). If the rate of SLR is too fast, the entire marsh will drown and transform into a tidal flat (Mariotti and Fagherazzi, 2010). The marsh hydroperiod is expected to increase with SLR, which can allow for either more deposition on the marsh platform (therefore increasing productivity) or more erosion and drowning of vegetation (Friedrichs and Perry, 2001). Coastal morphology can also influence the response of salt marsh systems to SLR. Deposition from nearby eroded shorelines can be a sufficient sediment source for marshes; Phillips (1986) estimated that shoreline erosion along the Delaware Bay, U.S., supplies 4.5 times the amount of sediment required to maintain the elevation of the adjacent marsh platforms.

Microtidal marsh systems are more sensitive to SLR and changes in suspended sediment concentrations because they cannot readily adjust their mean platform elevation with respect to the tidal elevation. A relatively small increase in sea level or a decrease in accretion can cause a microtidal marsh to become submerged. If there is ample accretion, the marshes will advance

seaward more quickly than marsh systems in higher tidal ranges. This is because less vertical growth is required to reduce the duration and frequency of the submersion time, which allows available sediment to be deposited landward. Mesotidal and macrotidal marshes may be able to keep pace with accelerating SLR due to enhanced sediment concentrations and flood dominance as tidal range increases (Friedrichs and Perry, 2001). However, even if a marsh has exhibited the ability to keep pace with SLR in the recent past and near future, a critical rate of SLR exists at which the marsh will eventually drown out (Morris et al., 2002). If suitable uplands are not available, marshes will be unable to migrate landward under SLR as they have historically, which will result in loss (Stralberg et al., 2011). It is also important to note that other factors such as changes in large-scale processes or anthropogenic interventions may have as much of an influence on marsh systems as SLR (French and Burningham, 2003).

2.4.3 Marsh Modeling of Sea Level Rise

Various models have been developed to simulate marsh processes, including empirical and physical models of marsh sedimentation, coupled vegetation and marsh sedimentation models, marsh boundary evolution, coupled vegetation and sedimentary process models and below ground organic production (for detailed model reviews, see Fagherazzi et al. (2012)). However, developing models that combine realistic local processes of sediment feedback in marshes with larger estuarine-scale spatial dynamics is challenging (Stralberg et al., 2011). Determining the effects of accelerated SLR is also difficult since isolating SLR as a driver is not feasible in natural wetlands (Kirwin and Temmerman, 2009).

Numerical models can provide insight to the effects of SLR on marsh productivity because they are able to separate SLR as a driver of change (Fagherazzi et al., 2012). Many modelling approaches have been developed (see Kirwin and Temmerman (2009) and references therein), a few of which are highlighted herein. Morris et al. (2002) developed a theoretical model used to predict marsh biomass productivity under changes in sea level. The model is able to capture the interactions between accretion and biomass productivity through a feedback process; the net rate of change in elevation of the marsh platform is equivalent to the net rate of accretion, which is dependent on biomass productivity. As the sea level rises, the marsh constantly adjusts towards a new equilibrium (Morris et al., 2002). Kirwan and Murray (2007) expanded the model to include the coupling effects between vegetation influenced evolution of the channel network and accretion on the marsh platform. Schile et al. (2014) applied the Morris et al. (2002) Marsh Equilibrium Model to four marshes in San Francisco Bay, U.S., with varying SLR and suspended sediment scenarios to quantify potential changes in marsh distributions. At high SLR and low sediment concentrations, the marshes were dominated with mudflats. Areas with adjacent uplands were able to gain new marsh habitats under the highest rate of SLR, stressing the significance of these areas in conservation planning. The study also indicated that marshes can sustain vegetated elevations with rising sea level to a certain point, but accretion alone is not enough to support the marsh habitat. Temmerman et al. (2003) developed a zero-dimensional physically based model to simulate tidal marsh accumulation rates under changes in SLR and suspended sediment concentrations (SSC) with the ability to quantify the combined effect of SLR and SSC on accumulation rates. The model was applied to the Scheldt estuary in Belgium to evaluate historical growth; results signified the importance of considering temporal variations in SSC in the marsh

rather than a constant SCC, which led to an underestimation in growth. Rybczyk and Cahoon (2002) developed a cohort modeling approach to simulate sediment dynamics (accretion, decomposition, compaction and belowground productivity) and sediment height to determine marsh elevation. Biomass productivity was calculated using a coupled productivity and sediment dynamic model, while changes in decomposition, root distribution, sediment compaction, peat characteristics and marsh surface elevation were incorporated. An application of the model to two marshes in Louisiana, U.S., revealed that the model was most sensitive to changes in the rates of deep subsidence. Under the current rate of SLR, the marsh surface elevation at both sites would fall below mean sea level over the next 100 years. Stralberg et al. (2011) developed a hybrid modeling approach that involved a process-based model of accumulation, which included feedback mechanisms between elevation and sediment inputs to simulate accretion dynamics under climate change scenarios. However, the model lacked a hydrodynamic component to allow for spatial sediment transport. The model was applied to San Francisco Bay, U.S., and although it provided insight into marsh responses to SLR, the authors concluded that a high-resolution, process-based model coupled with a broad-scale spatial model incorporating hydrodynamics would be ideal. Numerical simulations using a one-dimensional marsh evolution model by Mariotti and Fagherazzi (2010) illustrated that low rates of SLR increase wave dissipation and sediment deposition, whereas high rates cause wave driven erosion and recession of the marsh shoreline. The authors suggest that as edge erosion increases, salt marshes will be wedged between increasing sea levels seaward, and increasing urbanization landward.

Ecosystem-based landscape models have also been developed to forecast effects of SLR on marsh systems. This goal of this modeling approach is to simulate the dynamic and spatial behaviors of

systems, taking into account important landscape variables such as ecosystem type, water flows, sedimentation, subsidence, salinity, productivity, nutrients and elevation (Sklar et al., 1985). These models are beneficial because they can be applied with high-resolution to large domains. Interactions of organisms (such as plants) with the surrounding environment are considered with either direct or indirect calculations. A direct calculation model allows for feedback mechanisms by calculating hydrodynamics and biological processes simultaneously. An indirect calculation model computes hydrodynamics first, and then uses model outputs to simulate biological processes. The benefit of these models is that they are often easy to implement and require less computational time than direct calculation models (Fagherazzi et al., 2012). Costanza et al. (1990) developed the Coastal Ecological Landscape Spatial Simulation (CELSS) model which incorporated forcing factors such as subsidence, SLR, river discharge and climate variability to determine marsh productivity at 1 km resolution. Hydrodynamics were approximated using a mass balance approach, which the authors recognized were not accurate for short term simulations. The model was applied to the Atchafalaya marsh in Louisiana, U.S., to determine marsh productivity under various SLR scenarios. Results indicated net gains in land under a rate of SLR equal to twice the eustatic rate, whereas higher rates drowned the marsh out. The authors concluded that healthy marshes with adequate sediment inputs can act as a buffer against moderate rates of SLR. Using the CELSS framework, Reyes et al. (2000) developed The Barataria-Terrebonne ecological landscape spatial simulation (BTELSS) model to predict future trends in marsh productivity under SLR, river discharge changes and climate variability in the Mississippi Delta, U.S. Hydrodynamic calculations were improved by incorporating a two-dimensional vertically integrated hydrodynamic module. This allowed biomass productivity to be simulated with a daily time step

at a resolution of 1 km². Other direct calculation models include those of Martin et al. (2002) and Reyes et al. (2004a). Based on Reyes et al. (2000), Reyes et al. (2004b) compared projected marsh losses under SLR for the Atchafalaya delta and the Barataria Basin in Louisiana. Under a SLR rate double that of the current, fresh and brackish marsh loss was between 30% and 50% for the two marshes. However, in a scenario with increased river discharge, losses were reduced as a result of additional nutrient and sediment input to the marshes.

One of the most well-known indirect calculation models is SLAMM (Sea Level Affecting Marshes Model), a spatial model that simulates dominant processes associated with wetland conversion to simulate the effects of SLR on productivity. The model considers the effects of SLR on inundation, erosion, overwash, salinity and soil saturation. Although the model is capable of simulating broad-scale spatial patterns it is unable to accurately model elevation and sediment dynamic feedbacks or crucial local processes (Craft et al., 2009). Using field and laboratory measurements in conjunction with SLAMM modeling, Craft et al. (2009) found that tidal marshes at lower and upper salinity ranges will be most affected with accelerated SLR, unless vertical accretion can allow marshes to migrate inland or keep pace with SLR.

2.5 Synergetic Studies of Sea Level Rise

Recently, more studies have aimed to incorporate multiple coastal processes to achieve a more holistic evaluation of the effects of SLR on coastal environments. Incorporating changes in land use/land cover (LULC) and coastal morphology in conjunction with SLR into hydrodynamic modeling allows for an improved understanding of the coastal response under future scenarios. For example, Bilskie et al. (2014) investigated the interaction between changes in LULC,

topography, and coastal flooding under past (1960), and present (2005) sea levels and shoreline positions, as well as under projections of future LULC and sea levels (2050) along the Mississippi and Alabama coast. To examine the nonlinear interaction and sensitivity of storm surge to the changes in landscape and sea level, the authors developed the Normalized Nonlinearity (NNL) Index:

$$NNL = \frac{\eta_2 - \eta_1 - \lambda}{\lambda} = \frac{\eta_2 - \eta_1}{\lambda} - 1 \quad (2)$$

where η_2 and η_1 are the maximum generated surges for the lower and higher sea levels, given an amount of SLR. Historic changes in the nearshore topography both amplified and reduced storm surge depending on location. Projections of future urbanization amplified maximum storm surge by 70% more than the applied SLR scenario. The authors recommend considering future landscape changes including LULC and coastal morphology, in addition to altering the sea level for a more comprehensive assessment of future flood inundation. Furthermore, Passeri et al. (2015) tested the sensitivity of a hydrodynamic model to projected shoreline changes and SLR along the Florida Panhandle. The projected shoreline changes had variable influences on tidal and storm surge hydrodynamics, including minimal changes in tidal prisms, increased barrier island overtopping during storm events, and increased volumes of storm surge in back-bays. It was concluded that the sensitivity of individual areas to projected shoreline changes should be assessed for a better evaluation of the effects of SLR on the coastal environment.

The effects of landscape changes and SLR on coastal flooding have also been examined in a tidally influenced river in Malaysia to observe modifications in the hydrodynamic behavior. Overall, SLR

was found to increase the river's peak stage level, and either increase or decrease peak velocities, depending on location. The results were compared with flooding scenarios that included runoff under past and present land cover conditions. Urbanization and increased runoff were found to have a greater impact on the hydrodynamics in the river than SLR alone (Sathiamurthy, 2013). Consideration of future landscape scenarios is also beneficial when evaluating future project proposals under SLR. Cobell et al. (2013) simulated hypothetical hurricanes to analyze storm surge and wind waves under current and future conditions in Louisiana, where future conditions implemented SLR, changes in landscape elevations due to subsidence and accretion, bottom roughness changes due to vegetation changes, and proposed hurricane protection projects such as levees and landscape restorations. All future scenarios that did not consider protection showed increased inland inundation, and increased significant wave heights in areas with higher water depths. Levees protected areas landward of the structure, but increased surge in areas seaward. Restored landscapes provided wave attenuation but had minimal effects on surge reduction. Accretion and increased vegetation due to sediment diversions dampened waves and surge and protected inland areas.

Marsh and hydrodynamic processes have also been integrated to simulate the dynamics within each process and observe changes in marsh productivity under SLR. Hagen et al. (2013) investigated the impacts of SLR on a salt marsh system in the St. Johns River, FL using a two-dimensional hydrodynamic model coupled with a zero-dimensional marsh model. Changes in the governing parameters of biomass productivity (MHW and MLW) under conservative (0.15 m) and modest (0.30 m) SLR scenarios were observed. The hydrodynamic simulations showed that MHW and MLW responded nonlinearly, elevating by amounts unequal to the amount of SLR; MLW was

elevated by less than the SLR, and MHW was elevated by more than the SLR, especially within the tidal creeks. The variability in MHW and MLW significantly affected the distribution of biomass productivity over the marsh. Without accretion, biomass productivity decreased, whereas with accretion, the marsh was able to maintain its productivity. Improving on this methodology, *Alizad et al.*, [manuscript in review, 2014] enhanced the coupled model to incorporate inorganic and organic marsh platform accretion, as well as changes in biomass density through biological feedback mechanisms. Nonlinear SLR scenarios are captured using a “coupling time step”, which incrementally advances and updates the solution. The model was applied to the same salt marsh system in the St. Johns River, FL to simulate biomass productivity under low (0.11 m) and high (0.48 m) SLR scenarios for the year 2050. On average, biomass density increased by 54% under the low SLR scenario, but declined by 21% under the high SLR scenario [*Alizad et al.*, *A coupled two-dimensional hydrodynamic marsh model with biological feedback*, in review at *PLoS ONE*, 2014].

Including coastal processes that modify morphology for delineating future inundation under SLR is difficult due to the lack of reliable models that predict erosion and accretion in response to SLR (Zhang, 2011). Ding (2012) used an integrated model to simulate hydrodynamic and morphologic responses to SLR scenarios during a storm event in the Tochien Estuary, Taiwan. Results indicated changes in erosion/deposition in areas due to SLR, and the model was considered to be effective for simulating nonlinear and unsteady hydrodynamic and morphodynamic processes in coastal areas under SLR scenarios. Using a two-dimensional hydrodynamic model coupled with a morphological scale factor to update bed morphology, Dissanayake et al. (2012) simulated the effects of SLR over a 110 year period in a large inlet/basin system. Applying a morphological

scale factor instead of a conventional morphodynamic model allowed for dynamic simulations of morphology and hydrodynamics to be accomplished at a reasonable computational cost. Model results indicated that the existing flood dominance of the system increases as SLR rates increase, which causes the ebb-tidal delta to erode and the basin to accrete. Erosion and accretion rates were positively correlated with the rate of SLR, and under the highest scenario the tidal flats eventually drowned out.

2.6 Additional Considerations

2.6.1 Additional Coastal Dynamics

Although not a main focus of this review, hydrologic changes and saltwater intrusion into groundwater should also be considered in future synergetic studies, as they contribute to changes in coastal landscapes and ecosystems. Increased rainfall intensity and temporal shifts of extreme rainfall events under climate change have the potential to increase flooding, and sediment and nutrient loading into estuaries, especially under SLR (Gordon et al., 1992; Wang et al., 2013). Runoff has the potential to increase sediment loading in river systems depending on the rainfall intensity, slope, soil, and LULC; increased sediment loading aids in salt marsh survival under SLR (Defersha and Melesse, 2012). Therefore, there is a need for integrated models that not only capture the dynamic effects of SLR on biomass productivity, but also include runoff impacts on sediment deposition in marsh systems.

Changes in precipitation patterns across the coastal watershed may modify the magnitude of aquifer discharge to the sea, inducing saltwater intrusion, which can be exacerbated under SLR.

Saltwater intrusion, or the infringement of coastal saltwater into fresh groundwater in the coastal aquifer regime, may penetrate landward as the sea level rises. The magnitude and rate of migration is a function of local hydrogeologic variables such as aquifer thickness, rate of recharge, hydraulic conductivity, groundwater discharge rate to the estuary, as well as anthropogenic actions such as over pumping and increase in paved areas from urbanization (Werner and Simmons, 2009; Chang et al., 2011). The landward migration of the saltwater fringe may impact the coastal ecosystem via nearshore and/or large-scale submarine discharge patterns and nutrient loading levels (Li et al., 1999; Robinson et al., 2007; Chang et al., 2011). Despite qualitative claims that saltwater intrusion may be exacerbated under SLR, quantitative studies are limited and are typically focused on site-specific observations or numerical studies, making it difficult to draw general conclusions (Werner and Simmons, 2009). Similarly, few studies have examined the combined effects of climate change and anthropologic impacts on saltwater intrusion (Chang et al., 2011).

In addition, the dynamic effects of SLR discussed herein should be considered in biologic assessments of SLR (e.g., oysters, sea turtles, shorebirds, and beach mice). Until recently, biological assessments have mostly focused on the effects of rising temperatures, precipitation changes, and extreme weather events rather than the effects of SLR. The impacts of SLR have the potential to be one of the greatest causes of global species extinctions and ecosystem disruption in the upcoming decades and centuries (Noss, 2011). Anthropogenic and climate change stressors often interact synergistically; therefore, integrated assessments of processes that threaten coastal species are needed for conservation efforts (Reece et al., 2013). Biological assessments should also implement a synergetic approach, considering alterations in hydrodynamic patterns, sediment transport, shoreline erosion, marsh migration/loss, and hydrologic changes.

2.6.2 Socioeconomic Considerations

Future socioeconomic change is potentially equally as significant as future climate change when evaluating impacts and mitigation strategies (Brown et al., 2011). Future socioeconomic conditions are a fundamental driver in influencing changes in coastal systems with and without climate change. Although SLR-driven impacts to coastal wetlands could potentially be significant, human induced direct and indirect effects may be much larger based on existing trends (Nicholls, 2004). If future SLR does not occur, the number of people flooded per year would still change depending on socio-economic changes such as growing populations and the desire to live in coastal areas (Nicholls and Tol, 2006). Human-induced changes including coastal defenses, wetland destruction, ports and harbors, reduced sediment supply to dams, drainage and groundwater withdrawal have convoluted the effects of climate-induced SLR during the 20th century. However, these effects are so extensive that they necessitate more systematic studies to better establish mitigation and adaptation strategies (Nicholls and Cazenave, 2010).

Socioeconomic impacts of SLR can be characterized as follows: (1) direct loss of economic, ecological, cultural and subsistence values as a result of loss of lands, infrastructure and habitats (2) increased flood risk to people, land, infrastructure and the previously discussed values (3) impacts related to water management, salinity and biological activities (Klein and Nicholls, 1999). Until recently, socioeconomic assessments have mostly focused on the coastal zone, economic effects, and considered SLR alone without other climate changing variables (IPCC, 2007). Assessments are now considering the combined effects of climate change variables and SLR, including changes in precipitation, temperature and extreme events (e.g., Houser et al. (2014)).

Numerous studies dating back to the early 1990s have examined the socioeconomic cost of SLR (Turner et al., 1995; Yohe et al., 1996; Yohe and Schlesinger, 1998; West et al., 2001; Nicholls and Tol, 2006; Hallegatte et al., 2011; Hallegatte et al., 2013; Hinkel et al., 2014). Early studies evaluated economic loss in terms of property value that was susceptible to SLR as well as estimates of protection costs (IPCC, 2001). Recent studies have expanded analyses to include impacts to coastal businesses, coastal erosion, loss of wetland value, consumer surplus losses, etc. (Wei and Chatterjee, 2013). As sea levels rise in the 21st century and socioeconomic development increases within coastal floodplains, flood damages are also expected to escalate. Considering future socioeconomic changes in addition to SLR, it is estimated that 0.2% to 4.6% of the global population will experience flooding annually in 2100 with a SLR of 25 cm to 123 cm without adaptation; global gross domestic product is expected to have a 0.3% to 9.3% annual loss (Hinkel et al., 2014). Projecting future socioeconomic changes alone, average global flood losses are projected to increase to \$52 billion per year by 2050, compared to \$6 billion per year estimated in 2005. If adaptation investments keep flooding probability constant, subsidence and SLR will still increase global flood losses to \$60 - \$63 billion per year in 2050 (Hallegatte et al., 2013). More studies estimating future damages and adaptation costs are essential for designing strategies to mitigate and adapt to increased coastal flooding (Hinkel et al., 2014).

2.6.3 *Managing Future Risk*

Regional and local managers are responsible for planning and responding to threats such as SLR (Gilmer et al., 2011). Planning for changes under future sea levels may require a more active role from managers to protect estuaries and natural systems (Nicholls et al., 1995). Many coastal

communities are not equipped for increases in extreme flooding frequency. Although large uncertainties in cyclone climatology, SLR, and morphology make planning difficult for coastal planners and policy makers, the high probability of increased flooding justifies preparations. Changes in sediment supply, and subsidence induced by groundwater, oil and gas extraction should also be considered, especially along barrier coasts and deltaic systems (Woodruff et al., 2013).

There are two potential responses to SLR: mitigation and adaptation. Mitigation is a global-scale activity whereas adaptation is sub-global (local to national scale); therefore SLR assessments need to operate on multiple scales. In coastal areas, the goal of mitigation is to reduce the risk of passing irreversible thresholds regarding major ice sheet breakdown, and limit the rate of SLR to be adaptable at reasonable economic and social costs. Adaptation involves strategies responding to both mean and extreme rises in sea level (Church et al., 2010). Adaptation can be accomplished with protection, accommodation, or planned retreat; choosing a viable option is both a technical and sociopolitical decision depending on which avenue is desirable, affordable, and sustainable in the long-term. Due to the uncertainties regarding the impacts of SLR, an improved understanding of the various adaptation strategies is necessary, as adaptation is one of the most influential elements discerning between impacts actually occurring rather than potentially occurring (Nicholls and Cazenave, 2010). It has been proposed that the most reasonable response to SLR involves a combination of adaptation strategies to handle the inevitable rise and mitigation strategies to restrict the long-term rise to a manageable level (Nicholls et al., 2007).

Quantification of the dynamic effects of SLR on inundation extents as well as social, economic and ecologic impacts will aid in creating comprehensive policies to reduce the risks associated

with future SLR (Zhang, 2011). There is a need for more integrated responses and management strategies that consider a balance between protecting socioeconomic activity and ecology in the coastal zone under rising seas (Nicholls and Klein, 2005; Church et al., 2010). Assessments of SLR impacts and responses within a coastal management context will address all of the potential drivers of change within the coastal zone (Church et al., 2010).

2.7 Conclusions

This review has examined the dynamic effects associated with SLR through various studies in the context of hydrodynamics, coastal morphology and marsh ecology. Hydrodynamic response to SLR is dynamic, with nonlinear changes in parameters such as tidal ranges, tidal prisms, tidal asymmetries, increased flooding depths and inundation extents during storm events. Coastal morphology strives to achieve equilibrium as sea levels rise, which may significantly reshape the coastal landscape. Marsh productivity is a function of tidal inundation and elevation; sediment accumulation and migration are vital aspects in marsh survival under future SLR. The studies discussed herein employ more complex approaches rather than the “bathtub” approach to account for the dynamic responses of the coastal system. Although these studies provide an improved understanding of the effects of SLR on coastal environments, synergetic studies that integrate multiple system dynamics allow for more comprehensive evaluations. These present and future dynamic, integrated studies can contribute to an overall paradigm shift in how coastal scientists and engineers approach SLR modeling, transitioning away from the “bathtub” approach.

Based on the above review, a number of current research needs are summarized:

1. A critical review comparing various hydrodynamic models used to simulate SLR and an established framework for incorporating SLR into hydrodynamic models. This will provide a more uniform methodology that can be applied to various models to produce better evaluations of the effects of SLR on hydrodynamics.
2. A more quantitative understanding of shoreline response to SLR. Long-term monitoring of shorelines and more efficient morphological models will improve understanding of shoreline dynamics and give insight to how higher seas may reshape the coast. Furthermore, since barrier islands are particularly vulnerable to SLR, a fifth tropical cyclone impact regime, namely “Recession” should be considered because of its unique effects on short-term morphology and post-event hydrodynamics.
3. More economic-cost evaluations considering the various dynamics of SLR. Presently, most studies only focus on the effects of SLR inundation without incorporating future changes to the landscape (such as shoreline erosion), which may alter projected costs.
4. Additional studies incorporating the impacts of human induced changes such as coastal defenses, wetland destruction, ports and harbors, reduced sediment supply to dams, drainage and groundwater fluid withdrawal. Understanding how these changes might affect coastal systems during normal and extreme conditions will aid in management decision making and adaptation planning.
5. A better understanding of feedback processes between the physical and ecological environment under SLR. Little work has examined the interactions and feedbacks

between coastal systems under SLR and climate change (e.g., hydrodynamics, marsh ecology, coastal morphology, hydrologic changes, and saltwater intrusion into groundwater). To make more informed decisions on adaptation planning, a holistic understanding of these synergetic processes is needed.

6. Integration of socio-economic implications into the overall synergistic process. At present, the vast majority of socio-economic evaluations are performed after the physical and process-based assessments are completed. Incorporating this human element will ultimately influence future management and planning activities.

2.8 Acknowledgments

This research was funded in part under Award No. NA10NOS4780146 from the National Oceanic and Atmospheric Administration (NOAA) Center for Sponsored Coastal Ocean Research (CSCOR). The authors would like to thank A. Warnock for her constructive comments. The statements and conclusions are those of the authors and do not necessary reflect the views of NOAA-CSCOR or their affiliates.

2.9 References

- Atkinson, J. H., Smith, J. M. and Bender, C. (2013). "Sea-level rise effects on storm surge and nearshore waves on the Texas coast: influence of landscape and storm characteristics." *Journal of Waterway, Port, Coastal, and Ocean Engineering* 139(2): 98-117.
- Aubrey, D. G. and Speer, P. E. (1985). "A study of non-linear tidal propagation in shallow inlet/estuarine systems part I: Observations." *Estuarine, Coastal and Shelf Science* 21: 185-205.

- Bilskie, M. V., Hagen, S. C., Medeiros, S. C. and Passeri, D. L. (2014). "Dynamics of sea level rise and coastal flooding on a changing landscape." *Geophysical Research Letters* 41(3): 927-234.
- Blanton, J., Lin, G. and Elston, S. (2002). "Tidal current asymmetry in shallow estuaries and tidal creeks." *Continental Shelf Research* 22: 1731-1743.
- Boon, J. D. and Byrne, R. J. (1981). "On basin hypsometry and the morphodynamic response of coastal inlet systems." *Marine Geology* 40: 27-48.
- Brown, S., Nicholls, R., Vafeidis, A., Hinkel, J. and Watkiss, P. (2011). "The impacts and economic costs of sea level rise on coastal zones in the EU and the costs and benefits of adaptation. Summary of Results from the EC RTD ClimateCost Project.". The ClimateCost Project. Final Report. P. Watkiss. **Volume 1: Europe.**
- Bruun, P. (1954). "Coast Erosion and the Development of Beach Profiles ". Beach Erosion Board.
- Bruun, P. (1962). "Sea-level rise as a cause of shore erosion." *Proceedings of the American Society of Civil Engineers, Journal of the Waterways and Harbors Division* 88: 117-130.
- Cahoon, D. R., Reed, D. J., Day, J. W., Steyer, G. D., Boumans, R. M., Lynch, J. C., McNally, D. and Latif, N. (1995). "The influence of Hurricane Andrew on sediment distribution in Louisiana coastal marshes." *Journal of Coastal Research* SI(21): 2890-2294.
- Cazenave, A. and Le Cozannet, G. (2013). "Sea level rise and its coastal impacts." *Earth's Future* 2: 15-34.
- Chang, S. W., Clement, T. P., Simpson, M. J. and Lee, K. (2011). "Does sea-level rise have an impact on saltwater intrusion?" *Advances in Water Resources* 34: 1283-1291.
- Chini, N., Stansby, P., Leake, J., Wolf, J., Roberts-Jones, J. and Lowe, J. (2010). "The impact of sea level rise and climate change on inshore wave climate: a case study for east Anglia (UK)." *Coastal Engineering* 57: 973-984.
- Christie, M. C., Dyer, K. R. and Turner, P. (1999). "Sediment flux and bed level measurements from a macro tidal mudflat." *Estuarine, Coastal and Shelf Science* 49: 667-688.
- Church, J. A., Clark, P. U., Cazenave, A., Gregory, J. M., Jevrejeva, S., Levermann, A., Merrifield, M. A., Milne, G. A., Nerem, R. S., Nunn, P. D., Payne, A. J., Pfeffer, W. T., Stammer, D. and Unnikrishnan, A. S. (2013). Sea Level Change. Climate Change 2013: The Physical Science Basis. Contribution of Working Group I to the Fifth Assessment Report of the Intergovernmental Panel on Climate Change. T. F. Stocker, D. Qin, G.-K. Plattner et al. Cambridge, United Kingdom and New York, NY, USA, Cambridge University Press.

- Church, J. A., et. al. (2001). "Changes in sea level". Climate Change 2001: The Scientific Basis. J. T. Joughton, Y. Ding, D. J. Griggs et al. New York: 639-694.
- Church, J. A. and White, N. J. (2006). "A 20th century acceleration in global sea-level rise." *Geophys. Res. Lett.* 33(1): L01602.
- Church, J. A. and White, N. J. (2011). "Sea-level rise from the late 19th to early 21st century " *Surveys in Geophysics* 32(4-5): 585-602.
- Church, J. A., Woodworth, P. L., Aarup, T. and Wilson, W. S. (2010). Understanding sea level rise and variability. UK, Wiley-Blackwell.
- Cobell, Z., Zhao, H., Roberts, H. J., Clark, F. R. and Zou, S. (2013). "Surge and wave modeling for Louisiana 2012 coastal master plan." *Journal of Coastal Research* SI(67): 88-108.
- Cooper, J. A. G. and Pilkey, O. H. (2004). "Sea-level rise and shoreline retreat: time to abandon the Bruun Rule." *Global and Planetary Change* 43(3-4): 157-171.
- Costanza, R., Sklar, F. H. and White, M. L. (1990). "Modeling coastal landscape dynamics." *BioScience* 40(2): 91-107.
- Cowell, P. J. and Kench, P. S. (2001). "The morphological response of atoll islands to sea level rise. Part 1: Modifications to the shoreface translation model." *Journal of Coastal Research* SI(34, (ICS 2000 New Zealand)): 633-344.
- Cowell, P. J., Roy, P. S. and Jones, R. A. (1995). "Simulation of large-scale coastal change using a morphological behaviour model." *Marine Geology* 126: 45-61.
- Cowell, P. J., Stive, M. J. F., Niedoroda, A. W., De Vriend, H. J., Swift, D. J. P., Kaminsky, G. M. and Capobianco, M. (2003a). "The coastal tract: Part 1: A conceptual approach to aggregated modelling of low-order coastal change." *Journal of Coastal Research* 19: 812-827.
- Cowell, P. J., Stive, M. J. F., Niedoroda, A. W., Swift, D. J. P., De Vriend, H. J., Buisjman, M. C., Nicholls, R. J., Roy, P. S. and Co-authors (2003b). "The coastal tract. Part 2: Applications of aggregated modelling of lower-order coastal change." *Journal of Coastal Research* 19: 828-848.
- Cowell, P. J. and Thom, B. G. (1994). Morphodynamics of coastal evolution. Coastal evolution: late quaternary shoreline morphodynamics. R. W. G. Carter and C. D. Woodroffe. Cambridge, Cambridge University Press: 33-86.

- Cowell, P. J., Thom, B. G., Jones, R. A., Everts, C. H. and Simanovic, D. (2006). "Management of uncertainty in predicting climate-change impacts on beaches." *Journal of Coastal Research* 22: 232-245.
- Cowell, P. J. and Zeng, T. Q. (2003). "Integrating uncertainty theories with GIS for modeling coastal hazards of climate change." *Marine Geology* 126: 5-8.
- Craft, C., Clough, J., Ehman, J., Joye, S., Park, R., Pennings, S., Guo, H. and Machmuller, M. (2009). "Forecasting the effects of accelerated sea-level rise on tidal marsh ecosystem services." *Front Ecol Environ* 7(2): 73-78.
- Crowell, M., Douglas, B. C. and Leatherman, S. P. (1997). "On Forecasting Future U.S. Shoreline Positions: A Test of Algorithms." *Journal of Coastal Research* 13(4): 1245-1255.
- Crowell, M. and Leatherman, S. P. (1999). "Coastal Erosion Mapping and Management." *Journal of Coastal Research* 28 (Special Issue): 196.
- Curry, J. R. (1964). Transgressions and regressions. Papers in Marine Geology-Shepard Commemorative Volume. R. L. Miller. New York, MacMillan and Co.: pp. 175-203.
- Davidson-Arnott (2005). "Conceptual model of the effects of sea level rise on sandy coasts." *Journal of Coastal Research* 21(6): 1166-1172.
- Davis, R. A. (1995). "Geological impact of Hurricane Andrew on Everglades coast of southwest Florida." *Environmental Geology* 25: 143-148.
- Davis, R. A. and Hayes, M. O. (1984). "What is a wave dominated coast?" *Marine Geology* 60: 313-329.
- Dean, R. G. (1991). "Equilibrium Beach Profiles: Characteristics and Applications." *Journal of Coastal Research* 7(1): 53-84.
- Dean, R. G. and Dalrymple, R. A. (2002). Coastal Processes with Engineering Applications. Cambridge, Cambridge University Press.
- Dean, R. G. and Maurmeyer, E. M. (1983). Models for beach profile response. Handbook of coastal processes and erosion. P. D. Komar. Boca Raton, FL, CRC Press: pp. 151-166.
- DECCW (2010). "Draft Guidelines for preparing Coastal Zone Management Plans", NSW Department of Environment, Climate Change and Water.
- Defersha, M. B. and Melesse, A. M. (2012). "Effect of rainfall intensity, slope and antecedent moisture content on sediment concentration and sediment enrichment ratio." *CATENA* 90(0): 47-52.

- Department of Environmental and Heritage Protection (2013). "Coastal Hazard Technical Guide, Determining Coastal Hazard Areas", The State of Queensland.
- Dias, J. M. and Picado, A. (2011). "Impact of morphologic anthropogenic and natural changes in estuarine tidal dynamics." *Journal of Coastal Research* SI(64 (Proceedings of the 11th International Coastal Symposium)): 1490-1494.
- Ding, Y. (2012). Sea-level rise and hazardous storms: impacts on coasts and estuaries. Handbook of climate change mitigation. W. Y. Chen, J. Seiner, T. Suzuki and M. Lackner, Springer Science+Business Media, LLC.
- Ding, Y., Nath Kuiry, S., Elgohry, M., Jia, Y., Altinakar, M. S. and Yeh, K. (2013). "Impact assessment of sea-level rise and hazardous storms on coasts and estuaries using integrated processes model." *Ocean Engineering* 71: 74-95.
- Dissanayake, D. M. P. K., Ranasinghe, R. and Roelvink, J. A. (2012). "The morphological response of large tidal inlet/basin systems to relative sea level rise." *Climatic Change* 113: 253-276.
- Fagherazzi, S., Kirwin, M. L., Mudd, S. M., Gunetenspergen, G. R., S., T., D'Alpaos, A., van de Koppel, J., Rybczyk, J. M., Reyes, E., Craft, C. and Clough, J. (2012). "Numerical models of salt marsh evolution: ecological, geomorphic and climatic factors." *Reviews of Geophysics* 50(RG1002).
- Fenster, M. S., Dolan, R. and Elder, J. F. (1993). "A new method for predicting shoreline positions from historical data." *Journal of Coastal Research* 9(1): 147-171.
- Fitzgerald, D. M., Fenster, M. S., Argow, B. A. and Buynevich, I. V. (2008). "Coastal Impacts Due to Sea Level Rise." *Annual Review Earth Planet Science* 36: 601-647.
- Francalanci, S., Bondoni, M., Rinaldi, M. and Solari, M. (2013). "Ecomorphodynamic evolution of salt marshes: experimental observations of bank retreat processes." *Geomorphology* 195: 53-65.
- French, J. R. (2008). "Hydrodynamic Modelling of Estuarine Flood Defence Realignment as an Adaptive Management Response to Sea-Level Rise." *Journal of Coastal Research* 24(2B): 1-12.
- French, J. R. and Burningham, H. (2003). "Tidal marsh sedimentation versus sea-level rise: a southeast England estuarine perspective". Coastal Sediments '03: crossing disciplinary boundaries - proceedings of the fifth international symposium on coastal engineering and science of coastal sediment processes. Corpus Christi, USA., East Meets West Productions (EMW): 1-13.

- French, J. R. and Spencer, T. (1993). "Dynamics of sedimentation in a tide-dominated backbarrier salt marsh, Norfolk, UK." *Marine Geology* 110(3-4): 315-331.
- Friedrichs, C. T. and Aubrey, D. G. (1988). "Non-linear tidal distortion in shallow well-mixed estuaries: A synthesis." *Estuarine, Coastal and Shelf Science* 27: 521-545.
- Friedrichs, C. T., Aubrey, D. J. and Speer, P. E. (1990). Impacts of relative sea level rise on evolution of shallow estuaries. Residual current and long-term transport. R. T. Cheng. New York, Springer-Verlag.
- Friedrichs, C. T. and Madsen, O. S. (1992). "Nonlinear diffusion of the tidal signal in frictionally dominated embayments." *Journal of Geophysical Research* 97(C4): 5637-5650.
- Friedrichs, C. T. and Perry, J. E. (2001). "Tidal Salt Marsh Morphodynamics: A Synthesis." *Journal of Coastal Research* SI 27.
- Galgano, F. A. and Douglas, B. C. (2000). "Shoreline position prediction: methods and errors." *Environmental Geosciences* 7(1): 1-10.
- Gilmer, B., Brenner, J. and Sheets, J. (2011). "Informing conservation planning using sea-level rise and storm surge impact estimates in the Grand Bay NERR/NWR area in Mississippi", The Nature Conservancy.
- Goff, J. A., Allison, M. A. and Gulick, S. P. S. (2010). "Offshore transport of sediment during cyclonic storms: Hurricane Ike (2008), Texas Gulf Coast, USA." *Geology* 38: 351-354.
- Gordon, H. B., Whetton, P. H., Pittock, A. B., Fowler, A. M. and Haylock, M. R. (1992). "Simulated changes in daily rainfall intensity due to enhanced greenhouse effect: implications for extreme rainfall events." *Climate Dynamics* 8: 83-102.
- Green, M. O., Black, K. P. and Amos, C. L. (1997). "Control of estuarine sediment dynamics by interactions between currents and waves at several scales." *Marine Geology* 144: 97-116.
- Green, M. O. and Coco, G. (2014). "Review of wave-driven sediment resuspension and transport in estuaries." *Reviews of Geophysics* 52: 77-117.
- Gutierrez, B. T., Plant, N. G. and Thieler, E. R. (2011). "A Bayesian network to predict coastal vulnerability to sea level rise." *Journal of Geophysical Research* 116(FO2009).
- Hagen, S. C. and Bacopoulos, P. (2012). "Coastal Flooding in Florida's Big Bend Region with Application to Sea Level Rise Based on Synthetic Storms Analysis." *Terr. Atmos. Ocean. Sci.* 23: 481-500.

- Hagen, S. C., Morris, J. T., Bacopoulos, P. and Weishampel, J. F. (2013). "Sea-Level Rise Impact on a Salt Marsh System of the Lower St. Johns River." *J. Waterway, Port, Coastal, Ocean Eng.* 139(2): 118-125.
- Hall, M. J., Young, R. S., Thieler, E. R., Priddy, R. D. and Pilkey Jr., O. H. (1990). "Shoreline response to Hurricane Hugo." *Journal of Coastal Research* 6(1): 211-221.
- Hallegatte, S., Green, C., Nicholls, R. J. and Corfee-Morlot, J. (2013). "Future flood losses in major coastal cities." *Nature Clim. Change* 3: 802-806.
- Hallegatte, S., Patmore, N., Mestre, O., Dumas, P., Corfee-Morlot, J., Herweijer, C. and Muir-Wood, R. (2011). "Assessing Climate Change Impacts, Sea Level Rise and Storm Surge Risk in Port Cities: A Case Study on Copenhagen." *Climatic Change* 104: 113-137.
- Hands, E. B. (1983). The Great Lakes as a test model for profile responses to sea level changes. CRC handbook of coastal processes and erosion. P. D. Komar. Boca Raton, FL, CRC Press: 167-189.
- Hanson, H. (1989). "Genesis - A Generalized Shoreline Change Numerical Model." *Journal of Coastal Research* 5(1): 1-27.
- Hapke, C. and Plant, N. (2010). "Predicting coastal cliff erosion using a Bayesian probabilistic model." *Marine Geology* 278: 140-149.
- Hay, C. C., Morrow, E., Kopp, R. E. and Mitrovica, J. X. (2015). "Probabilistic reanalysis of twentieth-century sea-level rise." *Nature* 517: 481-484.
- Hayes, M. O. (1979). Barrier island morphology as a function of tidal and wave regime. Barrier Islands. S. P. Leatherman. New York, NY, Academic Press: pp. 1-27.
- Hayes, M. O. and Fitzgerald, D. M. (2013). "Origin, Evolution and Classification of Tidal Inlets." *Journal of Coastal Research* 69: 14-33.
- Hinkel, J., Lincke, D., Vafeidis, A. T., Perrette, M., Nicholls, R. J., Tol, R. S. J., Marzeion, B., Fettweis, X., Ionescu, C. and Levermann, A. (2014). "Coastal flood damage and adaptation costs under 21st century sea-level rise." *Proceedings of National Academy of Science*.
- Hoitink, A. J. F., Hoekstra, P. and Van Maren, D. S. (2003). "Flow asymmetry associated with astronomic tides: implications for the residual transport of sediment." *Journal of Geophysical Research* 108(C10): 3315.
- Houser, T., Kopp, R., Hsiang, S., Muir-Wood, R., Larsen, K., Delgado, M., Jina, A., Wilson, P., Mohan, S., Rasmussen, D. J., Mastrandrea, M. and Rising, J. (2014). "American Climate Prospectus: Economic Risks in the United States". Oakland: Rhodium Group.

- Houston, J. R. (2013). "The economic value of beaches - a 2013 update." *Shore and Beach* 81(1): 3-11.
- IPCC (2001). "Climate Change 2001: Impacts, Adaptation & Vulnerability: Contribution of Working Group II to the Third Assessment Report of the IPCC". J. J. McCarthy, O. F. Canziani, N. A. Leary, D. J. Dokken and K. S. White. Cambridge, UK, Cambridge University Press: 1000.
- IPCC (2007). "Climate Change 2007: Impacts, Adaptation and Vulnerability. Contribution of Working Group II to the Fourth Assessment Report of the IPCC". M. L. Parry, O. F. Canziani, J. P. Palutikof, P. J. van der Linden and C. E. Hanson. Cambridge, UK, Cambridge University Press: 967.
- Jackson, N. L., Nordstrom, K. F., Eliot, I. and Masselink, G. (2002). "'Low energy' sandy beaches in marine and estuarine environments: a review." *Geomorphology* 48: 147-162.
- Jevrejeva, S., Grinsted, A., Moore, J. and Holgate, S. (2006). "Nonlinear trends and multiyear cycles in sea level records." *Journal of Geophysical Research* 111.
- Jevrejeva, S., Moore, J. C., Grinsted, A. and Woodworth, P. L. (2008). "Recent global sea level acceleration started over 200 years ago?" *Geophysical Research Letters* 35(L08715).
- Jewell, S. A., Walker, D. J. and Fortunato, A. B. (2012). "Tidal asymmetry in a coastal lagoon subject to a mixed tidal regime." *Geomorphology* 138: 171-180.
- Kilanehei, F., Naeeni, S. T. O. and Namin, M. M. (2011). "Coupling of 2DH-3D hydrodynamic numerical models for simulating flow around river hydraulic structures." *World Applied Sciences Journal* 15(1): 63-77.
- Kirwan, M. L. and Murray, A. B. (2007). "A coupled geomorphic and ecological model of tidal marsh evolution." *Proceedings of National Academy of Science* 104: 6118-6122.
- Kirwin, M. and Temmerman, S. (2009). "Coastal marsh response to historical and future sea-level acceleration." *Quaternary Science Reviews* 28: 1801-1808.
- Klein, R. J. T. and Nicholls, R. J. (1999). "Assessment of coastal vulnerability to climate change." *Ambio* 28(2): 182-187.
- Kopp, R. E., Horton, R. M., Little, C. M., Mitrovica, J. X., Oppenheimer, M., Rasmussen, D. J., Strauss, B. H. and Tebaldi, C. (2014). "Probabilistic 21st and 22nd century sea-level projections at a global network of tide-gauge sites." *Earth's Future* 2: 383-406.

- Krone, R. B. (1987). "A method for simulating historic marsh elevations ". *Coastal Sediments '87*. New York, ASCE.
- Leadon, M. E. (1999). "Beach, Dune and Offshore Profile Response to a Severe Storm Event." *ASCE Coastal Sediments* Long Island, NY.
- Leatherman, S. P. (1990). "Modeling shore response to sea-level rise on sedimentary coasts." *Progress in Physical Geology* 14(4): 447-464.
- Leatherman, S. P., Zhang, K. and Douglas, B. C. (2000). "Sea Level Rise Shown to Drive Coastal Erosion." *EOS Transactions* 81(6).
- Leonard, L. A. and Luther, M. E. (1995). "Flow hydrodynamics in tidal marsh canopies " *Limnology and Oceanography* 40: 1474-1484.
- Leorri, E., Mulligan, R., Mallinson, D. and Cearretta, A. (2011). "Sea-level rise and local tidal range changes in coastal embayments: An added complexity in developing reliable sea-level index points." *Journal of Integrated Coastal Zone Management* 11(3): 307-314.
- Li, L., Barry, D. A., Stagnitti, F. and Parlange, J. Y. (1999). "Submarine groundwater discharge and associated chemical input to a coastal sea." *Water Resources Research* 35(11): 3253-3259.
- Lin, B., Wicks, J. M., Falconer, R. A. and Adams, K. (2006). "Integrating 1D and 2D hydrodynamic models for flood simulation." *Water Management* 159(WMI): 19-25.
- List, J. H., Sallenger, A. H., Hansen, M. E. and Jaffe, B. E. (1997). "Accelerated relative sea level rise and rapid coastal erosion: testing a casual relationship for the Louisiana barrier islands." *Marine Geology* 140: 347-363.
- Mariotti, G. and Fagherazzi, S. (2010). "A numerical model for the coupled long-term evolution of salt marshes and tidal flats." *Journal of Geophysical Research* 115.
- Martin, J. F., Reyes, E., Kemp, G. P., Mashriqui, H. and Day, J. W. (2002). "Landscape modeling of the Mississippi Delta." *BioScience* 52(4): 357-365.
- Martin, J. F., Reyes, E., Kemp, G. P., Mashriqui, H. and Day, J. W. (2002). "Landscape Modeling of the Mississippi Delta: Using a series of landscape models, we examined the survival and creation of Mississippi Delta marshes and the impact of altered riverine inputs, accelerated sea-level rise, and management proposals on these marshes." *BioScience* 52(4): 357-365.
- Masetti, R., Fagherazzi, S. and Montanari, A. (2008). "Application of a barrier island translation model to the millennial-scale evolution of Sand Key, Florida." *Continental Shelf Research* 28: 1116-1126.

- Masselink, G., Hughes, M. G. and Knight, J. (2011). Coastal Processes & Geomorphology. London, UK., Hodder Education.
- McKee, K. L. and Patrick Jr., W. H. (1988). "The relationship of smooth cordgrass (*Spartina Alterniflora*) to total datums: a review." *Estuaries* 11(3): 143-151.
- Möller, I., Spencer, T., French, J. R., Leggett, D. J. and Dixon, M. (1999). "Wave Transformation Over Salt Marshes: A Field and Numerical Modelling Study from North Norfolk, England." *Estuarine, Coastal and Shelf Science* 49(3): 411-426.
- Moore, L. J., McNamara, D. E., Murray, A. B. and Brenner, O. (2013). "Observed changes in hurricane-driven waves explain the dynamics of modern cusped shorelines." *Geophysical Research Letters* 40: 1-5.
- Morris, J. T., Sundareshwar, P. V., Nietch, C. T., Kjerfve, B. and Cahoon, D. R. (2002). "Responses of Coastal Wetlands to Rising Sea Level." *Ecology* 83(10): 2869-2877.
- Morton, R. A. and Miller, T. L. (2005). "National Assessment of Shoreline Change: Part 2, Historical Shoreline Changes and Associated Coastal Land Loss Along the U.S. Southeast Atlantic Coast", USGS: 40p.
- Morton, R. A., Miller, T. L. and Moore, L. J. (2004). "National assessment of shoreline change: Part 1: Historical shoreline changes and associated coastal land loss along the U.S. Gulf of Mexico". Open-file Report 2004-1043. St. Petersburg, Florida, U.S. Geological Survey: 45p.
- Mousavi, M. E., Irish, J. L., Frey, A. E., Olivera, F. and Edge, B. L. (2011). "Global warming and hurricanes: the potential impact of hurricane intensification and sea level rise on coastal flooding." *Climatic Change* 104(3-4): 575-597.
- Mudd, S. M., D'Alpaos, A. and Morris, J. T. (2010). "How does vegetation affect sedimentation on tidal marshes? Investigation particle capture and hydrodynamic controls on biologically mediated sedimentation." *Journal of Geophysical Research* 115.
- National Research Council (1987). Responding to Changes in Sea Level: Engineering Applications. Washington DC, The National Academies Press.
- Nerem, R. S., Chambers, D., Choe, C. and Mitchum, G. T. (2010). "Estimating mean sea level change from the TOPEX and Jason Altimeter Missions." *Marine Geodesy* 33(1): 435.
- Nicholls, R. J. (2004). "Coastal flooding and wetland loss in the 21st century: changes under the SRES climate and socio-economic scenarios." *Global Environmental Change* 14: 69-86.

- Nicholls, R. J. and Cazenave, A. (2010). "Sea-Level Rise and Its Impact on Coastal Zones." *Science* 328(18): 1517-1520.
- Nicholls, R. J. and Klein, R. J. T. (2005). Climate change and coastal management on Europe's coast. Managing European Coasts: Past, Present and Future. J. E. Vermaat, L. Ledoux, K. Turner, W. Salomons and L. Bouwer. London, Springer, Environmental Science Monograph Series.
- Nicholls, R. J., Leatherman, S. P., Dennis, K. C. and Volante, C. R. (1995). "Impacts and responses to sea-level rise: qualitative and quantitative assessments." *Journal of Coastal Research* SI (14): 26-43.
- Nicholls, R. J. and Tol, R. S. J. (2006). "Impacts and responses to sea-level rise: a global analysis of the SRES scenarios over the twenty-first century." *Philosophical Transactions of the Royal Society A* 364: 1073-1095.
- Nicholls, R. J., Wong, P. P., Burkett, V. R., Codignotto, J. O., J.E., H., R.F., M., Ragoonaden, S. and Woodroffe, C. D. (2007). Coastal systems and low-lying areas. Climate Change 2007: Impacts, adaptation, and vulnerability. Contribution of working group II to the Fourth Assessment Report of the Intergovernmental Panel on Climate Change. M. L. Parry, O. F. Canziani, J. P. Palutikof, P. J. van der Linden and C. E. Hanson. Cambridge, Cambridge University.
- Nichols, M. M. (1989). "Sediment accumulate rates and relative sea-level rise in lagoons." *Marine Geology* 88: 201-219.
- Niedoroda, A. W., Reed, C. W., Swift, D. J. P., Arato, H. and Hoyanagi, K. (1995). "Modeling shore-normal large-scale coastal evolution." *Marine Geology* 126: 181-199.
- NOAA (2011). "The Gulf of Mexico at a Glance: A Second Glance". Washington DC: U.S. Department of Commerce, National Oceanic and Atmospheric Administration.
- Noss, R. F. (2011). "Between the devil and the deep blue sea: Florida's unenviable position with respect to sea level rise." *Climatic Change* 107: 1-16.
- Nyman, J. A., Walters, R. J., Delaune, R. D. and Patrick Jr., W. H. (2006). "Marsh vertical accretion via vegetative growth." *Estuarine, Coastal and Shelf Science* 69: 370-380.
- O'Callaghan, J. M., Pattiaratchi, C. B. and Hamilton, D. P. (2010). "The role of intratidal oscillations in sediment resuspension in a diurnal, partially mixed estuary." *Journal of Geophysical Research* 115: C07018.

- Parris, A., Bromirski, P., Burkett, V., Cayan, D., Culver, M., Hall, J., Horton, R., Knuuti, K., Moss, R., Obeysekera, J., Sallenger, A. and Weiss, J. (2012). "Global Sea Level Rise Scenarios for the United States National Climate Assessment". NOAA Tech Memo OAR CPO-1: 37.
- Passeri, D. L., Hagen, S. C., Bilskie, M. V. and Medeiros, S. C. (2015). "On the significance of incorporating shoreline changes for evaluating coastal hydrodynamics under sea level rise scenarios." *Natural Hazards* 75(2): 1599-1617.
- Passeri, D. L., Hagen, S. C. and Irish, J. L. (2014). "Comparison of shoreline change rates along the South Atlantic Bight and Northern Gulf of Mexico coasts for better evaluation of future shoreline positions." *Journal of Coastal Research* In: Huang, W. and Hagen, S.C. (eds.), *Climate Change Impacts on Surface Water Systems* (SI, 68): 20-26.
- Patterson, D. (2009). "Modeling the Shoreline Impacts of Richmond River Training Walls." *Proceedings of the 18th NSW Coastal Conference*.
- Pethick, J. S. (1992). Saltmarsh Geomorphology. Saltmarshes: morphodynamics, conservation and engineering significance. K. Pye. Cambridge, UK., Cambridge University Press: 41-62.
- Phillips, J. D. (1986). "Coastal submergence and marsh fridge erosion." *Journal of Coastal Research* 2: 427-436.
- Postma, H. (1967). Sediment transport and sedimentation in the estuarine environment Estuaries. G. H. Lauff. Washington, DC, American Association for the Advancement of Science: 158-179.
- Pugh, D. T. (1987). Tides, Surges and Mean Sea Level. London, John Wiley and Sons.
- Ralston, D. K. and Stacey, M. T. (2007). "Tidal and meteorological forcing of sediment transport in tributary mudflat channels." *Continental Shelf Research* 27(10-11): 1510-1527.
- Ranasinghe, R., Duong, T. M., Uhlenbrook, S., Roelvink, D. and M., S. (2012). "Climate-change impact assessment for inlet-interrupted coastlines." *Nature Climate Change* 3: 83-87.
- Ranasinghe, R. and Pattiaratchi, C. (2000). "Tidal inlet velocity asymmetry in diurnal regimes." *Continental Shelf Research* 20: 2347-2366.
- Reece, J. S., Passeri, D., Ehrhart, L., Hagen, S., Hays, A., Long, C., Noss, R. F., Bilskie, M., Sanchez, C., Schwoerer, M. V., Von Holle, B., Weishampel, J. and Wolf, S. (2013). "Sea level rise, land use, and climate change influence the distribution of loggerhead turtle nests at the largest USA rookery (Melbourne Beach, Florida)." *Marine Ecology Progress Series* 493: 259-274.

- Reed, D. J. (1990). "The impact of sea level rise on coastal marshes." *Progress in Physical Geology* 14(4): 465-481.
- Reyes, E., Day, J. W., Lara-Dominguez, A. L., Sanchez-Gil, P., Zarate Lomeli, D. and Yanez-Arancibia, A. (2004a). "Assessing coastal management plans using watershed spatial models for the Mississippi delta, USA, and the Ususmacinta-Griljalva delta, Mexico." *Ocean & Coastal Management* 47: 693-708.
- Reyes, E., Martin, J. F., Day, J. W., Kemp, G. P. and Mashriqui, H. (2004b). "River forcing at work: ecological modeling of prograding and regressive deltas." *Wetlands Ecology and Management* 12: 103-114.
- Reyes, E., White, M. L., Martin, J. F., Kemp, G. P. and Day, J. W. (2000). "Landscape modeling of coastal habitat change in the Mississippi Delta." *Ecology* 81(8): 2331-2349.
- Riggs, S. R. and Ames, S. V. (2003). "Drowning the North Carolina Coast: Sea level Rise and Estuarine Dynamics", North Carolina Department of Environmental and Natural Resources, Division of Coastal Management and North Carolina Sea Grant, North Carolina State University.
- Rilo, A., Freire, P., Guerreiro, M., Fortunato, A. B. and Taborda, R. (2013). "Estuarine margins vulnerability to floods for different sea level rise and human occupation scenarios." *Journal of Coastal Research* Special Issue No. 65: 820-825.
- Robinson, C., Li, L. and Prommer, H. (2007). "Tide-induced recirculation across the aquifer-ocean interface." *Water Resources Research* 43(W07428).
- Rosati, J. D., Dean, R. G. and Walton, T. L. (2013). "The modified Bruun Rule extended for landward transport." *Marine Geology* 340: 71-81.
- Rosen, P. S. (1978). "A regional test of the Bruun Rule on shoreline erosion." *Marine Geology* 26: M7-M16.
- Rossington, S. K. (2008). "Modelling Large Scale Estuarine Morphodynamics Using Equilibrium Concepts: Responses to Anthropogenic Disturbance and Climatic Change", University of Southampton. **Dissertation.**
- Rybczyk, J. M. and Cahoon, D. R. (2002). "Estimating the potential for submergence for two wetlands in the Mississippi River Delta." *Estuaries* 25(5): 985-998.
- Sallenger, A. H. J. (2000). "Storm impact scale for barrier islands." *Journal of Coastal Research* 16(3): 890-895.

- Sampath, D. M. R., Boski, T., Silva, P. and Martins, F. A. (2011). "Morphological evolution of the Guadiana estuary and intertidal zone in response to projected sea level rise and sediment supply scenarios." *Journal of Quaternary Science* 26(2): 156-170.
- Sanford, L. P. (1994). "Wave-forced resuspension of upper Chesapeake Bay muds." *Estuaries* 17(1B): 148-165.
- Sathiamurthy, E. (2013). "Potential Effect of Sea Level Rise on Rambai River, Malaysia." *World Applied Sciences Journal* 22(3): 359-367.
- Schile, L. M., Callaway, J. C., Morris, J. T., Stralberg, D., Parker, V. T. and Kelly, M. (2014). "Modeling Tidal Marsh Distribution with Sea-Level Rise: Evaluating the Role of Vegetation, Sediment and Upland Habitat in Marsh Resiliency." *PLoS ONE* 9(2): e88760.
- Schwartz, M. L. (1967). "The Bruun theory of sea level rise as a cause of shore erosion." *Journal of Geology* 73: 528-534.
- Schwartz, M. L. (1987). "The Bruun Rule - twenty years late." *Journal of Coastal Research* 3: ii-iv.
- Sheldon, J. E. and Alber, M. (2006). "The Calculation of Estuarine Turnover Times Using Freshwater Fraction and Tidal Prism Models: A Critical Evaluation." *Estuaries and Coasts* 29(1): 133-146.
- Sklar, F. H., Costanza, R. and Day, J. W. (1985). "Dynamic spatial simulation modeling of coastal wetland habitat succession." *Ecological Modelling* 29: 261-281.
- Small, C. and Nicholls, R. J. (2003). "A global analysis of human settlement in coastal zones." *Journal of Coastal Research* 19(3): 584-599.
- Smith, J. M., Cialone, M. A., Wamsley, T. V. and McAlpin, T. O. (2010). "Potential impact of sea level rise on coastal surges in southeast Louisiana." *Ocean Engineering* 37: 37-47.
- Smith, J. M., Cialone, M. A., Wamsley, T. V. and McAlpin, T. O. (2010). "Potential impact of sea level rise on coastal surges in southeast Louisiana." *Ocean Engineering* 37(37-47).
- Speer, P. E. and Aubrey, D. G. (1985). "A study of non-linear tidal propagation in shallow inlet/estuarine systems II: theory." *Estuarine, Coastal and Shelf Science* 21: 207-224.
- Stevens, S. (2010). "Estuarine Shoreline Response to Sea Level Rise". Prepared for Lake Macquarie City Council.

- Stive, M. J. F., Capobianco, M., Wang, Z. B., Ruol, P. and Buisjman, M. C. (1998). "Morphodynamics of a tidal lagoon and the adjacent coast". Eighth International Biennial Conference on Physics of Estuaries and Coastal Seas. The Hague: +8-407.
- Stive, M. J. F. and De Vriend, H. J. (1995). "Modelling shoreface profile evolution." *Marine Geology* 126: 235-248.
- Stive, M. J. F., Roelvink, J. A. and De Vriend, H. J. (1990). "Large-scale coastal evolution concept." *Proceedings of 22nd International Conference on Coastal Engineering*, New York, ASCE.
- Stolper, D., List, J. H. and Thieler, E. R. (2005). "Simulating the evolution of coastal morphology and stratigraphy with a new morphological-behavior model (GEOMBEST)." *Marine Geology* 218(1-4): 17-36.
- Storms, J. E. A., Weltje, G. J., van Dijke, J. J., Geel, C. R. and Kroonenberg, S. B. (2002). "Process-response modeling of wave-dominated coastal systems: simulating evolution and stratigraphy on geological timescales." *Journal of Sedimentary Research* 72(2): 226-239.
- Stralberg, D., Brennan, M., Callaway, J. C., Wood, J. K., Schile, L. M., Jongsomjit, D., Kelly, M., Parker, V. T. and Crooks, S. (2011). "Evaluating tidal marsh sustainability in the face of sea-level rise: a hybrid modeling approach applied to San Francisco Bay." *PLoS ONE* 6(11): e27388.
- Stumpf, R. P. (1983). "The process of sedimentation on the surface of a saltmarsh." *Estuarine, Coastal and Shelf Science* 17: 495-508.
- Tagliapietra, D., Sigovini, M. and Volpi Ghirardini, A. (2009). "A review of terms and definitions to categorise estuaries, lagoons and associated environments." *Marine and Freshwater Research* 60: 497-509.
- Temmerman, S., Govers, G., Meir, P. and Wartel, S. (2003). "Modelling long-term tidal marsh growth under changing tidal conditions and suspended sediment concentrations, Scheldt Estuary, Belgium." *Marine Geology* 193: 151-169.
- Thieler, E. R. and Hammar-Klose, E. S. (1999). "National Assessment of Coastal Vulnerability to Sea Level rise: Preliminary Results for the U.S. Atlantic Coast". Woods Hole, Massachusetts, U.S. Geological Survey.
- Thieler, E. R. and Hammar-Klose, E. S. (2000). "National Assessment of Coastal Vulnerability to Sea-Level Rise: Preliminary Results for the U.S. Gulf of Mexico Coast". Woods Hole, MA, U.S. Geological Survey.

- Thieler, E. R., Pikley, O. H., Young, R. S., Bush, D. M. and Chai, F. (2000). "The use of mathematical models to predict beach behavior for coastal engineering: A critical review." *Journal of Coastal Research* 16(1): 48-70.
- Townend, I., Fletcher, C., Knappen, M. and Rossington, K. (2011). "A review of salt marsh dynamics." *Water and Environment Journal* 25: 477-488.
- Turner, R. K., Adger, N. and Doktor, P. (1995). "Assessing the economic costs of sea level rise." *Environment and Planning A* 27(11): 1777-1796.
- Valentim, J. M., Vaz, L., Vaz, N., Silva, H., Duarte, B., Cacador, I. and Dias, J. (2013). "Sea level rise impact in residual circulation in Tagus estuary and Ria de Aveiro lagoon." *Journal of Coastal Research* Special Issue No. 65: 1981-1986.
- Van Goor, M. A., Zitman, T. J., Wang, Z. B. and Stive, M. J. F. (2003). "Impact of sea level rise on the morphological equilibrium state of tidal inlets." *Marine Geology* 202: 211-227.
- van Maren, D. S., Hoekstra, P. and Hoitink, A. J. F. (2004). "Tidal flow asymmetry in the diurnal regime: bed-load transport and morphologic changes around the Red River Delta." *Ocean Dynamics* 54: 424-434.
- Walton, T. L. and Dean, R. G. (2007). "Temporal and Spatial Change in Equilibrium Beach Profiles from the Florida Panhandle." *Journal of Waterway, Port, Coastal and Ocean Engineering* 133: 364-376.
- Wang, D., Hagen, S. C. and Alizad, K. (2013). "Climate change impact and uncertainty analysis of extreme rainfall events in the Apalachicola River basin, Florida." *Journal of Hydrology* 480(14): 125-135.
- Wang, P., Kirby, J. H., Haber, J. D., Horwitz, M. H., Knorr, P. O. and Krock, J. R. (2006). "Morphological and Sedimentological Impacts of Hurricane Ivan and Immediate Poststorm Beach Recovery along the Northwestern Florida Barrier-Island Coasts." *Journal of Coastal Research* 22(6): 1382-1402.
- Wang, Z. B., Jeuken, C. and De Vriend, H. J. (1999). "Tidal asymmetry and residual sediment transport in estuaries, A literature study and application to the Westerschelde, WL", Delft Hydraulics.
- Wei, D. and Chatterjee, S. (2013). "Economic impact of sea level rise to the city of Los Angeles". Los Angeles, CA, Price School of Public Policy and Center for Risk and Economic Analysis of Terrorism Events. University of Southern California.
- Werner, A. D. and Simmons, C. T. (2009). "Impact of sea-level rise on sea water intrusion in coastal aquifers." *Groundwater* 47(2): 197-204.

- West, J. J., Small, M. J. and Dowlatabadi, H. (2001). "Storms, investor decisions, and the economic impacts of sea-level rise." *Climatic Change* 48: 317-342.
- Woodroffe, C. D. (2003). Coasts: form, process and evolution. Cambridge, Cambridge University Press.
- Woodroffe, C. D. (2007). The natural resilience of coastal systems: primary concepts. Managing coastal vulnerability. L. McFadden, P.-R. E. and R. J. Nicholls. Amsterdam, Elsevier: 45-60.
- Woodruff, J. D., Irish, J. L. and Camargo, S. J. (2013). "Coastal flooding by tropical cyclones and sea level rise." *Nature* 504: 44-52.
- Yates, M. L. and Le Cozannet, G. (2012). "Evaluating European coastal evolution using Bayesian Networks." *Natural Hazards Earth System Sciences* 12: 1173-1177.
- Yohe, G. W., Neumann, J., Marshall, P. and Ameden, H. (1996). "The economic cost of greenhouse-induced sea level rise for developed property in the United States." *Climatic Change* 32: 387-410.
- Yohe, G. W. and Schlesinger, M. E. (1998). "Sea Level Change: the Expected Economic Cost of Protection or Abandonment in the United States." *Climatic Change* 38: 447-472.
- Zhang, K. (2011). "Analysis of non-linear inundation for sea-level rise using LIDAR data: a case study for South Florida." *Climatic Change* 106: 537-565.
- Zhang, K., Douglas, B. and Leatherman, S. (2002). "Do Storms Cause Long-Term Beach Erosion along the U.S. East Barrier Coast?" *The Journal of Geology* 110(4): 493-502.
- Zhang, K., Douglas, B. C. and Leatherman, S. P. (2004). "Global warming and coastal erosion." *Climatic Change* 64(1/2): 41-58.

CHAPTER 3. COMPARISON OF SHORELINE CHANGE RATES ALONG THE SOUTH ATLANTIC BIGHT AND NORTHERN GULF OF MEXICO COASTS FOR BETTER EVALUATION OF FUTURE SHORELINE POSITIONS UNDER SEA LEVEL RISE

The content in this chapter is published as: Passeri, D.L., Hagen, S.C., Irish, J.L. 2014. Comparison of shoreline change rates along the South Atlantic Bight and Northern Gulf of Mexico coasts for better evaluation of future shoreline positions under sea level rise. *Journal of Coastal Research, Special Issue 66*. 7-14.

3.1 Introduction

A large number of sandy shorelines along the U.S. Atlantic and Gulf Coasts are experiencing long-term erosion trends (Morton et al., 2004; Hapke et al., 2010) and research has indicated that sea level rise (SLR) is a major factor in long-term, gradual shoreline recession (Leatherman et al., 2000; Zhang et al., 2002). Long-term erosion rates are expected to escalate with increasing sea levels in the future (Zhang et al., 2004; Fitzgerald et al., 2008). Accurately predicting the impacts of SLR along sandy shorelines is challenging due to the highly dynamic nature of beaches (Fitzgerald et al., 2008). Several approaches have been taken to quantify shoreline retreat under SLR. One of the most well-known methods is the Bruun Rule (Bruun, 1962), which has served as a basis for many models predicting future shoreline retreat (Fitzgerald et al., 2008). Extrapolation of historical trends using past shoreline positions has also been widely applied for predicting future shoreline positions (Crowell and Leatherman, 1999). Although methods such as these have emerged to predict shoreline recession under a future rise in sea level, a universal approach that is applicable along a variety of coastlines has yet to be adopted (Fitzgerald et al., 2008).

The Coastal Vulnerability Index (CVI) was developed in 1999 by the United States Geological Survey (USGS) to establish a national-scale assessment of the relative vulnerability of coastal environments to SLR (Thieler and Hammar-Klose, 1999; Thieler and Hammar-Klose, 2000). The database covers the East, Gulf and Pacific coast shorelines of the U.S., dividing the shoreline into sections based on various risk variables including geomorphology, shoreline erosion and accretion rates, coastal slope, relative SLR, mean tidal range and mean wave height. The erosion and accretion rates for each section were derived from the Coastal Erosion Information System (CEIS), created in 1982. The CEIS database was assembled based on a collection of published reports, historical shoreline change maps, field surveys and aerial images. Due to the lack of a standard method for analyzing shoreline changes, the data utilized a variety of reference features, measurements and methods for rate of change calculations. Out of all of the variables included in the CVI, the erosion rates are the most complex and poorly documented due to low resolution data sets (Thieler and Hammar-Klose, 2000).

In 2004, the USGS National Assessment of Shoreline Change determined long-term shoreline change rates along the continental U.S. coastlines. The long-term rates (herein referred to as LT rates) were calculated every 50 m along the shoreline by applying a linear regression to four shoreline positions (mid to late 1800s, 1920s-1930s, 1970s, and 2000s). Early shorelines were collected from historic shoreline databases including National Oceanic and Atmospheric Administration (NOAA) Topographic Sheets (T-sheets) and aerial photographs. The most recent shoreline was derived from Light Detection and Ranging (lidar) data, collected circa 2001. To measure the average shoreline change, linear regression was applied; this is the most statistically robust quantitative method given a limited number of shorelines, and is the most commonly

applied statistical technique for defining shoreline movement and change rates. The largest error in assembling the change rates was positioning error, attributed to the scales and inaccuracies of the original surveys. However, the influence of any large position errors is reduced because the period of analysis is long (Morton et al., 2004; Morton and Miller, 2005). The Bruun Rule (Bruun, 1962), a two-dimensional cross-shore model, evaluates the recession of an active beach profile under a rise in mean sea level. The model is based on the equilibrium beach profile concept, which represents a balance of constructive and destructive forces acting on a beach, where turbulence induced by wave breaking in the surf zone is the dominant destructive force (Bruun, 1954; Dean, 1991). Higher sea levels facilitate high-energy, short waves to act further landward on the beach profile and transport sand offshore (Leatherman et al., 2000). Bruun (1962) determined the horizontal recession R of a beach profile by assuming the active profile extends out to a depth of closure (DOC) where bed sediments are no longer significantly transported by wave forces, and that the volume of sand that is eroded in the upper shoreface is conserved and deposited offshore while the profile maintains its shape. Shoreline recession is calculated from the relationship

$$R = S \frac{L^*}{b+h^*} \quad (3)$$

where S is the rise in mean sea level, b is the elevation of the berm, h^* is the DOC, and L^* is the width of the active beach profile. Since the Bruun Rule is a cross-shore model, it does not take into account the effects of longshore transport, coastal structures such as inlets or jetties, or Aeolian transport, and is often considered a first approximation (DECCW, 2010). Numerous applications have tested the validity of the Bruun Rule and have come to conflicting conclusions about its applicability (Schwartz, 1967; Rosen, 1978; Hands, 1983; Schwartz, 1987; List et al., 1997;

Leatherman et al., 2000; Zhang et al., 2004). Studies have also adapted the Bruun Rule to incorporate additional parameters other than the landward translation of the active beach profile (Davidson-Arnott, 2005; Ranasinghe et al., 2012; Rosati et al., 2013).

The purpose of this study is to compare and contrast the CVI, LT, and erosion rates predicted by the Bruun Rule under historic SLR. This analysis is not meant to deem one method better than another, but rather to explore the similarities and differences between the methods and offer recommendations on how to quantify shoreline positions under future scenarios. Transects are analyzed along stretches of sandy beach in the Northern Gulf of Mexico (NGOM) and the South Atlantic Bight (SAB) to compare results in two different wave environments. The effect of beach nourishment on the change rates is also explored.

3.2 Study Area

The NGOM portion of the study area spans from St. Andrew Bay, FL to Mobile Bay, AL (Figure 3.1). This section was selected due to the vast expanse of sandy shorelines encountering wave and tidal forces from the Gulf of Mexico, as well as the availability of data for all three methodologies. The study area spans five bay systems (Mobile Bay, AL; Perdido Bay, FL; Pensacola Bay, FL; Choctawhatchee Bay, FL and St. Andrew Bay, FL), four barrier islands that are in contact with the mainland, and one mainland beach. This portion of the NGOM is a wave dominated, microtidal environment and includes the Gulf Intracoastal Waterway, which travels through the barrier island chain to Mobile Bay. Any shorelines in the vicinity of inlet ebb shoals are excluded due to increased longshore transport that the Bruun Rule is unable to account for.

The SAB domain encompasses the sandy shorelines along the Atlantic Ocean from Miami, FL to Cape Hatteras, NC (Figure 3.1). Within the SAB is the Georgia Bight (from the Florida-Georgia border to Pawleys Island, SC), where the continental shelf widens and flattens, increasing the amplification of tidal waves and reducing the deep-water wave energy. (Davis Jr and Fitzgerald, 2004). This results in a mixed energy coast, characterized with short barrier islands and marshes separated by large tidal inlets with sand shoals. Since the Bruun Rule is derived from the equilibrium beach profile concept and the assumption that turbulence due to wave breaking is the dominant force for sediment transport, it is not applicable along this stretch because processes other than waves may be dominant forces of erosion. Therefore, the Bruun Rule is not applied to this area, and the corresponding CVI and LT rates are excluded for comparison. The SAB also contains four capes, namely Canaveral, FL, Fear, NC, Lookout, NC, and Hatteras, NC. Capes are highly dynamic areas with shoals that trap sediment and influence wave breaking, refraction, and longshore currents (Park and Wells, 2005). Because of the complex processes associated with cape evolution, shorelines within cape shoals are also excluded from the analysis. Again, any areas within the vicinity of inlet ebb shoals are also not included.



Figure 3.1: NGOM and SAB study area where the Bruun Rule, CVI and LT rates are compared.

3.3 Methodology

The CVI database is divided into 4800 m sections along the U.S. East and Gulf shorelines. Each span provides a single erosion/accretion rate, whereas the LT change rates from the National Assessment are calculated every 50 m along the shoreline. Since each CVI span is longer than the 50 m spaced LT transects, the range and average of the LT rates are calculated over each CVI span. For both databases, positive values indicate accretion, and negative values indicate erosion. If the LT transects within the span contained both eroding and accreting sections, an average

erosion rate is determined by selecting the eroding transects only; this allows for a better comparison with the Bruun Rule, which only predicts erosion. Areas influenced by beach nourishment are identified in The National Assessment of Shoreline Change database.

The Bruun Rule is applied along the coastline to predict erosion rates under local historic SLR rates at 4 km spaced locations. The historic SLR rate is obtained from long-term mean sea level trends at nearby NOAA tidal gauging stations (Figure 3.2). The DOC varies spatially along shorelines due to differing wave climates and can be determined using high quality profile data or predictive wave equations. Hallermeier (1978) proposed that the DOC is a result of erosion by the largest waves, and developed equation 2 to quantify it:

$$h^* = 2.28H_{e,t} - 68.5\left(\frac{H_{e,t}^2}{gT_{e,t}^2}\right) \quad (4)$$

where $H_{e,t}$ is the effective wave height that is exceeded 12 hours per t years (0.137 percent of the time), and $T_{e,t}$ is the associated wave period. Birkemeier (1985) evaluated the Hallermeier equation by comparing it with beach profile data in Duck, NC and found a good approximation to be:

$$h^* = 1.57H_{e,t} \quad (5)$$

The effective wave height can be related to the mean wave height using:

$$H_{e,t} = \bar{H} + 5.6\sigma_H \quad (6)$$

where \bar{H} is the mean annual significant wave height and σ_H is the standard deviation of the significant wave height (USACE, 1995). It is important to note that nearshore wave data must be used when predicting the DOC, as deep-water wave data will over-predict the location.

Dean and Grant (1989) determined spatially varying DOC values along Florida's shorelines using a blend of long-term nearshore wave data and beach profile data from beach nourishment projects. Similarly, Nicholls et al. (1996) used high quality profile data and wave data to determine the DOC in Duck, NC. In this study, the Dean and Grant (1989) values are used to assign the DOC in the NGOM at each location. For the SAB, the Dean and Grant (1989) values are used in conjunction with those found by Nicholls et al. (1996), as well applying the Birkemeier equation using 20 years of wave data recorded at National Data Buoy Center (NDBC) buoy 41008 in Grays Reef, GA. The buoy floats at a depth of 20 m, seaward of the breaking zone (similar to the buoys used in Nicholls et al. (1996)) just north of Jacksonville, FL.

Plotting the DOC values at Miami, FL, Melbourne, FL, Jacksonville, FL, Grays Reef, GA, and Duck, NC, with Miami representing the 0-km marker, illustrates that the DOC increases nearly linearly along the SAB coastline (Figure 3.3). Therefore, the DOC is assigned based on location using a linear regression equation. For simplicity, an average value can be assigned to areas where the wave climate does not vary. This can be confirmed by examining if the nearshore bathymetric contours run parallel with the shoreline; irregular bottom topography can cause complex wave refraction, producing significant variations in wave height and energy along the coastline (Masselink et al., 2011). Values are averaged over 80 km spans along the SAB and NGOM study areas (Figure 3.4).

To determine the width of the active profile, the DOC contour is extracted at each section using a bathymetric Digital Elevation Model (DEM) assembled from National Ocean Service (NOS) hydrographic surveys. The width is then determined by measuring the distance from the mean high

water (MHW) line to the DOC contour at each location. Finally, the elevation of the berm is determined by plotting elevation profiles using a 3 m lidar-derived DEM at each location. The profile is compared with aerial imagery to locate the vegetation line, and the corresponding elevation of the dune toe, which is assumed to be characteristic of the elevation of the berm. The final output is shoreline recession expressed as a rate (m/yr).

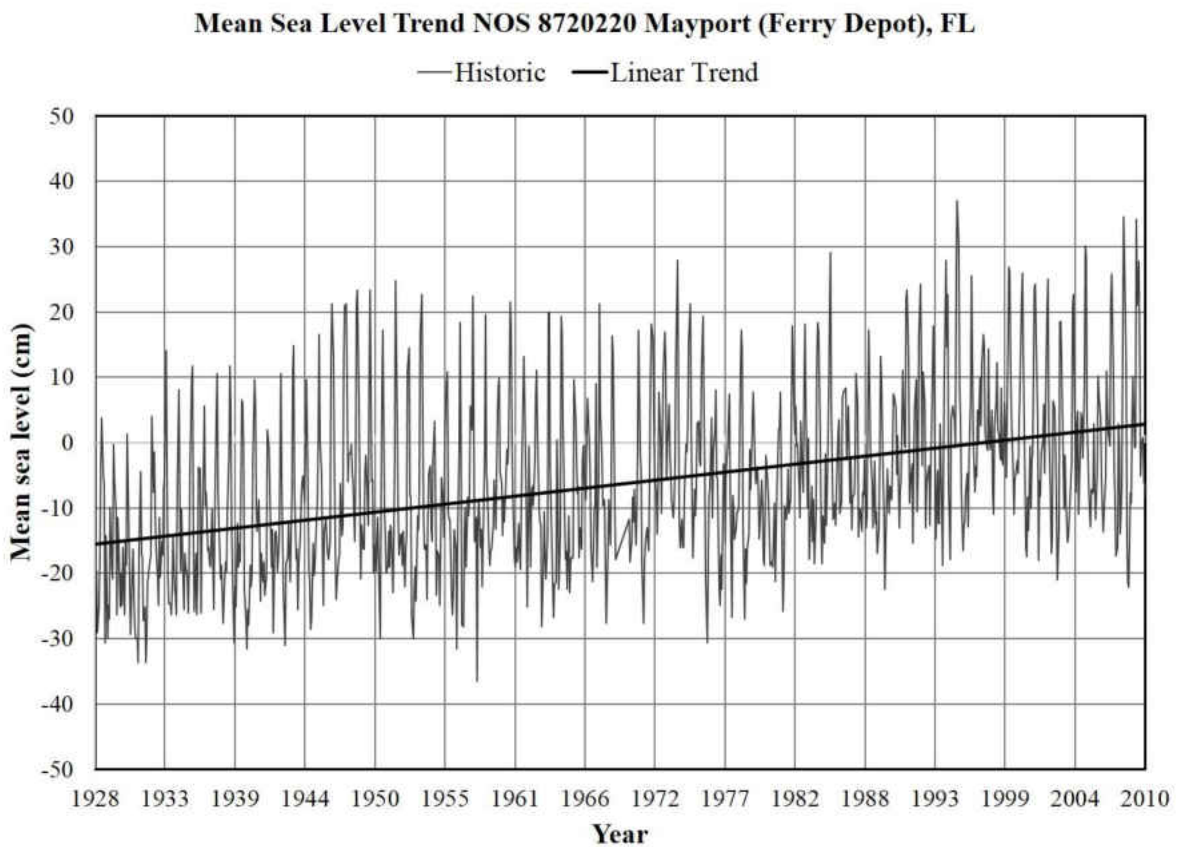


Figure 3.2: Example of historic mean SLR at NOS station in Mayport, FL.

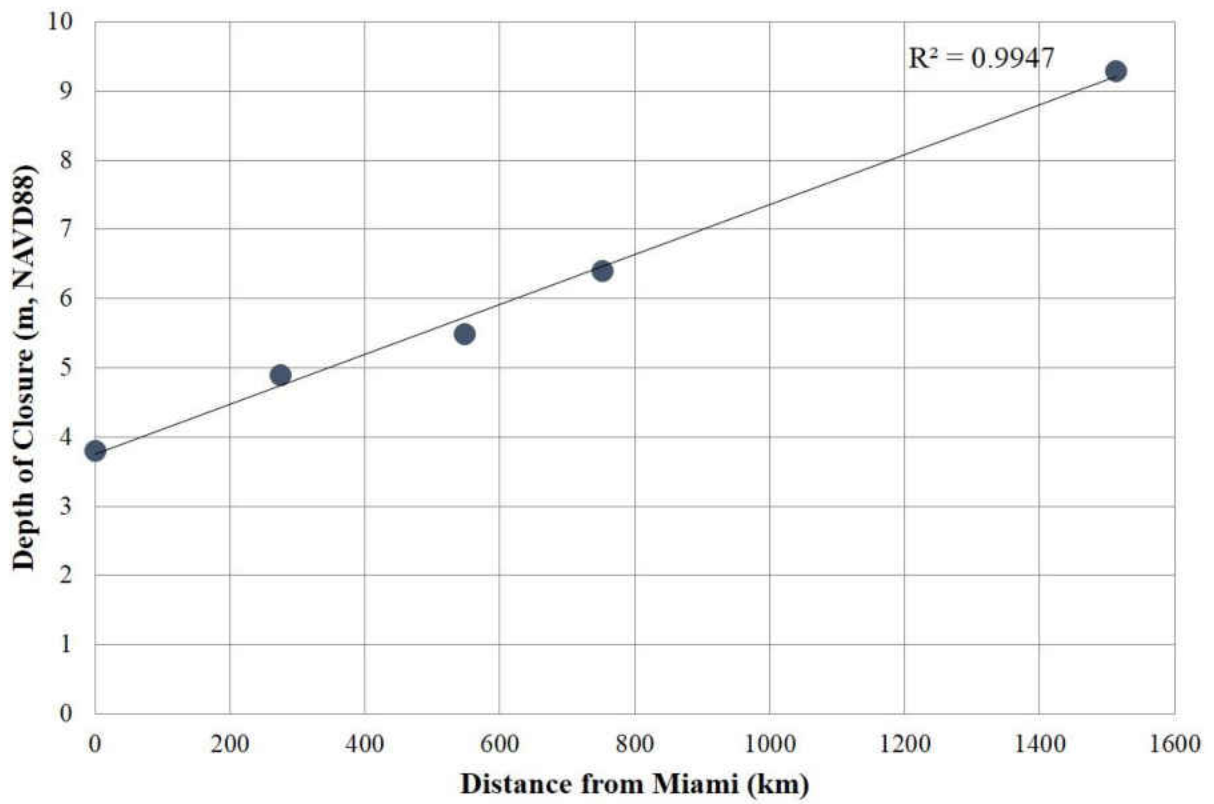


Figure 3.3: DOC estimates along the SAB derived from Dean and Grant (1989), Nicholls et al. (1996) and wave data at NDBC buoy 41008.

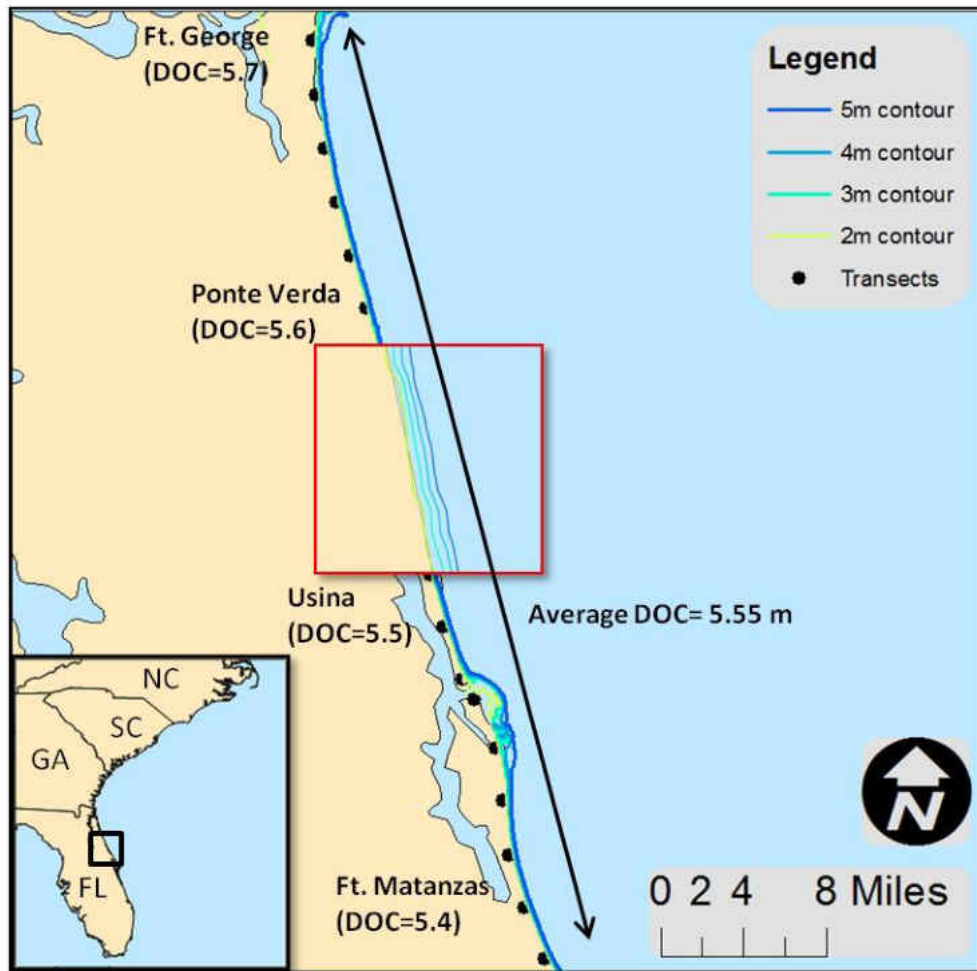


Figure 3.4: Average DOC value is assigned along SAB span where wave climate does not change using the linear regression equation; contours running parallel with the coast indicate unchanging wave climate.

3.4 Results

Percent differences and absolute differences are calculated to compare the CVI, LT and Bruun Rule shoreline change (Table 3.1, Table 3.2). Because the Bruun Rule predicts shoreline erosion rather than accretion, it is only compared with areas where the CVI and LT rates indicate erosion.

For the areas that are influenced by beach nourishment, the LT rates are re-evaluated using the historic shorelines that existed before nourishment occurred.

3.4.1 Coastal Vulnerability Index vs. Long-Term Rates

CVI rates are typically higher than the LT rates. Differences between the CVI and LT average rates are large when there is disagreement on which spans are accreting or eroding. This may be due to a difference in time frames used to establish the historic change rates or a result of areas that have been influenced by recent nourishment (the CVI does not specify which years were used to determine change rates, only that it was based on the CEIS data from 1982 which is older than the most recent shoreline used in the LT rates). In addition, there is not a strong correlation between the two data sets, with an R^2 value of 0.26. Isolating areas where both databases show erosion reduces the average difference from 1.16 m/yr to 0.61 m/yr (223% difference to 100%), with smaller differences in the SAB than the NGOM.

3.4.2 Bruun Rule vs. Coastal Vulnerability Index and Long-Term Rates

The predicted Bruun Rule erosion rates are slightly closer to the LT erosion rates than the CVI erosion rates with average differences of 0.55 m/yr (89% difference) and 0.75 m/yr (121% difference), respectively. There is a larger average difference in the NGOM study area than the SAB for the Bruun Rule compared with the CVI erosion rates (1.27 m/yr in NGOM and 0.49 m/yr in SAB), as well as the Bruun Rule compared with the LT erosion rates (0.52 m/yr for NGOM and 0.25 m/yr for SAB). The larger variation between the CVI and Bruun Rule in the two study areas may be attributed to the various methodologies used to derive the CVI rates, as the difference with

the LT erosion rates is smaller. A few areas in northeast Florida including Flagler Beach, New Smyrna, and Melbourne show little to no difference between the Bruun Rule and the LT erosion rates (0 m/yr, 0.05 m/yr and 0.01 m/yr, respectively). However, areas such as Knoll Ceders, NC and Hurricane Island, FL show large differences on the order of 3.50 m/yr and 3.16 m/yr.

3.4.3 Effect of Beach Nourishment

For sections influenced by nourishment, the date of nourishment is estimated by consulting beach nourishment project documents, as well as visual inspection of the different shorelines used in the USGS National Assessment for Shoreline Change (recall, the shorelines were grouped as mid to late 1800s, 1920s-1930s, 1970s, and 2000s). Erosion rates are then recalculated by measuring the change in position between the shorelines over time. Comparing pre-nourished erosion rates with the Bruun Rule reduces the average difference to 0.27 m/yr (average percent difference of 84%) with an average difference of 0.31 m/yr in the SAB and 0.11 m/yr in the NGOM.

Table 3.1: Percent differences across the NGOM and SAB between CVI, CVI erosion rates (CVI-E), LT, LT erosion rates (LT-E), the Bruun Rule (BR), and pre-nourished rates (PN)

Area	CVI LT (%)	CVI-E LT-E (%)	BR LT-E (%)	CVI-E BR (%)	BR PN (%)
Knoll Ceders, NC	250	--	186	--	140
Surf City, NC	229	--	55	73	96
Holden, NC	28	28	87	63	106
N. Myrtle, SC	264	--	--	122	9
Myrtle Beach, SC	170	--	187	--	48
Pawleys Island, SC	94	94	129	51	--
Flagler Beach, FL	207	--	0	129	--
New Smyrna, FL	358	--	48	129	--
Melbourne, FL	173	--	11	--	--
Palm Beach, FL	33	33	80	50	--
Hollywood, FL	229	--	106	79	21
Miami, FL	700	--	--	167	137
Hurricane Island, FL	750	--	192	--	--
Laguna Beach, FL	241	--	86	195	166
Miramar Beach, FL	155	155	145	192	--
Santa Rosa, FL	44	--	50	--	--
Pensacola, FL	157	157	88	182	--
Perdido Key, FL	174	--	--	--	--
Gulf Shores, AL	50	--	13	--	33
Cedar Grove, AL	160	130	59	148	--
Average	223	100	89	121	84
SAB Average	228	52	89	96	79
NGOM Average	216	148	90	179	100

Table 3.2: Absolute differences across the NGOM and SAB between CVI erosion rates (CVI-E), LT erosion rates (LT-E), the Bruun Rule (BR), and pre-nourished rates (PN)

Area	CVI-E LT-E (m)	BR LT-E (m)	CVI-E BR (m)	BR PN (m)
Knoll Ceders, NC	--	3.5	--	0.6
Surf City, NC	0.22	0.06	0.16	0.26
Holden, NC	0.16	0.4	0.24	0.58
N. Myrtle, SC	--	--	1.97	0.05
Myrtle Beach, SC	--	0.85	--	0.34
Pawleys Island, SC	0.32	0.66	0.34	--
Flagler Beach, FL	0.47	0	0.47	--
New Smyrna, FL	0.52	0.05	0.47	--
Melbourne, FL	--	0.01	--	--
Palm Beach, FL	0.08	0.16	0.08	--
Hollywood, FL	0.26	0.09	0.17	0.03
Miami, FL	--	--	0.82	0.35
Hurricane Island, FL	--	3.16	--	--
Laguna Beach, FL	1.45	0.03	1.48	0.20
Miramar Beach, FL	1.31	0.16	1.47	--
Santa Rosa, FL	--	0.04	--	--
Pensacola, FL	1.32	0.11	1.43	--
Perdido Key, FL	--	--	--	--
Gulf Shores, AL	--	0.01	--	0.03
Cedar Grove, AL	0.58	0.10	0.68	--
Average	0.61	0.55	0.75	0.27
SAB Average	0.29	0.25	0.49	0.31
NGOM Average	1.17	0.52	1.27	0.11

3.5 Discussion

The large differences between the CVI and the LT rates illustrate the need to define a benchmark methodology for determining erosion and accretion rates. This would yield better estimates when extrapolating historical trends to identify future shoreline positions. Since the methodology used to determine the CVI rates is not well documented, care should be taken when using them to project future shoreline positions.

Areas with little to no difference between the Bruun Rule and LT erosion rates, such as northeast Florida, are locations where shoreline retreat can be assumed to be completely attributed to forces associated with rising seas. These are areas with little to no background erosion, where the Bruun Rule can be applied to estimate shoreline recession under future SLR scenarios. On the contrary, erosion in areas such as Knoll Ceders, NC and Hurricane Island, FL is most likely due background processes in addition to SLR, such as increased gradients of longshore transport resulting from local bathymetry. If the Bruun Rule is applied to these areas, a factor should be incorporated to account for the background erosion processes. For example, Dean and Dalrymple (2002) recognize that at most locations the long-term erosion rates are not in agreement with the Bruun Rule and offer the following equation to compute the volume of sand required for shoreline stability, taking into consideration the background erosion rate, as well as SLR.

$$\frac{\partial V}{\partial t} = (h * +B) \frac{\partial R_0}{\partial t} + W * \left(\frac{\partial S}{\partial t} - \frac{\partial S_0}{\partial t} \right) \quad (7)$$

where $\frac{\partial R_0}{\partial t}$ is the existing background erosion and $\frac{\partial S_0}{\partial t}$ is the present rate of SLR. The first term on the right-hand side represents the volume required for the present rate of SLR, and the second term

represents the volume due to the increased SLR rate; all components contributing to the present shoreline erosion (including background effects such as longshore transport) are taken into consideration. Identifying nourished shorelines when using historic shoreline change rates or applying the Bruun Rule is necessary, as nourishment causes artificial shoreline accretion and may not provide an accurate estimate of the natural shoreline erosion rate.

3.6 Summary and Recommendations

Shoreline change rates from the CVI and National Assessment of Shoreline Change have been compared with erosion rates predicted by the Bruun Rule along the South Atlantic Bight and Northern Gulf of Mexico shorelines. Results showed large differences between the CVI and LT rates, signifying caution should be taken when projecting these change rates to determine future shoreline positions. Applying the Bruun Rule using historic rates of SLR predicted erosion rates closer to the LT rates than the CVI rates. The following is recommended for evaluating shoreline changes under future scenarios using these three approaches:

- 1) The Bruun Rule can be used to determine recession in areas where historic shoreline retreat can be assumed to be completely attributed to forces related to SLR (i.e., there is little to no background erosion). This can be accomplished through the comparison of long-term erosion rates with results predicted by the Bruun Rule, using the historic rate of SLR. When doing so, it is important to identify any nourished shorelines within a study domain.

- 2) A hybrid approach that takes into account background erosion in addition to cross-shore erosion predicted by the Bruun Rule may be appropriate in areas where shoreline retreat cannot be completely attributed to SLR (i.e., there is moderate to high background erosion).
- 3) Care should be taken when extrapolating shoreline change rates determined by the CVI or National Assessment of Shoreline Change to predict future shoreline positions. Projected CVI rates could be used when considering extreme future SLR scenarios (i.e., scenarios greater than the historic rise), as they are typically larger than long-term erosion rates.

Selecting a methodology for projecting future shoreline positions under SLR is a complex process. The recommendations provided herein will benefit future assessments of the impacts of SLR, including future shoreline changes, to better evaluate the effects of SLR on coastal environments.

3.7 Acknowledgments

This research was funded in part under Award No. NA10NOS4780146 from the National Oceanic and Atmospheric Administration (NOAA) Center for Sponsored Coastal Ocean Research (CSCOR). The statements and conclusions are those of the authors and do not necessarily reflect the views of NOAA-CSCOR or their affiliates. The authors would like to thank A. Warnock and the anonymous reviewer for their constructive comments.

3.8 References

- Birkemeier, W. A. (1985). "Field data on seaward limit of profile change." *Journal of Waterway, Port, Coastal and Ocean Engineering* 111(3): 598-602.
- Bruun, P. (1954). "Coast Erosion and the Development of Beach Profiles ". Beach Erosion Board.
- Bruun, P. (1962). "Sea-level rise as a cause of shore erosion." *Proceedings of the American Society of Civil Engineers, Journal of the Waterways and Harbors Division* 88: 117-130.
- Crowell, M. and Leatherman, S. P. (1999). "Coastal Erosion Mapping and Management." *Journal of Coastal Research* 28 (Special Issue): 196.
- Davidson-Arnott (2005). "Conceptual model of the effects of sea level rise on sandy coasts." *Journal of Coastal Research* 21(6): 1166-1172.
- Davis Jr, R. A. and Fitzgerald, D. M. (2004). Beaches and Coasts, Wiley-Blackwell.
- Dean, R. G. (1991). "Equilibrium Beach Profiles: Characteristics and Applications." *Journal of Coastal Research* 7(1): 53-84.
- Dean, R. G. and Dalrymple, R. A. (2002). Coastal Processes with Engineering Applications. Cambridge, Cambridge University Press.
- Dean, R. G. and Grant, J. (1989). "Development of Methodology for Thirty-Year Shoreline Projections in the Vicinity of Beach Nourishment Projects". Tallahassee, FL, Division of Beaches and Shores, Florida Department of Natural Resources.
- DECCW (2010). "Draft Guidelines for preparing Coastal Zone Management Plans", NSW Department of Environment, Climate Change and Water.
- Fitzgerald, D. M., Fenster, M. S., Argow, B. A. and Buynevich, I. V. (2008). "Coastal Impacts Due to Sea Level Rise." *Annual Review Earth Planet Science* 36: 601-647.
- Hallermeier, R. J. (1978). "Uses for a calculated limit depth to beach erosion." *Proceedings, 16th Coastal Engineering Conference*, New York, American Society of Civil Engineers.
- Hands, E. B. (1983). The Great Lakes as a test model for profile responses to sea level changes. CRC handbook of coastal processes and erosion. P. D. Komar. Boca Raton, FL, CRC Press: 167-189.

- Hapke, C. J., Himmelstoss, E. A., Kratzmann, M., List, J. H. and Thieler, E. R. (2010). "National assessment of shoreline change; historical shoreline change along the New England and Mid-Atlantic coasts". Open-File Report 2010-1118, U.S. Geological Survey: 57p.
- Leatherman, S. P., Zhang, K. and Douglas, B. C. (2000). "Sea Level Rise Shown to Drive Coastal Erosion." *EOS Transactions* 81(6).
- List, J. H., Sallenger, A. H., Hansen, M. E. and Jaffe, B. E. (1997). "Accelerated relative sea level rise and rapid coastal erosion: testing a casual relationship for the Louisiana barrier islands." *Marine Geology* 140: 347-363.
- Masselink, G., Hughes, M. G. and Knight, J. (2011). Coastal Processes & Geomorphology. London, UK., Hodder Education.
- Morton, R. A. and Miller, T. L. (2005). "National Assessment of Shoreline Change: Part 2, Historical Shoreline Changes and Associated Coastal Land Loss Along the U.S. Southeast Atlantic Coast", USGS: 40p.
- Morton, R. A., Miller, T. L. and Moore, L. J. (2004). "National assessment of shoreline change: Part 1: Historical shoreline changes and associated coastal land loss along the U.S. Gulf of Mexico". Open-file Report 2004-1043. St. Petersburg, Florida, U.S. Geological Survey: 45p.
- Nicholls, R. J., Birkemeier, W. A. and Hallermeier, R. J. (1996). "Application of the depth of closure concept." *25th International Conference on Coastal Engineering*.
- Park, J. and Wells, J. T. (2005). "Longshore transport at Cape Lookout, North Carolina: Shoal Evolution and the Regional Sediment Budget." *Journal of Coastal Research* 21(1): 1-17.
- Ranasinghe, R., Duong, T. M., Uhlenbrook, S., Roelvink, D. and M., S. (2012). "Climate-change impact assessment for inlet-interrupted coastlines." *Nature Climate Change* 3: 83-87.
- Rosati, J. D., Dean, R. G. and Walton, T. L. (2013). "The modified Bruun Rule extended for landward transport." *Marine Geology* 340: 71-81.
- Rosen, P. S. (1978). "A regional test of the Bruun Rule on shoreline erosion." *Marine Geology* 26: M7-M16.
- Schwartz, M. L. (1967). "The Bruun theory of sea level rise as a cause of shore erosion." *Journal of Geology* 73: 528-534.
- Schwartz, M. L. (1987). "The Bruun Rule - twenty years late." *Journal of Coastal Research* 3: ii-iv.

- Thieler, E. R. and Hammar-Klose, E. S. (1999). "National Assessment of Coastal Vulnerability to Sea Level rise: Preliminary Results for the U.S. Atlantic Coast". Woods Hole, Massachusetts, U.S. Geological Survey.
- Thieler, E. R. and Hammar-Klose, E. S. (2000). "National Assessment of Coastal Vulnerability to Sea-Level Rise: Preliminary Results for the U.S. Gulf of Mexico Coast". Woods Hole, MA, U.S. Geological Survey.
- USACE (1995). "Beach-Fill Volume Required to Produce Specified Dry Beach Width", US Army Engineer Waterways Experiment Station, Coastal Engineering Research Center, Vicksburg, MS. **Coastal Engineering Technical Note.**
- Zhang, K., Douglas, B. and Leatherman, S. (2002). "Do Storms Cause Long-Term Beach Erosion along the U.S. East Barrier Coast?" *The Journal of Geology* 110(4): 493-502.
- Zhang, K., Douglas, B. C. and Leatherman, S. P. (2004). "Global warming and coastal erosion." *Climatic Change* 64(1/2): 41-58.

CHAPTER 4. ON THE SIGNIFICANCE OF INCORPORATING SHORELINE CHANGES FOR EVALUATING COASTAL HYDRODYNAMICS UNDER SEA LEVEL RISE

The content in this chapter is published as: Passeri, D.L., Hagen, S.C., Bilskie, M.V., Medeiros, S.C. 2015. On the significance of incorporating shoreline changes for evaluating coastal hydrodynamics under sea level rise. *Natural Hazards*, 75 (2), 1599-1617 doi: 10.1007/s11069-014-1386-y.

4.1 Introduction

SLR threatens coastal environments with loss of land, inundation of coastal wetlands, and increased flooding during extreme storm events (Nicholls et al., 1999). Hydrodynamics may be altered with increased tidal ranges, tidal prisms, surge heights, and inundation of shorelines (National Research Council, 1987). The most straightforward approach to assess the response of shorelines to SLR is to consider inundation under a static rise (or fall) in sea level, often referred to as the “drowned valley concept” (Leatherman, 1990) or the “bathtub” approach. Under this approach, the shoreline migrates landward according to the slope of the coast as the sea level rises; the shore becomes submerged, but otherwise unaltered. This concept is suitable for regions with rocky or armored shorelines, or where the wave climate is subdued (Leatherman, 1990).

Along sandy shorelines and coastal marshes, shoreline retreat has a more dynamic effect than inundation, including permanent or long-term erosion of sand from beaches as a result of complex, feedback-dependent processes that occur within the littoral zone, as well as migration and loss of marshes (Fitzgerald et al., 2008). Unlike inundation, erosion is a physical process in which sand is removed from the shoreface and deposited elsewhere, typically offshore. Currently, 90% of coastlines worldwide are affected by coastal erosion, with a large portion of beaches along the

U.S. Atlantic and Gulf Coasts experiencing long-term erosion trends (Morton et al., 2004; Williams, 2004; Hapke et al., 2010). Direct anthropogenic causes are not considered a primary driver of coastal erosion, as erosion has also been observed on sparsely populated, undeveloped coasts (Leatherman, 1990). Although high energy storms can cause drastic beach erosion over a relatively short period of time, shorelines tend to recover to their pre-storm equilibrium conditions. The long-term, gradual recession of shorelines is believed to be a result two processes, (1) SLR, which enables high-energy waves to act further on the shoreline and (2) variations in sediment supplies (Zhang et al., 2002). As sea levels continue to rise, long-term erosion rates are expected to increase (Zhang et al., 2004), which may ultimately lead to the deterioration of barrier islands and embayments along the U.S. East and Gulf Coasts (Williams et al., 1992; Fitzgerald et al., 2007).

Several studies have examined the potential effects of SLR on coastal flooding during storm events (Resio et al., 2008; Irish et al., 2009; Woodruff et al., 2013), and hydrodynamic models have been extensively applied to study the influence of SLR on storm surge and astronomic tides. Responses have been shown to be nonlinear (Smith et al., 2010; Mousavi et al., 2011; Hagen et al., 2013), and dependent on local topography (Hagen and Bacopoulos, 2012; Atkinson et al., 2013). Changes to the landscape over time, such as the past migration of the offshore barrier islands in Mississippi, may further influence storm surge inundation (Bilskie et al., 2014). Therefore, to capture the dynamic interactions in the cases of storm surge and astronomic tides, SLR must be modeled as a dynamic process, as opposed to a static process (i.e., “bathtub” approach); this may lead to a greater or lesser increase in future tidal and storm surge inundation (Hagen and Bacopoulos, 2012). Although previous studies have emphasized the importance of recognizing the dynamics

associated with SLR in hydrodynamic modeling, little research has considered the impact of future shoreline changes in conjunction with SLR on hydrodynamics over large expanses of coastline with multiple embayments. Most studies incorporating shoreline changes into hydrodynamic modeling studies have focused on simulating the coastal processes responsible for past and present shoreline changes (Vitousek et al., 2007; Dawson et al., 2012), or have considered the effects of hypothetical morphological scenarios for management purposes (Reyes et al., 2005; Cobell et al., 2013). Similarly, economic impact assessments of climate change have accounted for subsidence and increased exposure to mean sea level and storm surge under future sea levels (Hallegatte et al., 2011; Hallegatte et al., 2013) but have not incorporated the effects of future shoreline changes on coastal inundation.

This study examines the influence of incorporating future shoreline migration and associated nearshore bathymetric changes into hydrodynamic modeling to evaluate the response of a coastal system under future SLR scenarios. This study is not intended to be a future projection, but rather a sensitivity analysis of the response of hydrodynamics to the inclusion of long-term shoreline change estimates. The study area spans the Northern Gulf of Mexico (NGOM) from Mobile Bay, AL to St. Andrew Bay, FL in the Florida Panhandle (Figure 4.1). This section of the NGOM was selected due to the vast expanse of sandy shorelines that encounter wave and tidal forces from the Gulf of Mexico. Within the study area are five bay systems, four barrier islands and one mainland beach. The western half of the study area from Fort Morgan to Santa Rosa Island is comprised of long barrier islands immediately backed by lagoons and sounds that connect to larger bay systems. The eastern stretch between Destin and Panama City contains mainland beach, followed by a small barrier island backed by St. Andrew Bay. This portion of the NGOM is a wave dominant,

microtidal environment and has endured a number of powerful storms including the recent hurricanes Ivan (2004), Dennis (2005) and Katrina (2005). Shoreline change rates provided by the Coastal Vulnerability Index (CVI) (Thieler and Hammar-Klose, 2000) are used in conjunction with a translation of the nearshore profile to reflect the projected 2050 shoreline and nearshore morphology. A large scale hydrodynamic model is used to simulate astronomic tides and hurricane storm surge under present and future sea levels to test the sensitivity of the system to the projected shoreline changes under normal and extreme flooding conditions.

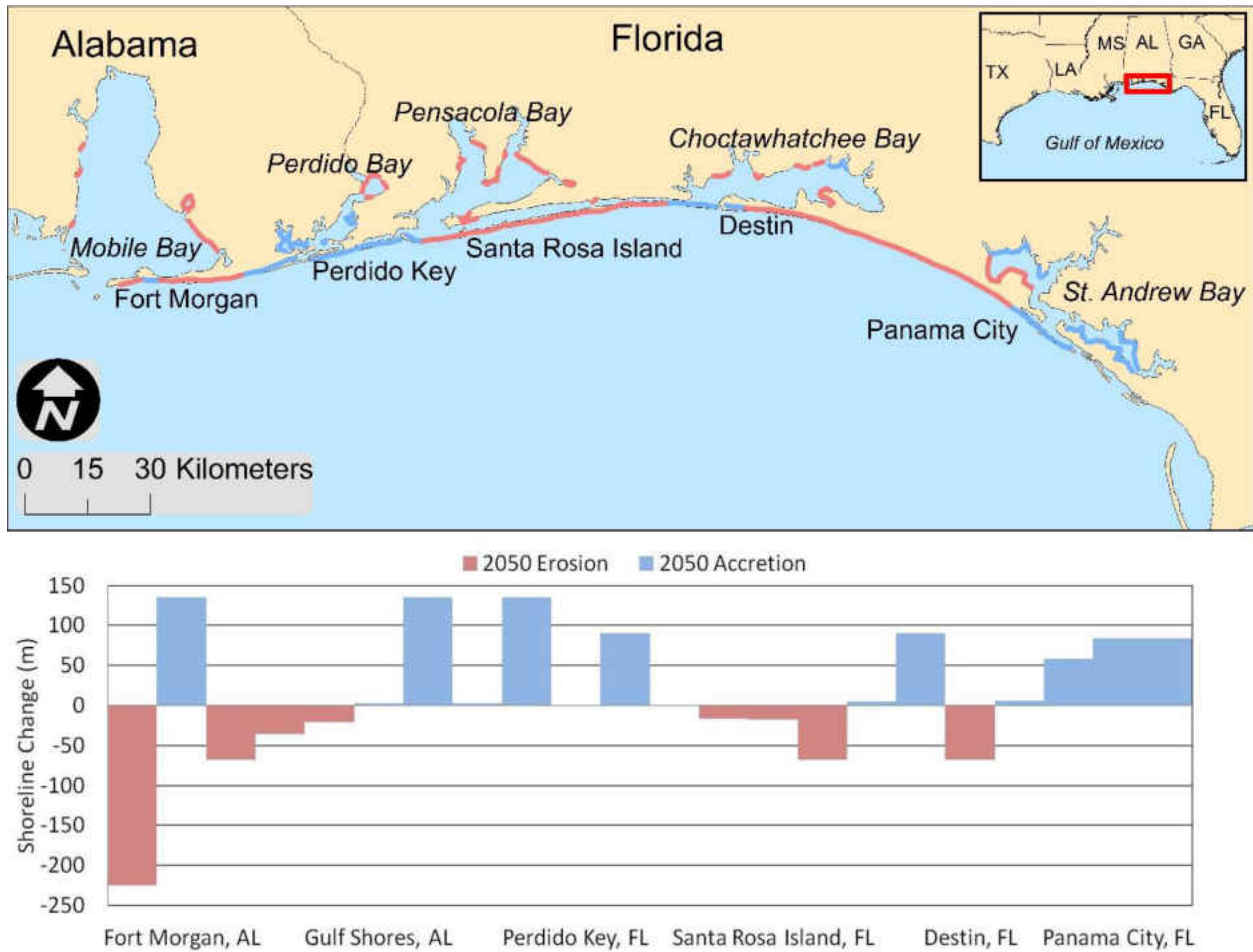


Figure 4.1: Top: Study area with projected erosion and accretion along Gulf and non-hardened bay shorelines from CVI database Bottom: 2050 shoreline change along Gulf shoreline estimated with CVI erosion and accretion rates.

4.2 Methods

4.2.1 Projected 2050 Shoreline and Nearshore Morphology

Due to the complex nature of beaches, coastal scientists do not have a reliable, universal model to accurately predict the impacts of SLR along a variety of coastlines (Fitzgerald et al., 2008). Extrapolation of historical trends using past shoreline data has been widely applied for predicting

future shoreline positions (Fenster et al., 1993; Crowell et al., 1997; Crowell and Leatherman, 1999; Galgano and Douglas, 2000). Historic shoreline erosion and accretion rates have been calculated by a variety of studies and compiled into databases such as the CVI, developed in 1999 by the United States Geological Survey (USGS) (Thieler and Hammar-Klose, 1999; Thieler and Hammar-Klose, 2000). The database covers the U.S. Pacific, Atlantic and Gulf shorelines (inclusive of embayments) and is governed by risk variables including shoreline erosion and accretion rates. The shoreline change rates were derived from the Coastal Erosion Information System (CEIS) (May et al., 1982) based on published reports, historical shoreline change maps, field surveys and aerial images. In comparison with the long-term historic shoreline change rates along the NGOM provided by the National Assessment of Shoreline Change (Miller et al., 2004), the CVI change rates are typically much larger, and can therefore be considered a high estimate of shoreline changes.

Many recently developed coastal response models acknowledge that shoreline response to SLR involves the movement of the entire shoreface (Davidson-Arnott, 2005; Ranasinghe et al., 2007; Ranasinghe et al., 2012; Rosati et al., 2013). Observations of beach profiles led to the development of the equilibrium beach profile concept, which assumes that the beach profile maintains an average, constant shape (aside from periods of storm induced changes) as the profile moves parallel to itself seasonally (Bruun, 1954). Assuming conditions other than sea level remain unchanged, the active beach profile extending from the shoreline to a seaward boundary denoted as the depth of closure will translate upward and landward to keep pace with rising seas, while maintaining shape (equilibrium) (Bruun, 1962). This concept remains a central assumption in

many coastal response models (Hanson, 1989; Dean, 1991; Patterson, 2009; Ranasinghe et al., 2012).

Shoreline change under SLR is not limited to beaches, it can be a major factor in estuaries as well; this may result in the loss of inter-tidal areas, erosion of shorelines and increased flooding in low lying areas (Rossington, 2008). Estuarine shoreline response to SLR is dependent upon the amount of energy acting on the shoreline; if the energy is high enough, the shoreline will erode and deposit sediment along other shorelines within the basin, whereas if the energy is low, the shoreline will be inundated (Stevens, 2010; Department of Environmental and Heritage Protection, 2013).

Since a goal of this research is to demonstrate the sensitivity of the model results to a central facet of the coastal dynamics of SLR, namely the inclusion of projected shoreline morphology, the year 2050 is chosen to contrast with the majority of published work which uses extreme SLR values (on the order of one meter or greater). In addition, shoreline changes are presently significant within the study area and extrapolating historical trends to the near-term (2050) will reduce uncertainty in long-term shoreline dynamics. The position of the 2050 Gulf shoreline is estimated by extrapolating the historic CVI change rates, which typically span 4800 m sections along the coast with negative rates indicating erosion and positive rates indicating accretion. Although SLR typically induces landward retreat of shorelines, many shorelines especially within the vicinity of inlets are projected to accrete. Total projected shoreline change along the Gulf shoreline ranges from -220 m to 140 m (Figure 4.1).

In order to account for the dynamic movement of the shoreface under SLR, the beach profile is translated upwards by the amount of SLR, and landwards/seawards by the amount of projected erosion/accretion while maintaining shape. This assumes that the beach profile is currently in equilibrium, and will remain so in the year 2050. A study by Walton and Dean (2007) found that beach profiles measured in the Florida panhandle directly after storms did not correlate with equilibrium conditions, and reformation of the nearshore occurs within one month to one year after the storm, with recovery of eroded sand after two years (Leadon, 1999; Wang et al., 2006). Since the data used to assemble the hydrodynamic model's nearshore Gulf bathymetric DEM was collected in 1990, five years after a hurricane affected the Florida panhandle (this was the best available and most recent data), it is presumed that the nearshore had been restored at the time of the surveys and the data is representative of equilibrium conditions. The profile translation is implemented for each CVI section by shifting the active zone portion of the DEM defined from the shoreline (0 m contour) to the depth of closure contour, estimated by Dean and Grant (1989) to be approximately 5 m along the coastline. Bathymetry and topography outside of the active zone remain the same.

All five inlets in the study area are dredged and hardened with a variety of structures including jetties, terminal groins and seawalls (Rice, 2012), and are therefore considered fixed. Non-hardened estuarine shorelines within the bay systems are also translated landward or seaward in accordance with the extrapolated CVI change rates. Because the depth of closure is difficult to measure in low energy estuarine environments, it is assumed to be very shallow (0 m), and therefore only the shoreline is translated in these regions. Total projected shoreline change along estuarine shorelines ranges from -67.5 m to 90 m. Estuarine shorelines with CVI shoreline change

rates of zero as well as hardened shorelines are assumed to be areas affected by inundation only, i.e., no erosion or accretion occurs.

4.2.2 Projected 2050 Sea Level

Sea level has been rising globally at a rate of 1.7 mm/yr (Church and White, 2006). Although there are large variations in future projections, all agree that there will be a continuous rise (Donoghue, 2011). Parris et al. (2012) identified four scenarios of global mean SLR by 2100, ranging from 0.2 m to 2.0 m; these SLR curves are considered to be plausible trajectories of global mean SLR for use in assessing vulnerability, impacts and adaptation strategies. Since the extrapolation of the CVI change rates can be considered a high projection of future shoreline positions in comparison with extrapolation of shoreline change rates from the National Assessment of Shoreline Change (Miller et al., 2004), the highest scenario of SLR is selected to observe the response of the system under both an extreme SLR and a high projection of shoreline changes. The highest SLR scenario for 2050 is approximately 0.46 m (Parris et al., 2012).

4.2.3 Hydrodynamic Model and Simulations

Hydrodynamics are simulated using ADCIRC-2DDI, a two dimensional code that solves the depth-integrated shallow water equations for water surface elevations and currents (Luettich et al., 1992). The finite element mesh, originally developed for a Federal Emergency Management Agency (FEMA) Flood Insurance Study along the Florida Panhandle and Alabama coast (Hagen et al., 2011), describes the Western North Atlantic Tidal (WNAT) model domain west of the 60° W meridian, including the Caribbean Sea and the Gulf of Mexico. Higher resolution elements (on

the order of 20 m to 100 m) are incorporated within the Florida Panhandle and Alabama. Further information on mesh development and topographic elevations can be found in Hagen et al. (2011). An extensive validation was performed for the FEMA study to evaluate the performance of the ADCIRC model. Model results were compared with available historical storm surge data for Hurricanes Ivan, Katrina, and Dennis, including assessments of high water mark data and time-series gauge data. Wave setup was incorporated for these hurricanes through wave radiation stress provided by a loosely coupled 2D SWAN model (Slinn, 2013). An astronomic tidal validation was also performed at fifteen tide gauge stations located throughout the study domain to compare resynthesized observed and simulated tidal signals. For brevity, only the assessment of high water mark data is included herein (Figure 4.2). Model results are biased slightly lower than the measured high water marks, although overall comparison between the modeled and historic data indicates a skillful model (University of Central Florida, 2011).

The hydrodynamic model is applied to test the sensitivity of the coastal system to the projected shoreline changes through simulations of astronomic tides, and hurricane storm surge with wave setup. Tides and surge are each simulated for three scenarios: a) present day sea level with present day shorelines (i.e., hindcast for hurricanes), b) projected 2050 sea level (+0.46 m of SLR) with present day shorelines and nearshore bathymetry and c) projected 2050 sea level (+0.46 m of SLR) with projected 2050 shorelines and nearshore bathymetry, herein referred to as the 2005, 2050, and 2050-S simulations, respectively. For the 2050-S simulations, surface roughness in the form of Manning's n (resistance to flow) is altered for newly wetted (erosional) and dry (accretional) areas (e.g., along a Gulf shoreline, areas now wetted due to erosion are assigned a water Manning's n of 0.02, and areas now dry due to accretion are assigned a beach Manning's n of 0.03).

Boundary conditions for tidal simulations include seven harmonic constituents (K_1 , O_1 , M_2 , S_2 , N_2 , K_2 and Q_1) that force water surface elevations along the open ocean boundary. Model output consists of time-dependent water levels. Storm surge with wave setup is simulated for each of the three scenarios with winds and pressures supplied by Ocean Weather Inc. (OWI), representative of Hurricanes Ivan (2004), Dennis (2005) and Katrina (2005). The selection of the hurricanes was based on their use in the model validation, as well as the landfall locations in relation to the study area. In order to observe the individual responses of tides and storm surge to the projected shoreline changes, the storm surge simulations do not include astronomic tidal forcing. Output includes time series water surface elevations as well as maximum elevations obtained at each node of the mesh for the duration of the simulation.

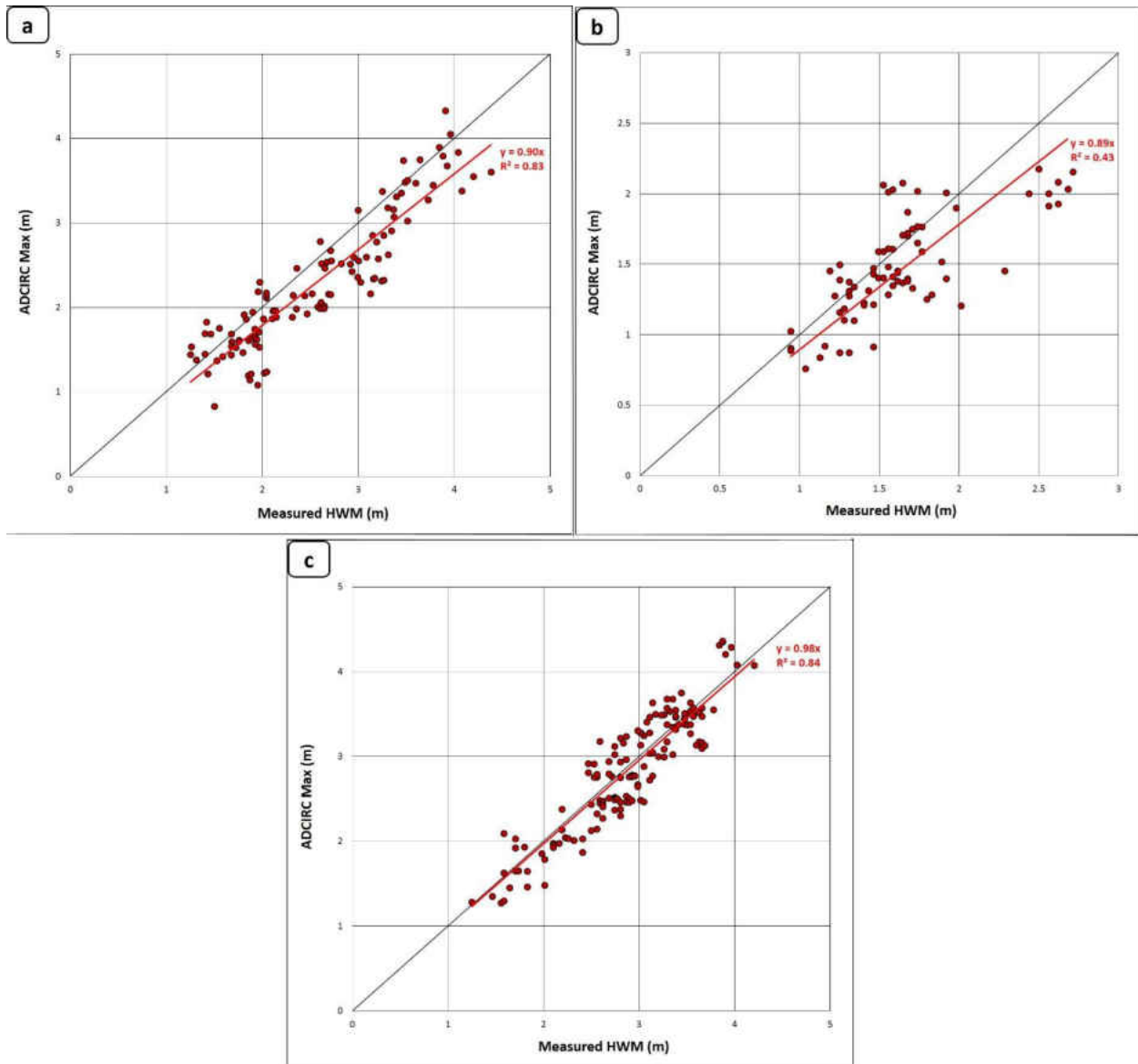


Figure 4.2: Comparison of measured and modeled high water mark (HWM) data for (a) Hurricane Ivan, (b) Hurricane Dennis and (c) Hurricane Katrina.

4.3 Results

4.3.1 Astronomic Tides

Tidal ranges within each bay are calculated as the maximum vertical difference between the high tide and subsequent low tide during the spring tidal cycle. The tidal prism is calculated as the volume of water that enters the bay during the flood flow. Tidal ranges, tidal prisms, and differences in the wetted area and volume of each bay at high and low tide for the 2005, 2050 and 2050-S simulations are summarized in Table 4.1 and

Table 4.2. Overall, tidal ranges increase in each bay system in the 2050 scenario compared to the 2005 scenario as a result of the larger volume of water entering the bay; Perdido and Choctawhatchee bays experience the largest increases of 40% and 34%, respectively. Similarly, tidal prisms increase in the 2050 scenario due to the amplified tidal ranges as well as the enlargement in the planform area of the bays resulting from shoreline inundation. In the 2050-S scenarios, the tidal ranges remain the same as the 2050 scenario, as no additional water is entering the bay system since the inlets are considered fixed. The projected bay shoreline changes have variable influences on the tidal prisms; in Perdido and Choctawhatchee bays, the tidal prisms increase from the 2050 scenario, in Mobile and Pensacola bays tidal prisms remain relatively the same as the 2050 scenario, and in St. Andrew Bay the tidal prism decreases from the 2050 scenario. This variability is dependent on whether the bay undergoes shoreline erosion, accretion, or both. Mobile and Pensacola bays only had projected shoreline erosion, which increased the overall planform area of the bay. The erosion increased the wetted area at low and high tide, which increased the volume of water at low and high tide from the 2050 scenario. However, the increase was not substantial enough to alter the tidal prism from the 2050 scenario. Although Perdido and Choctawhatchee bays had shoreline erosion and accretion, the planform area increased as a result of net erosion. The accretion within these bays decreased the wetted area and volume of water at low tide, whereas the erosion increased the wetted area and volume at high tide; this resulted in 12% and 6% increases in the tidal prism in each bay, respectively. St. Andrew Bay also had shoreline erosion and accretion, but the planform area was decreased as a result of net accretion. Although the accretion decreased the wetted area at low tide, the volume of water at low tide

increased. The wetted area and volume at high tide also increased, and the tidal prism minimally decreased by 1%.

Inspection of residual currents in each of the bay systems yields minimal differences between the 2050-S, 2050 and 2005 scenarios. Comparing the 2050 simulations to the 2005 simulations, the magnitude of the residual currents negligibly changes within the bays (less than 1 mm/s difference), although currents within the Perdido and Choctawhatchee Bay inlets increase by as much as 4 cm/s; these bays also have the largest increase in tidal prisms from 2005 to 2050. Again this is a result of the higher water levels increasing the current velocities and allowing more water to enter the bays on the flood tides. Differences between the 2050-S and 2050 scenarios are negligible within the bays as well as the inlets, since the inlets are considered fixed and no additional water is entering the bay systems.

Table 4.1: Calculated tidal ranges and tidal prisms for each bay under 2005, 2050 and 2050-S scenarios

Location	Scenario	Area (m ²)	Tidal range (m)	Tidal prism (m ³)
Mobile Bay	2005	9.95E+08	0.50	5.39E+08
	2050	1.01E+09	0.53	5.71E+08
	2050-S	1.02E+09	0.53	5.73E+08
Perdido Bay	2005	9.76E+07	0.24	2.28E+07
	2050	9.88E+07	0.33	3.46E+07
	2050-S	9.91E+07	0.33	3.88E+07
Pensacola Bay	2005	3.30E+08	0.49	1.78E+08
	2050	3.45E+08	0.51	1.95E+08
	2050-S	3.46E+08	0.51	1.96E+08
Choctawhatchee Bay	2005	3.18E+08	0.17	4.40E+07
	2050	3.21E+08	0.23	6.31E+07
	2050-S	3.21E+08	0.23	6.69E+07
St. Andrew Bay	2005	2.40E+08	0.52	1.14E+08
	2050	2.66E+08	0.53	1.19E+08
	2050-S	2.65E+08	0.53	1.18E+08

Table 4.2: Difference between low tide and high tide wetted area and volume of bay systems, and percent increase in tidal range and tidal prisms under 2005, 2050 and 2050-S scenarios

Location	Scenario	Difference (m ²)				% increase	
		Low tide area	High tide area	Low tide volume	High tide volume	Tidal range	Tidal prism
Mobile Bay	2050 - 2005	7.99E+07	5.09E+07	5.12E+08	5.45E+08	6%	6%
	2050-S - 2050	4.91E+06	2.67E+06	1.33E+06	3.48E+06	0%	0%
Perdido Bay	2050 - 2005	1.19E+07	1.21E+07	4.82E+07	6.01E+07	40%	52%
	2050-S - 2050	-1.71E+06	2.79E+05	-2.32E+06	1.93E+06	0%	12%
Pensacola Bay	2050 - 2005	4.94E+07	5.59E+07	1.70E+08	1.87E+08	5%	10%
	2050-S - 2050	7.00E+05	1.42E+06	3.44E+04	7.46E+04	0%	0%
Choctawhatchee Bay	2050 - 2005	1.92E+07	6.62E+07	1.43E+08	1.63E+08	34%	44%
	2050-S - 2050	-9.11E+04	1.42E+06	-2.12E+06	1.72E+06	0%	6%
St. Andrew Bay	2050 - 2005	3.75E+07	3.38E+07	1.29E+08	1.35E+08	2%	5%
	2050-S - 2050	-2.74E+06	3.30E+04	5.28E+05	-3.74E+05	0%	-1%

4.3.2 Hurricane Storm Surge

Hurricane Ivan, Dennis and Katrina made landfall in Gulf Shores, AL, Santa Rosa Island, FL and southeastern Louisiana, respectively, each as Category 3 storms. Values and locations for peak surges for each hurricane are summarized in Table 4.3. Comparison of peak surges for the 2005 and 2050 simulations demonstrates the nonlinear response of the surge to SLR; the peak surge produced in each of the 2050 simulations is unequal to the 2005 peak surge elevated by 0.46 m of SLR. Results from each storm surge simulation and scenario are analyzed by comparing differences in the maximum elevations of water (the maximum elevation reached at each node in the mesh for a particular simulation (Figure 4.3), barrier island inundation (Table 4.4) and volume of surge within bay systems (Table 4.5).

The dry area and inundation index of the Fort Morgan peninsula, Perdido Key, Santa Rosa Island and St. Andrew barrier island for each hurricane simulation and scenario are summarized in Table 4.4. The dry area, defined as the area of land not wetted during each simulation, is indicative of the inundation extent. The inundation index of each barrier island is used as a relative comparison of barrier island inundation from 2005 to 2050-S conditions, and is calculated as follows:

$$\text{Inundation Index} = \frac{A_i - A_f}{A_i} \quad (8)$$

where A_i is the initial dry area of the barrier island (for either the 2005 or the 2050-S scenario) and A_f is the total area of the barrier that is not wetted during each simulation. The inundation index ranges from 0 to 1, with 1 indicating all areas of the barrier island have become submerged, and 0 indicating no inundation.

Comparison of the inundation index for each barrier island indicates that SLR increases the area of inundation along all of the islands for each storm surge simulation as a result of the higher water levels. The St. Andrew barrier experiences the largest increase in the inundation indices for all three storm surge simulations, despite being located the furthest away from the landfall location of all three hurricanes. SLR also leads to higher increases of the inundation index on barrier islands where the simulated hurricanes made landfall. Perdido Key (close to where Ivan made landfall) experiences a larger increase in the inundation index from the 2005 to the 2050 simulation for Ivan than Dennis and Katrina. Likewise, the inundation index along Santa Rosa Island increases more during the Dennis simulation than the Ivan and Katrina simulations.

Santa Rosa Island is affected the most with increased inundation when the projected shorelines are included due to narrow width of the island (about 500 m wide in the 2005 scenario). The extensive projected erosion (about 67 m) on the Gulf side of the island allows more water to inundate the island in the 2050-S scenario, which initiates overtopping at more locations than in the 2050 simulations. Dennis has the most severe impact due to it making landfall on the island, which almost doubles the inundation index from the 2050 simulation as a result of overtopping at many new locations (Figure 4.4). Since the majority of the island was overtopped in the 2050 Ivan simulation, the effect of the projected shoreline erosion is not as dramatic in the 2050-S simulation, although the inundation index still increases.

Despite the projected erosion along the Fort Morgan peninsula, the inundation index remains relatively the same in the 2050-S and the 2050 simulations. The Fort Morgan peninsula is much wider than the Santa Rosa Island (on average over twice as wide), and is not as affected with increased overtopping when the projected shoreline erosion is included. However, a few small areas that were not overtopped in the 2050 simulation become overtopped in the 2050-S simulation due to the projected erosion.

The inundation index along Perdido Key slightly increases for all three the 2050-S simulations, despite the projected accretion. Inspection of the dry areas indicates the island is slightly inundated more during the 2050-S Ivan simulation than in the 2050 simulation; this occurs on the bayside of the island due to the additional overtopping of the Santa Rosa Island in conjunction with the hurricane's nearby landfall location. The inundation index increases the most for the Katrina simulation because the dry area for the 2050 and 2050-S simulations are almost equal. The

inundation index along the St. Andrew barrier also slightly increases in all three 2050-S simulations for the same reason; however, this barrier was not as impacted with storm surge due to its distance from the landfall locations of each hurricane.

Comparing the differences in maximum elevations of water for the 2050 and 2050-S Ivan and Dennis simulations shows the largest variation within Santa Rosa Sound (maximum increase in water levels of approximately 0.20 m and 0.65 m, respectively, Figure 4.3). Because Santa Rosa Island experiences increased overtopping when the 2050 shoreline is included, water levels elevate in Santa Rosa Sound and Pensacola Bay. The largest increase in the volume of surge occurred during Dennis (24% increase in Santa Rosa Sound; 7% increase in Pensacola Bay) again due to the landfall location of the hurricane. Similarly, overtopping also increased the volume of surge during the Ivan simulation (3% increase in Santa Rosa Sound; 3% increase in Pensacola Bay). The overtopping was not extensive enough to significantly increase the volume of surge in the bays during the Katrina simulations, as a result of the hurricane making landfall further away. Water levels in Perdido Bay do not significantly increase in any of the storm surge simulations when the projected shoreline changes are included because Perdido Key does not experience additional overtopping. The volume of surge in Mobile Bay minimally increases during the Ivan and Katrina simulations, resulting from some additional overtopping of the Fort Morgan peninsula. This also slightly increases flooding depths north of Mobile Bay in the floodplain during the Katrina simulation. Choctawhatchee Bay experiences increases in surge during the Ivan and Dennis simulations, most likely as a result of the increased volume of surge in Santa Rosa Sound, but is unaffected during Katrina, again as a result of the landfall location.

Differences in maximum elevations of water indicate the mainland beach from Destin to Panama City remains unaffected in all three storm surge simulations despite the projected erosion. Including projected shoreline changes increases the overall inundation of the floodplain by 63.41 km², 147.47 km², 5.57 km², during the Ivan, Dennis and Katrina simulations, respectively. Again, this is a result of increased overtopping along the barrier islands allowing additional surge into the back-bays, thereby increasing the inland inundation extent and magnitude.

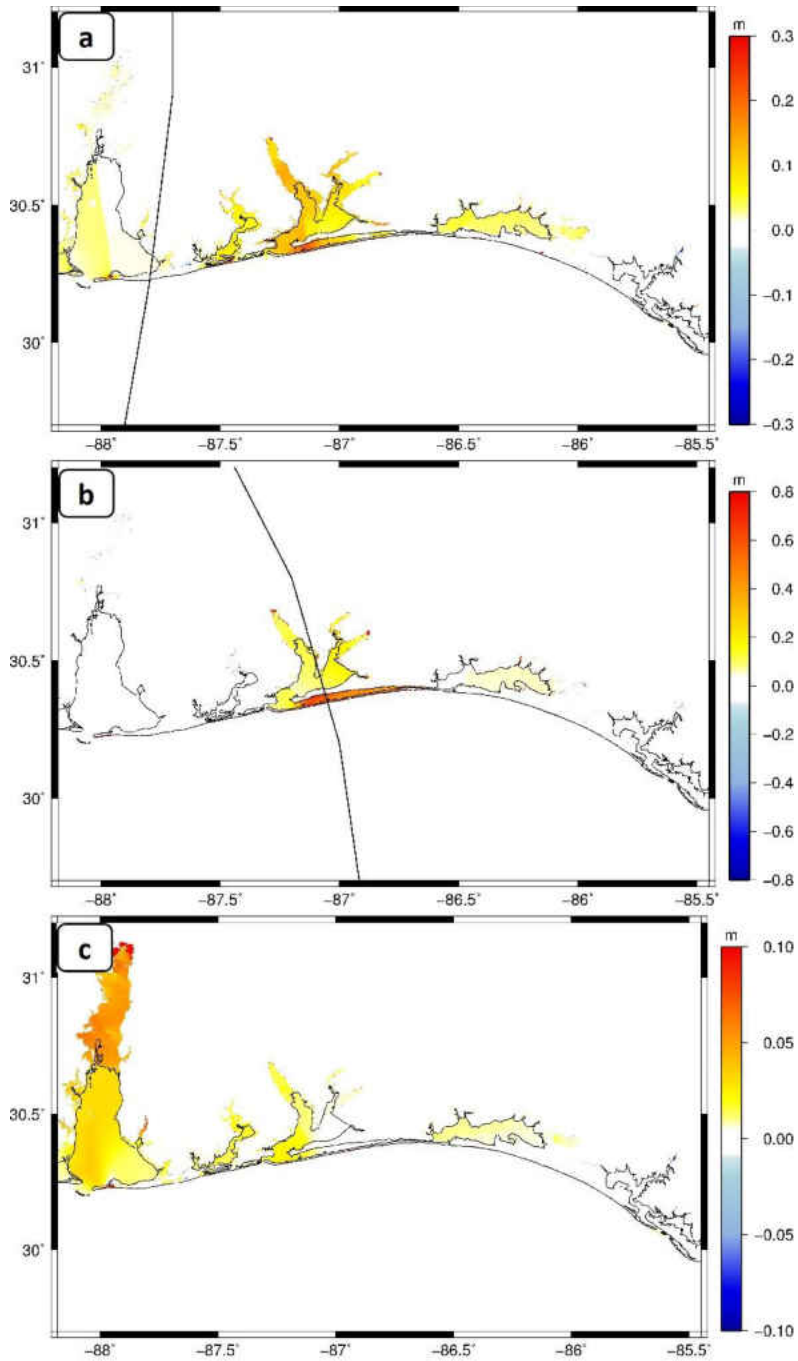


Figure 4.3: Difference in maximum elevations of water for 2050-S and 2050 simulations of (a) Hurricane Ivan (b) Hurricane Dennis and (c) Hurricane Katrina, solid black line represents hurricane track; color scale bar changes in each plot.

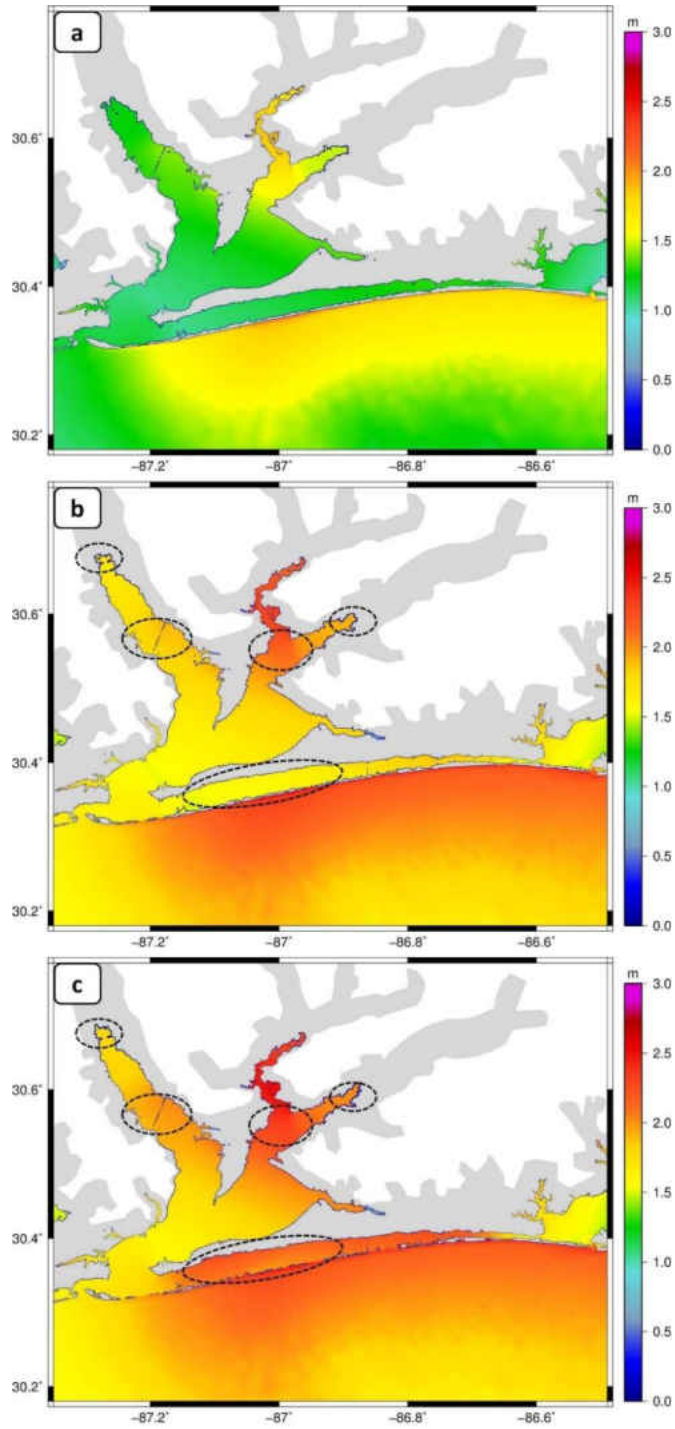


Figure 4.4: Maximum elevations of water for Hurricane Dennis (a) 2005, (b) 2050 (c) 2050-S simulations, illustrating extent of overtopping of Santa Rosa Island; dotted ovals indicate notable regions of increased inundation.

Table 4.3: Peak surge values and location for Hurricanes Ivan, Dennis and Katrina under 2005, 2050 and 2050-S scenarios

Hurricane	Peak surge location	Peak surge (m)		
		2005	2050	2050-S
Ivan	NE Pensacola	4.31	4.8	4.93
Dennis	Santa Rosa Island	2.08	2.53	2.54
Katrina	Mobile Bay floodplain	3.55	4.15	3.15

Table 4.4: Dry area and inundation index for barrier islands under 2005, 2050 and 2050-S scenarios for Hurricanes Ivan, Dennis and Katrina

Location	Hurricane	Dry Area (km ²)			Inundation Index			% increase in index from 2050 to 2050-S
		2005	2050	2050-S	2005	2050	2050-S	
Fort Morgan Peninsula	Ivan	14.6	9.58	9.28	0.39	0.60	0.59	-1%
	Dennis	23.36	18.43	17.07	0.03	0.23	0.25	8%
	Katrina	14.91	10.55	9.97	0.38	0.56	0.56	0%
Perdido Key	Ivan	6.10	3.80	3.58	0.53	0.71	0.74	5%
	Dennis	12.81	11.48	11.65	0.02	0.12	0.16	36%
	Katrina	12.82	11.53	11.55	0.02	0.11	0.17	47%
Santa Rosa Island	Ivan	21.04	19.28	14.73	0.51	0.55	0.63	15%
	Dennis	41.89	34.09	23.96	0.03	0.21	0.40	93%
	Katrina	42.26	40.66	36.15	0.02	0.06	0.10	75%
St. Andrew Barrier	Ivan	7.08	4.59	4.61	0.37	0.59	0.64	7%
	Dennis	6.54	4.07	4.10	0.42	0.64	0.68	6%
	Katrina	10.53	8.22	8.64	0.06	0.27	0.32	18%

Table 4.5: Volumes of surge and percent increases for bay systems under 2005, 2050 and 2050-S scenarios for Hurricanes Ivan, Dennis and Katrina

		Volume of Surge (km ³)			% increase from 2050 to 2050-S
Location	Hurricane	2005	2050	2050-S	
Mobile Bay	Ivan	1.32	1.78	1.79	1%
	Dennis	0.81	1.26	1.26	0%
	Katrina	2.30	2.83	2.85	1%
Perdido Bay	Ivan	0.19	0.24	0.24	0%
	Dennis	0.08	0.12	0.12	0%
	Katrina	0.11	0.15	0.15	0%
Santa Rosa Sound	Ivan	0.29	0.37	0.38	3%
	Dennis	0.15	0.21	0.26	24%
	Katrina	0.12	0.18	0.18	0%
Pensacola Bay	Ivan	0.88	1.06	1.09	3%
	Dennis	0.40	0.56	0.59	7%
	Katrina	0.35	0.50	0.50	0%
Choctawhatchee Bay	Ivan	0.42	0.58	0.59	2%
	Dennis	0.30	0.46	0.47	3%
	Katrina	0.25	0.39	0.39	0%
St. Andrew Bay	Ivan	0.33	0.43	0.43	0%
	Dennis	0.34	0.45	0.45	0%
	Katrina	0.15	0.25	0.25	0%

4.4 Discussion

Tidal ranges increased in each of the bay systems in the 2050 scenario. If a static approach was taken, the water levels would be elevated by the amount of SLR but the increase in tidal range would not be captured. Tidal prisms also increased nonlinearly with tidal ranges in the 2050 scenario, and either increased, decreased, or remained the same in the 2050-S scenario depending on whether the bay experienced a net increase or decrease in the planform area as a result of the shoreline erosion and accretion. A change in tidal range (and therefore tidal prisms) may affect the productivity of salt marsh systems, as tidal range and inundation depth are fundamental parameters governing suspended sediment transport and deposition on the marsh platform (Fitzgerald et al., 2008). Residual currents were minimally altered in both the 2050 and 2050-S scenarios. Although tidal parameters had a relatively small nonlinear response to SLR and the projected shoreline changes in comparison with storm surge, it is important to note that this is a microtidal system; in systems with greater tidal influences, the response could be more significant. In addition, changes to the inlet geometry could potentially further alter the tidal range, tidal prisms and residual velocities.

Simulating storm surge under future sea levels and shoreline changes highlighted the vulnerability of the barrier islands to increased flooding. Although Perdido Key and Santa Rosa Island experienced increased inundation during the 2050 Ivan and Dennis simulations as compared to the 2005 simulations, the St. Andrew Barrier experienced the largest increase in inundation from the 2005 scenarios. This indicates that elevated water levels due to SLR not only affect barrier island inundation where hurricanes make landfall, but may also affect barrier islands further away.

Santa Rosa Island was especially susceptible to additional overtopping when the projected shoreline changes were included. Unlike the other barrier islands in the study area, the island is long and narrow, and backed with a wide, enclosed Sound. The projected shoreline erosion along the Gulf side of the island increased the flooding inundation during all three storm surge simulations, which caused many new areas to overtop. The increase in overtopping allowed additional water to inundate the back-bays, and furthered the inundation extent and depth in the nearby floodplain, especially during Dennis. Although not considered in this study, it is important to note that overtopping could induce erosion of the foreshore and dunes, and if the island was submerged long enough, fast moving flows and wave forces could initiate breaching. This could lead to additional flooding in the back-bays and floodplain, and amplify effects of the storm surge recession.

Inundation in the 2050-S simulation remained relatively the same as the 2050 simulation along Perdido Key despite the projected accretion. However, the back-bay of this barrier did not experience any increases in the volume of surge; the only way for higher water levels to enter the back-bays would be through additional overtopping of the barrier island. The stretch of mainland beach between Destin and Panama City was not affected by additional storm surge inundation, illustrating the greater susceptibility of barrier island systems to SLR and shoreline changes, including their back-bays.

4.5 Conclusions

The results of this study reinforce the necessity to model SLR as a dynamic process due to nonlinearities in the hydrodynamic response. Incorporating estimates of future shoreline and

barrier island morphology had varying impacts on the astronomic tide and storm surge hydrodynamics. The increases in tidal range and tidal prism in the 2050 simulation demonstrate the nonlinear nature of the tidal response to SLR, which would not be evident if a static approach was used. Although incorporating the projected Gulf and bay shoreline changes did not alter tidal ranges, tidal prisms responded with both increases and decreases depending on whether the projected shoreline changes increased or decreased the planform of the bay.

Santa Rosa Island was vulnerable to increased overtopping from storm surge when the projected erosion was included, due to the narrow geometry of the island. An increase in overtopping allowed additional water to inundate back-bays, and furthered the inundation extent and depth in the nearby floodplain. This is an important consideration for future coastal vulnerability studies, including hurricane-induced coastal erosion hazard studies. Storm surge inundation along the accretional barrier islands remained relatively the same; however, the accretion prevented additional overtopping and limited more water from entering the back-bays. The stretch of mainland beach between Destin and Panama City was not affected by additional storm surge inundation, illustrating the greater susceptibility of barrier island systems to SLR and shoreline changes, including their back bays.

Future hydrodynamic studies investigating the response of coastal systems to SLR should not only consider modeling dynamic SLR but also, at a minimum, an assessment of related dynamic shoreline changes. The sensitivity of a coastal system to future shoreline changes should be uniquely evaluated for individual areas; if assessment results indicate sensitivity, estimates of shoreline and morphological changes should be incorporated into the model to evaluate future

hydrodynamics under SLR. Such approaches will benefit interdisciplinary studies such as analyses of coastal ecohydraulics and ecohydrology, to yield better assessments of the effects of SLR on the built and natural coastal environment and lead to more informed management decisions.

4.6 Acknowledgments

This research was funded in part under Award No. NA10NOS4780146 from the National Oceanic and Atmospheric Administration (NOAA) Center for Sponsored Coastal Ocean Research (CSCOR). The STOKES Advanced Research Computing Center (ARCC) (webstokes.ist.ucf.edu) provided computational resources for the simulations (System Administrators: C. Finch and S. Tafur). The authors would like to thank A. Warnock, S. Stephens, K. Alizad and the two anonymous reviewers for their constructive comments. The statements and conclusions are those of the authors and do not necessary reflect the views of NOAA-CSCOR, STOKES ARCC, or their affiliates.

4.7 References

- Atkinson, J. H., Smith, J. M. and Bender, C. (2013). "Sea-level rise effects on storm surge and nearshore waves on the Texas coast: influence of landscape and storm characteristics." *Journal of Waterway, Port, Coastal, and Ocean Engineering* 139(2): 98-117.
- Bilskie, M. V., Hagen, S. C., Medeiros, S. C. and Passeri, D. L. (2014). "Dynamics of sea level rise and coastal flooding on a changing landscape." *Geophysical Research Letters* 41(3): 927-234.
- Bruun, P. (1954). "Coast Erosion and the Development of Beach Profiles ". Beach Erosion Board.
- Bruun, P. (1962). "Sea-level rise as a cause of shore erosion." *Proceedings of the American Society of Civil Engineers, Journal of the Waterways and Harbors Division* 88: 117-130.

- Church, J. A. and White, N. J. (2006). "A 20th century acceleration in global sea-level rise." *Geophys. Res. Lett.* 33(1): L01602.
- Cobell, Z., Zhao, H., Roberts, H. J., Clark, F. R. and Zou, S. (2013). "Surge and wave modeling for Louisiana 2012 coastal master plan." *Journal of Coastal Research* SI(67): 88-108.
- Crowell, M., Douglas, B. C. and Leatherman, S. P. (1997). "On Forecasting Future U.S. Shoreline Positions: A Test of Algorithms." *Journal of Coastal Research* 13(4): 1245-1255.
- Crowell, M. and Leatherman, S. P. (1999). "Coastal Erosion Mapping and Management." *Journal of Coastal Research* 28 (Special Issue): 196.
- Davidson-Arnott (2005). "Conceptual model of the effects of sea level rise on sandy coasts." *Journal of Coastal Research* 21(6): 1166-1172.
- Dawson, A. G., Gomez, C., Ritchie, W., Batstone, C., Lawless, M., Rowan, J. S., Dawson, S., McIlveny, J., Bates, R. and Muir, D. (2012). "Barrier island geomorphology, hydrodynamic modeling, and historic shoreline change: An example from South Uist and Benbecula, Scottish Outer Hebrides." *Journal of Coastal Research* 28(6): 1462-1476.
- Dean, R. G. (1991). "Equilibrium Beach Profiles: Characteristics and Applications." *Journal of Coastal Research* 7(1): 53-84.
- Dean, R. G. and Grant, J. (1989). "Development of Methodology for Thirty-Year Shoreline Projections in the Vicinity of Beach Nourishment Projects". Tallahassee, FL, Division of Beaches and Shores, Florida Department of Natural Resources.
- Department of Environmental and Heritage Protection (2013). "Coastal Hazard Technical Guide, Determining Coastal Hazard Areas", The State of Queensland.
- Donoghue, J. F. (2011). "Sea level history of the northern Gulf of Mexico coast and sea level rise scenarios for the near future." *Climatic Change* 107(1-2): 17-33.
- Fenster, M. S., Dolan, R. and Elder, J. F. (1993). "A new method for predicting shoreline positions from historical data." *Journal of Coastal Research* 9(1): 147-171.
- Fitzgerald, D. M., Fenster, M. S., Argow, B. A. and Buynevich, I. V. (2008). "Coastal Impacts Due to Sea Level Rise." *Annual Review Earth Planet Science* 36: 601-647.
- Fitzgerald, D. M., Howes, N., Kulp, M., Hughes, Z., Georgiou, I. and Penland, S. (2007). "Impacts of rising sea level to backbarrier wetlands, tidal inlets, and barriers: Barataria Coast, Louisiana." *Proceedings of Coastal Sediments 2007 CD-ROM13*.

- Galgano, F. A. and Douglas, B. C. (2000). "Shoreline position prediction: methods and errors." *Environmental Geosciences* 7(1): 1-10.
- Hagen, S., Daranpob, A., Bacopoulos, P., Medeiros, S., Bilskie, M., Coggin, D., Salisbury, M., Atkinson, J. and Roberts, H. (2011). "Storm Surge Modeling for FEMA Flood Map Modernization for the Northwest Florida and Alabama Coast, Digital Elevation Model and Finite Element Mesh Development". University of Central Florida.
- Hagen, S. C. and Bacopoulos, P. (2012). "Coastal Flooding in Florida's Big Bend Region with Application to Sea Level Rise Based on Synthetic Storms Analysis." *Terr. Atmos. Ocean. Sci.* 23: 481-500.
- Hagen, S. C., Morris, J. T., Bacopoulos, P. and Weishampel, J. F. (2013). "Sea-Level Rise Impact on a Salt Marsh System of the Lower St. Johns River." *J. Waterway, Port, Coastal, Ocean Eng.* 139(2): 118-125.
- Hallegatte, S., Green, C., Nicholls, R. J. and Corfee-Morlot, J. (2013). "Future flood losses in major coastal cities." *Nature Clim. Change* 3: 802-806.
- Hallegatte, S., Patmore, N., Mestre, O., Dumas, P., Corfee-Morlot, J., Herweijer, C. and Muir-Wood, R. (2011). "Assessing Climate Change Impacts, Sea Level Rise and Storm Surge Risk in Port Cities: A Case Study on Copenhagen." *Climatic Change* 104: 113-137.
- Hanson, H. (1989). "Genesis - A Generalized Shoreline Change Numerical Model." *Journal of Coastal Research* 5(1): 1-27.
- Hapke, C. J., Himmelstoss, E. A., Kratzmann, M., List, J. H. and Thieler, E. R. (2010). "National assessment of shoreline change; historical shoreline change along the New England and Mid-Atlantic coasts". Open-File Report 2010-1118, U.S. Geological Survey: 57p.
- Irish, J. L., Resio, D. T. and Cialone, M. A. (2009). "A surge response function approach to coastal hazard assessment. Part 2: Quantification of spatial attributes of response functions." *Natural Hazards* 51: 183-205.
- Leadon, M. E. (1999). "Beach, Dune and Offshore Profile Response to a Severe Storm Event." *ASCE Coastal Sediments* Long Island, NY.
- Leatherman, S. P. (1990). "Modeling shore response to sea-level rise on sedimentary coasts." *Progress in Physical Geology* 14(4): 447-464.
- Luetlich, R. A., Westerink, J. J. and Scheffner, N. W. (1992). "ADCIRC: An Advanced Three-Dimensional Circulation Model For Shelves, Coasts, and Estuaries, I: Theory and Methodology of ADCIRC-2DDI and ADCIRC-3DL", U.S. Army Corps of Engineers.

- May, S. K., Kimball, W. H., Grady, N. and Dolan, R. (1982). "CEIS: The coastal erosion information system." *Shore and Beach* 50: 19-26.
- Miller, T. L., Morton, R. A., Sallenger, A. H. and Moore, L. J. (2004). "The National Assessment of Shoreline Change: A GIS Compilation of Vector Shorelines and Associated Shoreline Change Data for the US Gulf of Mexico". USGS Open File Report 2005-1089. St. Petersburg, Florida, US Geological Survey, St. Petersburg Coastal and Marine Science Center.
- Morton, R. A., Miller, T. L. and Moore, L. J. (2004). "National assessment of shoreline change: Part 1: Historical shoreline changes and associated coastal land loss along the U.S. Gulf of Mexico". Open-file Report 2004-1043. St. Petersburg, Florida, U.S. Geological Survey: 45p.
- Mousavi, M. E., Irish, J. L., Frey, A. E., Olivera, F. and Edge, B. L. (2011). "Global warming and hurricanes: the potential impact of hurricane intensification and sea level rise on coastal flooding." *Climatic Change* 104(3-4): 575-597.
- National Research Council (1987). Responding to Changes in Sea Level: Engineering Applications. Washington DC, The National Academies Press.
- Nicholls, R. J., Hoozemans, F. M. J. and Marchand, M. (1999). "Increasing flood risk and wetland losses due to sea-level rise: regional and global analyses." *Global Environmental Change* 9: S69-S87.
- Parris, A., Bromirski, P., Burkett, V., Cayan, D., Culver, M., Hall, J., Horton, R., Knuuti, K., Moss, R., Obeysekera, J., Sallenger, A. and Weiss, J. (2012). "Global Sea Level Rise Scenarios for the United States National Climate Assessment". NOAA Tech Memo OAR CPO-1: 37.
- Patterson, D. (2009). "Modeling the Shoreline Impacts of Richmond River Training Walls." *Proceedings of the 18th NSW Coastal Conference*.
- Ranasinghe, R., Duong, T. M., Uhlenbrook, S., Roelvink, D. and M., S. (2012). "Climate-change impact assessment for inlet-interrupted coastlines." *Nature Climate Change* 3: 83-87.
- Ranasinghe, R., Watson, P., Lord, D., Hanslow, D. and Cowell, P. (2007). "Sea Level Rise, Coastal Recession and the Bruun Rule." *Proceedings of the 18th Australasian Coastal and Ocean Engineering Conference*.
- Resio, D. T., Irish, J. L. and Cialone, M. A. (2008). "A surge response function approach to coastal hazard assessment - Part 1: basic concepts." *Natural Hazards* 51: 163-182.

- Reyes, E., Georgiou, I., Reed, D. and McCorquodale, A. (2005). "Using models to evaluate the effects of barrier islands on estuarine hydrodynamics and habitats: a numerical experience." *Journal of Coastal Research* 44: 176-185.
- Rice, T. M. (2012). "Inventory of habitat modifications to tidal inlets in the coastal migration and wintering range of the piping plover (*Charadrius melodus*). Appendix 1B in Draft Comprehensive Conservation Strategy for the Piping Plover (*Charadrius melodus*) Coastal Migration and Wintering Range", U.S. Fish and Wildlife Service: 35.
- Rosati, J. D., Dean, R. G. and Walton, T. L. (2013). "The modified Bruun Rule extended for landward transport." *Marine Geology* 340: 71-81.
- Rossington, S. K. (2008). "Modelling Large Scale Estuarine Morphodynamics Using Equilibrium Concepts: Responses to Anthropogenic Disturbance and Climatic Change", University of Southampton. **Dissertation.**
- Slinn, D. (2013). "Wave Setup Validation Report for the Alabama-Florida Panhandle Flood Study". Gainesville, FL, University of Florida.
- Smith, J. M., Cialone, M. A., Wamsley, T. V. and McAlpin, T. O. (2010). "Potential impact of sea level rise on coastal surges in southeast Louisiana." *Ocean Engineering* 37: 37-47.
- Stevens, S. (2010). "Estuarine Shoreline Response to Sea Level Rise". Prepared for Lake Macquarie City Council.
- Thieler, E. R. and Hammar-Klose, E. S. (1999). "National Assessment of Coastal Vulnerability to Sea Level rise: Preliminary Results for the U.S. Atlantic Coast". Woods Hole, Massachusetts, U.S. Geological Survey.
- Thieler, E. R. and Hammar-Klose, E. S. (2000). "National Assessment of Coastal Vulnerability to Sea-Level Rise: Preliminary Results for the U.S. Gulf of Mexico Coast". Woods Hole, MA, U.S. Geological Survey.
- University of Central Florida (2011). "Flood Insurance Study: Florida Panhandle and Alabama, Model Validation". Technical Study Documentation Notebook, FEMA.
- Vitousek, S., Fletcher, C. H., Merrifield, M. A., Pawlak, G. and Storlazzi, C. D. (2007). "Model scenarios of shoreline change at Kaanapali Beach, Maui, Hawaii: Seasonal and Extreme Events." *Coastal Sediments*, ASCE.
- Walton, T. L. and Dean, R. G. (2007). "Temporal and Spatial Change in Equilibrium Beach Profiles from the Florida Panhandle." *Journal of Waterway, Port, Coastal and Ocean Engineering* 133: 364-376.

- Wang, P., Kirby, J. H., Haber, J. D., Horwitz, M. H., Knorr, P. O. and Krock, J. R. (2006). "Morphological and Sedimentological Impacts of Hurricane Ivan and Immediate Poststorm Beach Recovery along the Northwestern Florida Barrier-Island Coasts." *Journal of Coastal Research* 22(6): 1382-1402.
- Williams, S. J. (2004). "Coastal Erosion and Land Loss Around the United States: Strategies to Manage and Protect Coastal Resources – Examples from Louisiana." *Coastal Ecosystems and Federal Activities Technical Training Symposium Proceedings*, Gulf Shores State Park, AL.
- Williams, S. J., Penland, S. and Sallenger, A. H. J. (1992). "Louisiana Barrier Island erosion study. Atlas of shoreline changes in Louisiana from 1853 to 1989". USGS Reston, VA, USGS/La. State University Misc. Investig. Ser. I-2150-A.
- Woodruff, J. D., Irish, J. L. and Camargo, S. J. (2013). "Coastal flooding by tropical cyclones and sea level rise." *Nature* 504: 44-52.
- Zhang, K., Douglas, B. and Leatherman, S. (2002). "Do Storms Cause Long-Term Beach Erosion along the U.S. East Barrier Coast?" *The Journal of Geology* 110(4): 493-502.
- Zhang, K., Douglas, B. C. and Leatherman, S. P. (2004). "Global warming and coastal erosion." *Climatic Change* 64(1/2): 41-58.

CHAPTER 5. IMPACTS OF HISTORIC MORPHOLOGY AND SEA LEVEL RISE ON TIDAL HYDRODYNAMICS

The content in this chapter is submitted as: Passeri, D.L., Hagen, S.C., Medeiros, S.C., Bilskie, M.V. 2015. Impacts of historic morphology and sea level rise on tidal hydrodynamics in a microtidal estuary (Grand Bay, Mississippi). *Continental Shelf Research, Under Review*.

5.1 Introduction

SLR has the potential to alter astronomic tidal hydrodynamics by increasing tidal ranges, tidal prisms and inundation, as well as changing current velocities and circulation patterns (French, 2008; Leorri et al., 2011; Hall et al., 2013; Valentim et al., 2013). Within estuaries, tidal asymmetries and resulting sediment transport patterns may be fundamentally altered if rising seas increase channel depths or alter the volume of water stored in the intertidal zone (Friedrichs et al., 1990). In addition, changes in coastal topography can influence the hydrodynamic response under SLR (Bilskie et al., 2014; Passeri et al., 2015). Changes in tidal hydrodynamics have important implications for navigation, fisheries, coastal flooding, and the evolution of the coastline. However, the complexities in coastal processes make determining the future impacts of SLR and coastal topography a difficult task. Evaluating historic changes in hydrodynamics under a changing landscape in conjunction with SLR can provide insight as to how water levels and currents may change in the future.

The marine dominant Grand Bay estuary is one of the few remaining coastal marsh environments in Mississippi. Over the past century, the estuary has undergone natural and anthropogenic induced landscape changes including the diversion of the estuary's sediment source and the erosion of its protective barrier island, Grand Batture. As a result, marshes in Grand Bay are being eroded away

faster than any other marsh in the state (Mississippi Department of Marine Resources, 1999). The fate of the estuary depends on scientifically informed managerial decisions regarding factors such as SLR and changes in coastal morphology. This research examines the geophysical influence of SLR and historic morphology on tidal hydrodynamics. A high resolution large-domain hydrodynamic model was used to simulate present (circa 2005) and past conditions (circa 1848, 1917, and 1960) with unique sea levels, bathymetry, topography and shorelines that represent the conditions at those times. Additionally, a hypothetical scenario was performed in which Grand Batture Island exists under 2005 conditions to observe the influence of the island on tidal hydrodynamics. Changes in variables such as harmonic constituent amplitudes, phases and current velocities were examined. Comparison of past and present conditions illustrates the tidal hydrodynamic response of the system to SLR and the changing landscape. This yields a better understanding of the function of coastal morphology and the role of SLR on tidal hydrodynamics, and provides insight into potential future changes.

5.2 Study Domain

The Grand Bay estuary is located within the Mississippi Sound at the MSAL border in the northern Gulf of Mexico (Figure 5.1). The estuary is comprised of two bays (Point aux Chenes Bay and Grand Bay), bayous, and marsh shorelines. The bays are shallow with average water depths ranging from 0.5 m to 1.8 m, and up to 3.0 m at the tidally scoured entrance to Point aux Chenes Bay (Peterson et al., 2007). The estuary supports recreational and commercial fisheries with an abundance of marine life including shrimp, crabs and oysters (Eleuterius and Criss, 1991). This portion of the Gulf of Mexico is a diurnal, microtidal environment. The offshore MSAL barrier

islands (namely Cat Island, Ship Island, Horn Island, Petit Bois Island and Dauphin Island) define the boundary between the Mississippi Sound and the Gulf of Mexico. Three of the barrier island inlets have been modified and connected to mainland ports via navigation channels (Mobile Ship Channel at the inlet to Mobile Bay, Pascagoula Channel at Horn Island Pass, and Gulfport Ship Channel at Ship Island Pass). In addition, the Gulf Intracoastal Water Way (GIWW) extends east to west through the Sound.

Historically, the Escatawpa River flowed south-southeast and emptied into the Mississippi Sound at Grand Bay, creating a delta that encompassed the entire estuary and was sheltered by Dauphin Island. At this time, erosion was limited due to weak tidal and wave forces within the Sound, and was typically counteracted by sediment deposited by the Escatawpa River. However, prior to 1848 (exact time unknown) the river diverted its course and became a tributary of the Pascagoula River, which terminated the direct sediment supply to Grand Bay (Eleuterius and Criss, 1991). During the period of 1740-1766, a hurricane bisected Dauphin Island, creating an inlet and a new island called Petit Bois (Otvos, 1979). By 1848, waves and currents in Grand Bay had shaped deposited deltaic sediments into the Grand Batture Island, an elongated barrier island that sheltered the estuary from northerly directed waves (Eleuterius and Criss, 1991). Dredging of the navigational channels began in the mid-1800s. By 1857, the Mobile Ship Channel was in place; as early as 1880, construction began on the Pascagoula Channel, and in 1899, the Ship Island Pass began. Various studies have examined the influence of the shipping channels on sediment transport in the Sound and have found strong evidence that the channels prevent sediment bypassing around the ebb-tidal deltas thereby depriving downdrift shorelines of the barrier islands (Morton, 2008).

During the 20th century, Grand Bay and the Mississippi Sound underwent major landscape changes due to erosion from normal tidal and wave forces, as well as hurricanes. The eastern end of Dauphin Island, fixed by its Pleistocene core, remained in place but the western end grew through lateral spit accretion (Byrnes et al., 1991; Morton, 2008; Rosati and Stone, 2009). Petit Bois Island began narrowing and rotated counterclockwise on the eastern spit as a result of wave refraction and storm driven overwash, which widened the pass to Dauphin Island. The eroded sediment was deposited on the western end of Petit Bois Island and in Horn Island Pass (Morton, 2008). Horn Island and Horn Island Pass also migrated westward (Byrnes et al., 1991). By 1921, multiple hurricanes and tropical storms within the area had fragmented the Grand Batture Island into several islands (Eleuterius and Criss, 1991). Meanwhile, the pass between Petit Bois Island and Dauphin Island continued to widen. In the late 1920's, Highway 90 was constructed in Mississippi, solidifying the diversion of the Escatawpa River from Grand Bay. Since 1957, the western end of Petit Bois Island has remained in place against the Horn Island Pass due to the maintained navigation channel (Byrnes et al., 1991). The Grand Batture Island continued to erode until 1969 when Hurricane Camille reduced the majority of the island to sand shoals (Eleuterius and Criss, 1991). By 1980, all remnants of the former islands were submerged (Peterson et al., 2007). Lack of protection from the Grand Batture Island and the offshore barriers allowed continuous erosion to reshape Grand Bay's shoreline under normal and extreme conditions. In addition, higher saline waters entering the estuary from the Sound altered marine life, significantly reducing the oyster population in the estuary over the past century (Peterson et al., 2007).

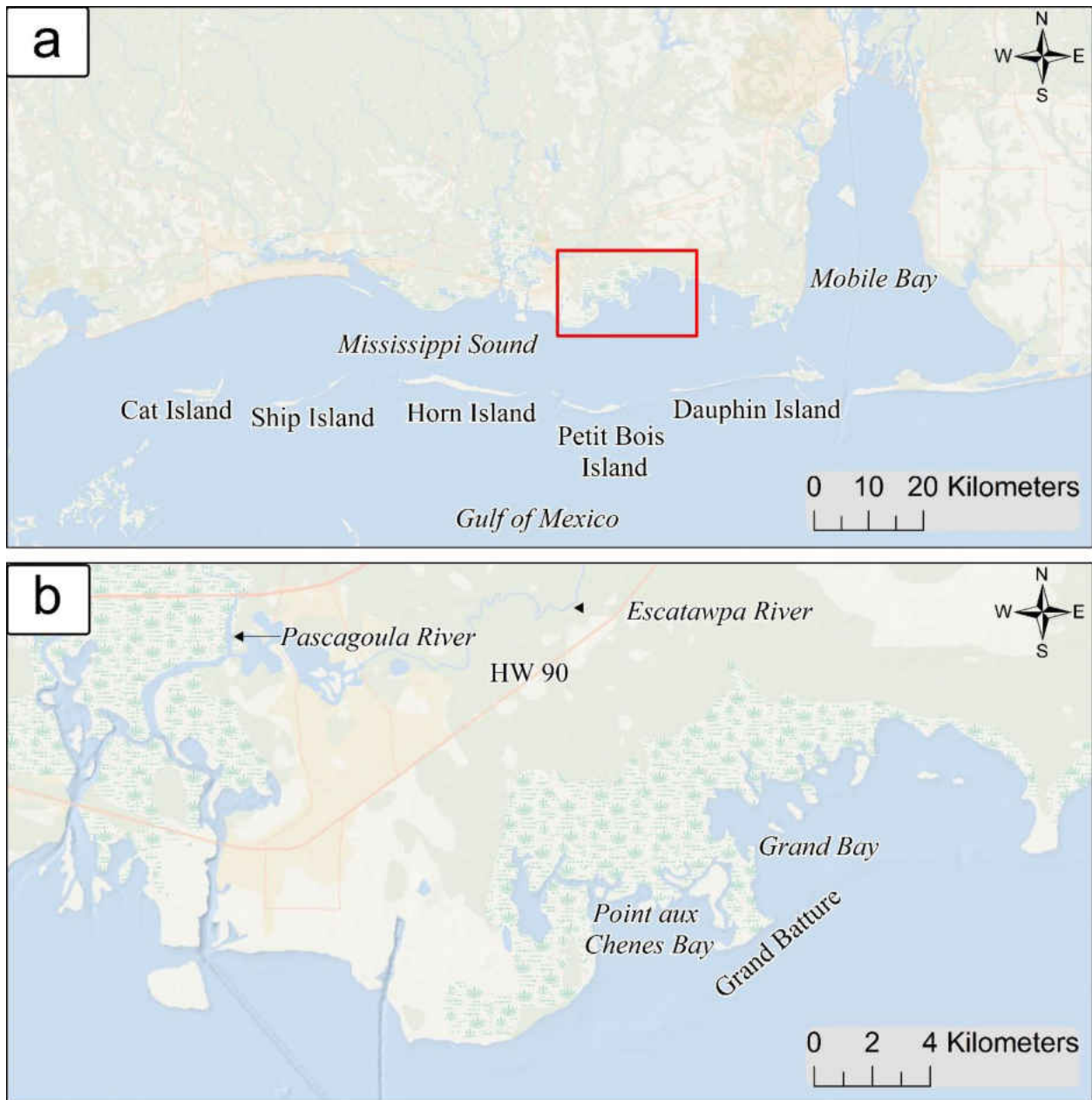


Figure 5.1: Mississippi Sound study area (a) with zoomed in inset of Grand Bay estuary (b) for present day conditions.

5.3 Methodology

5.3.1 Hydrodynamic Model

To simulate tidal hydrodynamics, ADCIRC-2DDI (Luettich et al., 1992), a two-dimensional code that solves the depth-integrated shallow water equations for water surface elevations and currents was employed. The unstructured finite element mesh describes the Western North Atlantic Tidal (WNAT) model domain west of the 60° W meridian (open ocean boundary), including the Caribbean Sea and the Gulf of Mexico. Higher resolution elements (on the order of 20 m to 100 m) were incorporated within the MSAL coast, which permits localized adjustments of the landscape to be made. The model was developed to represent elevations circa 2005 (post-Katrina) using a Digital Elevation Model (DEM) constructed with lidar data, as well as NOS (National Ocean Service) hydrographic surveys, U.S. Army Corps of Engineers (USACE) channel surveys and NOAA (National Oceanographic and Atmospheric Administration) nautical charts. Within the Grand Bay marsh, an elevation correction based on biomass density was employed to adjust the lidar-derived elevations. This technique uses ASTER and IfSAR satellite imagery along with lidar-derived canopy heights to classify the above-ground biomass density as high, medium or low. This biomass density class was then used to lower the lidar DEM by 32, 23 and 16 cm, respectively (Medeiros et al., 2015). Further information on mesh development and topographic elevations can be found in Bilskie et al. (2015).

The hydrodynamic model was validated with available historical storm surge data for Hurricane Katrina (Bilskie et al., 2015) and astronomic tide data. The tidal validation was performed at 18 NOAA tide gauges located throughout the study domain. Astronomic tides were simulated for 45

days beginning from a cold start with a 10-day hyperbolic tangent ramp function. The model was forced with water surface elevations of eight harmonic constituents (K1, O1, M2, S2, N2, K2, Q1, and P1) along the open ocean boundary (Egbert et al., 1994; Egbert and Erofeeva, 2002). Model output consisted of 23 tidal constituents, which were validated against reported tidal constituents at each of the tidal gauging stations (<http://tidesandcurrents.noaa.gov/>) by comparing resynthesized observed and simulated tidal signals. Overall, the model matches well in phase and amplitude, with an average root mean square error (RMSE) of approximately 4 cm.

5.3.2 *Historic Simulations*

When conducting historical (or future) evaluations of the effects of SLR, it is necessary to properly represent the dynamics in the physical system; this study aims to recreate historic conditions to observe the changing tidal hydrodynamic response. Historic shoreline positions in the Grand Bay estuary circa 1848, 1917 and 1960 were obtained from the Mississippi Department of Environmental Quality Office of Geology. Historic bathymetric DEMs within the Mississippi Sound for the time periods of 1847 to 1856, 1917 to 1920, and 1960 to 1970 were obtained from Buster and Morton (2011). The DEMs were constructed using historic bathymetric soundings and digitized shoreline positions from historic NOAA T-sheets. The most significant changes in the bathymetry were surrounding the MSAL barrier islands as a result of the migration of the islands, as well as the construction of the dredged shipping channels; elsewhere, changes were minimal. The overall vertical uncertainty in the DEMs is 0.5 m (Buster and Morton, 2011).

Using the historic data, the hydrodynamic model representing present day (i.e., 2005) conditions was altered to reflect historic conditions circa 1848, 1917 and 1960. To do so, the DEM was

updated with the historic shoreline positions and bathymetric data. This included removing the dredged shipping channels and the GIWW within the Mississippi Sound, altering depths within the Mississippi Sound according to the historic bathymetry, and shifting shoreline positions within the Grand Bay estuary and along the MSAL barrier islands. In addition, the DEM was altered with historic marsh surface elevations in Grand Bay, estimated assuming that the marsh is currently in equilibrium. The historic marsh elevation is equal to the present elevation minus the amount of sea level change, determined from the mean sea level trend. Historic sea levels were estimated using the linear mean sea level trend at a nearby NOAA gauge located along Dauphin Island; the mean sea level trend is 2.98 mm/year, based on monthly mean sea level data from 1966 to 2006. Therefore, historic sea levels were 0.47 m, 0.26 m, and 0.13 m below present day sea level (circa 2005) for the years 1848, 1917, and 1960, respectively. Lastly, a fifth hypothetical scenario was devised in which Grand Batture Island exists under 2005 conditions; the Grand Bay shoreline in the 2005 model was modified to include the Grand Batture Island (this is herein referred to as the 2005-GBI scenario). This scenario aids in examining the influence of the island if it were to be reconstructed in the near future.

Inspection of the model elevations illustrates the elevation changes in the barrier islands (Figure 5.2). In 1848, Petit Bois Island was longer than in 2005 and sheltered most of the Grand Bay estuary. The significant erosion of the eastern spit is visible in the 1917 and 1960 DEMs. In addition, Dauphin Island had elongated westward from 1848 to 1917, although a large breach existed in the middle of the island in 1917 as a result of a hurricane. In 1960, the island was reconnected, but was breached again in 2005 by Hurricane Katrina. In Grand Bay, the Grand

Batture Island was still in place in 1848, was breached in two locations in the center in 1917, and was reduced almost completely to a sand shoal in 1960 as it remains today.

For each of the five scenarios (1848, 1917, 1960, 2005, and 2005-GBI) astronomic tides were simulated for 45 days from a cold start with a 10 day ramp. In addition to forcing the eight harmonic constituents at the open ocean boundary, a ninth “steady” component was included with an amplitude equal to the amount of sea level change for the given scenario to lower the sea level accordingly. As the goal is to simulate tidal hydrodynamics in response to SLR and landscape changes, morphologic processes were not simulated concurrently. Model output consisted of depth-integrated velocities, amplitudes and phases of harmonic constituents, as well as maximum elevations of water and maximum velocities obtained at each node of the mesh for the duration of the simulation.

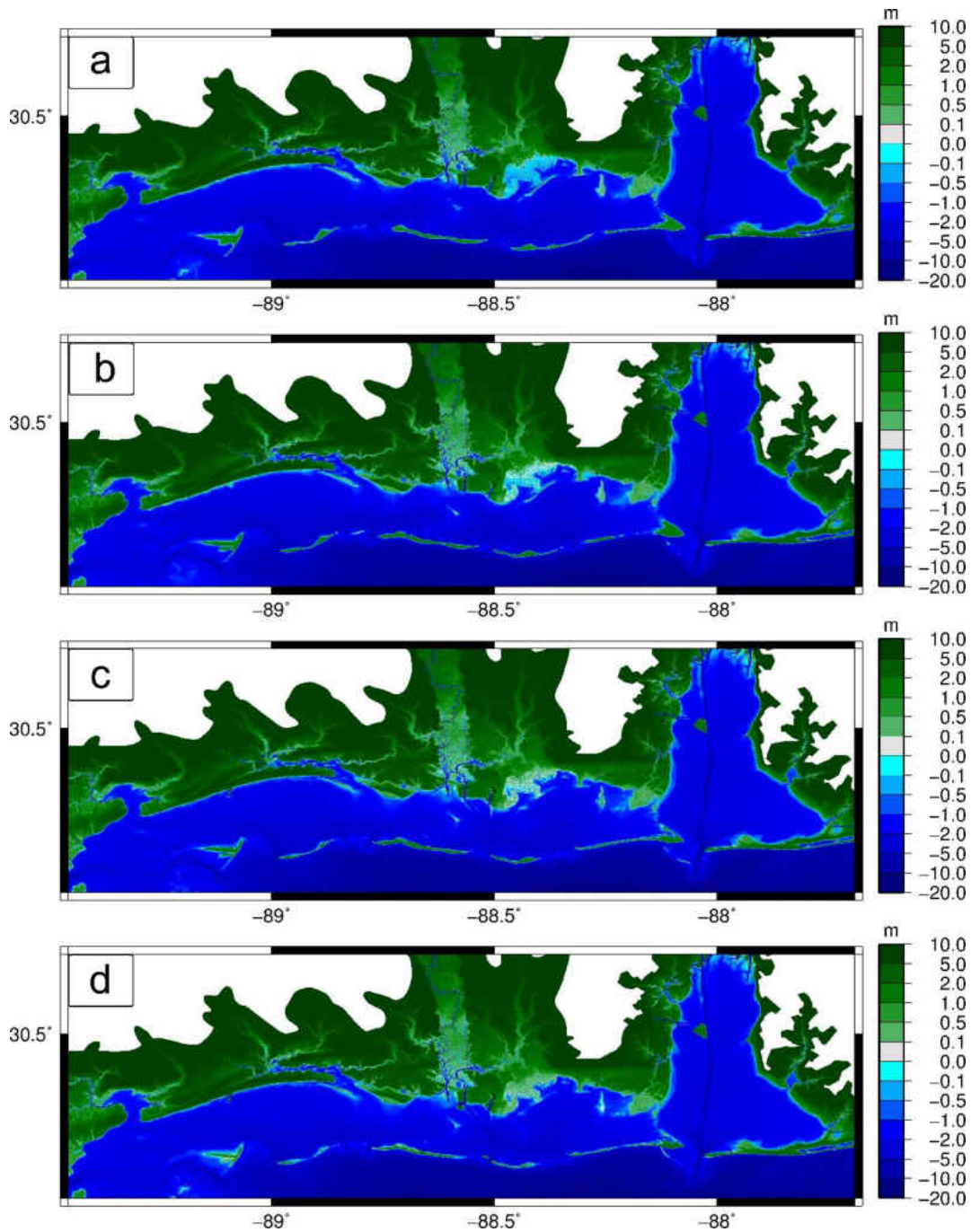


Figure 5.2 Model elevations circa (a) 1848, (b) 1917, (c) 1960 and (d) 2005 using historic bathymetry and shoreline positions in the Mississippi Sound; notable changes include gains and losses of land along the offshore MSAL barrier islands, presence and size of inlets, the existence of the dredged shipping channels, and the submergence of the Grand Batture Island in the Grand Bay estuary.

5.4 Results

The diurnal K1 (principal lunar and solar) and O1 (principal lunar) harmonic constituents dominate tides along this portion of the Gulf of Mexico; the semidiurnal M2 (principal lunar) tide is almost an order of magnitude smaller than the diurnal tides. In 2005, the simulated total tidal amplitude was 45 cm west of Cat Island, 50 cm to 55 cm within the Mississippi Sound, and 45 cm to 50 cm in Mobile Bay. Tides propagate parallel to the coast from east to west and enter the Sound through the inlets of the MSAL barrier islands. Tidal current speeds increase up to 30 cm/s within the inlets. Inside the Sound, current speeds decrease. Semidiurnal overtides and compound tides, which are more prominent within the inlets, result in an asymmetric distortion of the tides with maximum ebb-directed currents and double peaked flood currents (Seim and Sneed, 1988).

5.4.1 Water Levels

Percent changes in the total tidal amplitude from the historic conditions to 2005 were examined (Figure 5.3). Differences greater than 0 indicate the tidal amplitude increased from the historic condition, differences less than 0 indicate the tidal amplitude decreased from the historic condition and differences equal to 0 indicate the tidal amplitude is unchanged from the historic condition. Overall, the magnitude of change was relatively small as a result of the system being microtidal. The largest change occurred west of Cat Island, with increases of 28% (10.0 cm), 15% (6.2 cm) and 13% (5.3 cm) from 1848, 1917 and 1960, respectively. Tidal amplitudes were also altered in Mobile Bay, with increases of 11% (4.4 cm), 7% (3.0 cm) and 20% (7.5 cm) from 1848, 1917 and 1960, respectively. The increase in Mobile Bay from the 1960 scenario resulted from the submergence of the southern spit off of eastern Dauphin Island; the spit was longer in 1960 which

restricted tidal flow through the inlet. Within the Mississippi Sound, changes in tidal amplitudes were not as significant. Amplitudes minimally increased in the western portion of the Sound by 5% (2.7 cm), 4% (2.2 cm) and 5% (2.7 cm) from 1848, 1917 and 1960. In the eastern portion of the Sound and within Grand Bay, amplitudes were unaltered from 1848 and 1917, and minimally increased by 3% (1.6 cm) from 1960. This indicates that barrier island migration was not impactful in altering tidal amplitudes. SLR was more influential in altering amplitudes in Mobile Bay than the Sound, most likely due to the bay having a semi-enclosed shoreline that connects to the Gulf of Mexico with a single inlet. There were no changes in tidal amplitudes offshore, illustrating the greater influence of SLR on the embayments than in the open ocean. Also, there were no changes in the 2005 vs. 2005-GBI scenario, again illustrating the greater influence of SLR than the morphological changes.

To further examine changes in tidal amplitudes, percent changes in the K1, O1 and M2 constituents at the locations specified in Figure 5.3 were examined (Table 5.1). Spatial changes in the amplitudes of the diurnal K1 and O1 constituents were similar in magnitude and pattern. As seen with the total tidal amplitudes, the largest increases from the historic conditions occurred west of Cat Island and within Mobile Bay (as much as 3.1 cm increase west of Cat Island, and 2.5 cm increase in Mobile Bay from 1848). In the eastern portion of the Sound, changes from the historic conditions were minimal. In Mobile Bay, increases in the diurnal constituent amplitudes from 1848 to 2005 were almost equivalent to the increases from 1960 to 2005, indicating that the combined effects of SLR and morphological changes influenced the constituent amplitude, rather than the effects of SLR alone. Within the Sound, the percent change in the M2 amplitude was larger than

the changes in the diurnal constituents; however, changes were small relative to the total tidal amplitude and therefore were not influential.

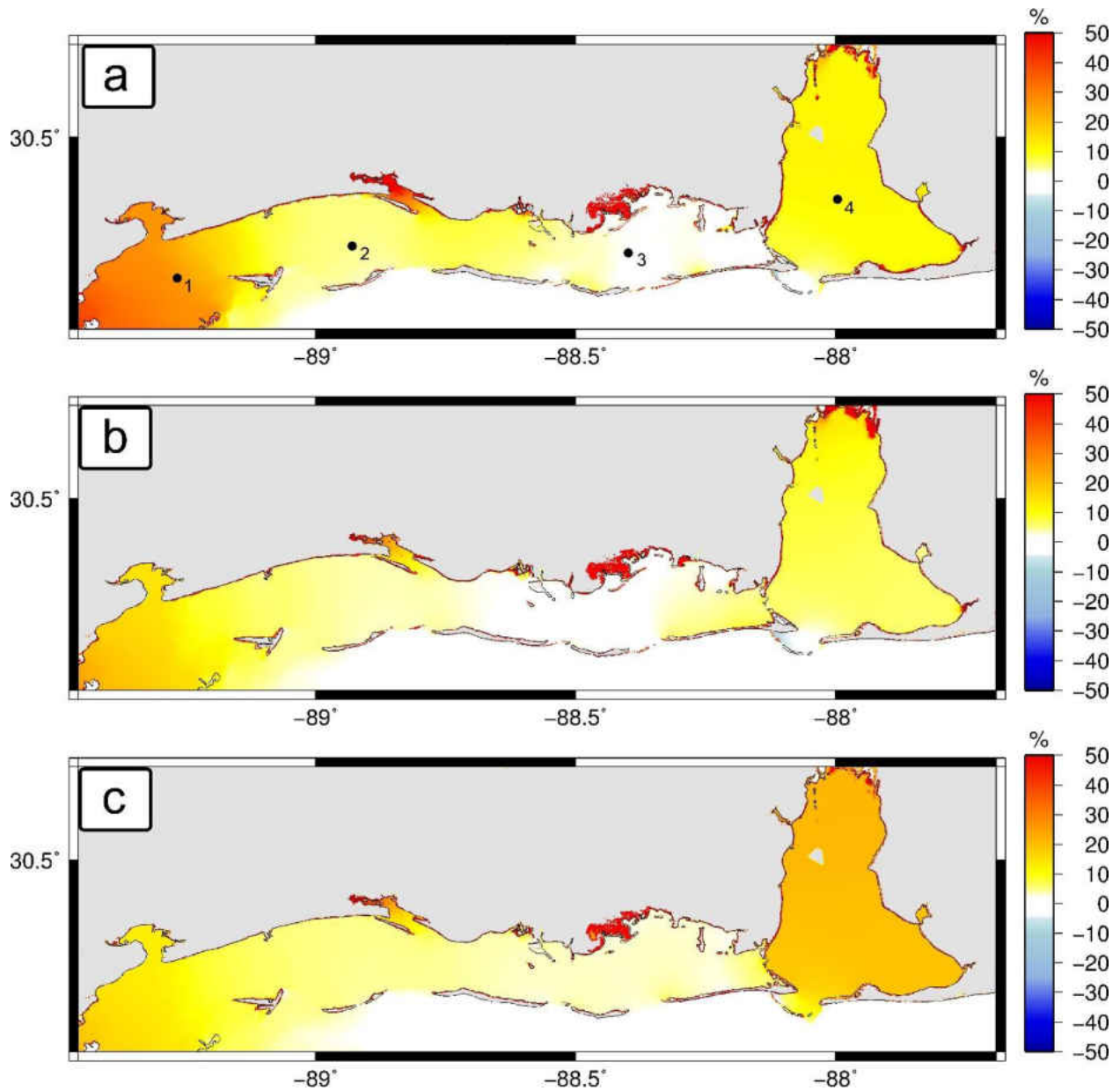


Figure 5.3: Percent change in total tidal amplitude from (a) 1848 to 2005, (b) 1917 to 2005 and (c) 1960 to 2005. The black line represents the 2005 shoreline; differences greater than 0 indicate percent increases in tidal amplitude from the historic condition to 2005, differences less than 0 indicate percent decreases in the tidal amplitude from the historic condition to 2005. The dots in (a) represent locations where constituent amplitudes are measured in Table 1.

Table 5.1: Percent change in constituent amplitudes from 1848 to 2005, 1917 to 2005 and 1960 to 2005 at locations 1-4, illustrated in Figure 5.3.

	2005 Amplitude			% Change from 1848			% Change from 1917			% Change from 1960		
	<i>K1</i>	<i>O1</i>	<i>M2</i>	<i>K1</i>	<i>O1</i>	<i>M2</i>	<i>K1</i>	<i>O1</i>	<i>M2</i>	<i>K1</i>	<i>O1</i>	<i>M2</i>
1	0.16	0.14	0.02	24%	24%	20%	12%	11%	14%	8%	8%	18%
2	0.19	0.18	0.03	5%	4%	6%	4%	3%	5%	3%	3%	12%
3	0.17	0.16	0.02	-1%	0%	60%	1%	1%	15%	2%	2%	16%
4	0.16	0.15	0.01	18%	13%	2%	14%	9%	-13%	16%	17%	34%

Tidal propagation throughout the Mississippi Sound and Grand Bay also changed from the historic conditions. In the 2005 simulation, constituent phases were equal inside of the Sound and offshore of Ship Island. East of Horn Island, phases were lagged within the Sound in comparison with the offshore, indicating slower propagation through the eastern inlets. Differences in harmonic constituent phases were examined to observe changes in tidal propagation; the difference in the *K1* amplitude from the historic conditions to 2005 is summarized in Figure 5.4. Differences equal to 0 indicate the constituent phase was unchanged in 2005 from the historic scenario, differences greater than 0 indicate the constituent phase sped up from the historic scenario, and differences less than 0 indicate the constituent phase was slower than in the historic scenario.

Similar to the constituent amplitudes, changes in the *K1* and *O1* phases were nearly the same in pattern and magnitude. The effects of SLR strongly influenced tidal propagation within the Mississippi Sound. In 2005, the *K1* phase was approximately 19 minutes faster in the Sound and 28 minutes faster in Mobile Bay than in 1848. Directly behind the 1848 location of Petit Bois Island and within Grand Bay, the phase sped up in the 2005 scenario as a result of the westward migration of the island; within Grand Bay, the *K1* phase was faster by approximately 90 minutes in 2005. Overall, the magnitude of change in the *K1* phase in the 1917 vs. 2005 scenario was less

than in the 1848 vs. 2005 scenario. The 1917 breach in Dauphin Island influenced tidal propagation into the Sound. Immediately behind the breach (which also existed in 2005, but was wider in 1917) there was no difference in the K1 phase, although the phase was faster by approximately 10 minutes on the eastern side of Dauphin Island in 1917. In the 1960 vs. 2005 scenario, differences in the K1 phase were more uniform across the Sound, with phases being approximately 17 minutes faster in 2005. This is most likely influenced by SLR, since changes in barrier island morphology were minimal from 1960 to 2005. In Mobile Bay, phases were faster by 47 minutes in 2005 than in 1960, further illustrating the influence of the spit off of Dauphin Island inhibiting tidal flows. No phase changes were observed in the diurnal or semidiurnal constituents in the 2005 vs. 2005-GBI scenario.

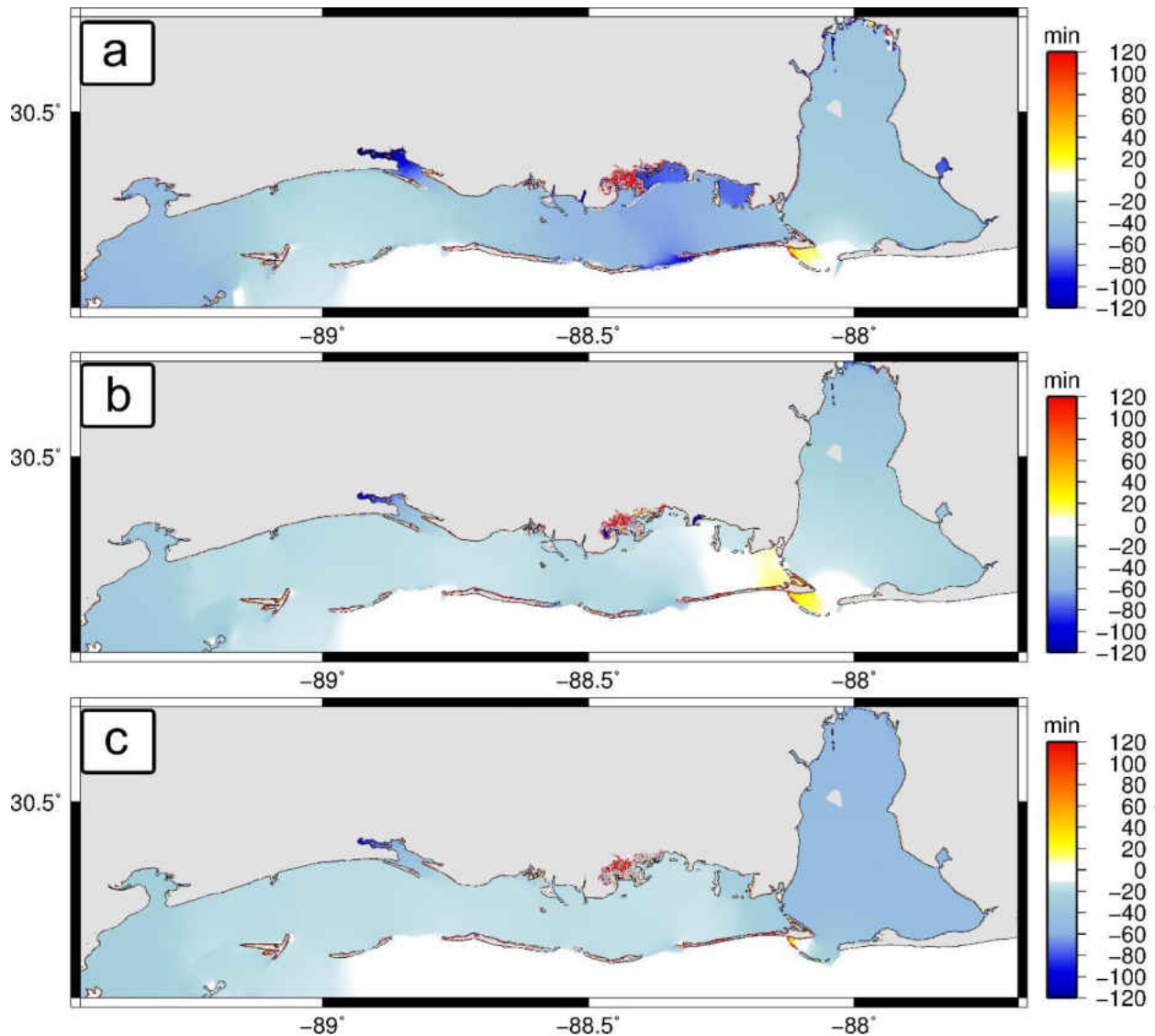


Figure 5.4: Phase differences of the K1 constituent from (a) 1848 to 2005, (b) 1917 to 2005 and (c) 1960 to 2005. The black line represents the 2005 shoreline; differences equal to 0 indicate the constituent phase is unchanged from the historic scenario, differences greater than 0 indicate the constituent phase is slower in 2005 than the historic scenario, and differences less than 0 indicate the constituent phase is faster in 2005 than the historic scenario.

5.4.2 Currents

The migration of the MSAL barrier islands also influenced tidal currents within the Mississippi Sound and Grand Bay. Changes in the maximum tidal velocities between the 1848 vs. 2005, 1917 vs. 2005, 1960 vs. 2005 and 2005 vs. 2005-GBI scenarios are summarized in Figure 5.5. Differences larger than 0 indicate the maximum velocity has increased from historic conditions, differences less than 0 indicate the maximum velocity has decreased from historic conditions. Maximum differences on the order of 20 cm/s occurred within the historic and present locations of the inlets between the MSAL barrier islands, further illustrating the role of the barrier islands in tidal propagation to the Sound. The size and position of the inlets not only control the strength of the currents, but also where the currents are directed in the Sound. As Petit Bois Pass migrated westward, stronger tidal velocities were centered along Grand Batture Island (approximately 5 cm/s stronger in 2005 than in 1848, and 10 cm/s stronger in 2005 than in 1917). This could have aided in the erosion of the island. Maximum tidal velocities did not change within Point aux Chenes Bay, but were approximately 5 cm/s (63%) faster in Grand Bay in 1848 than in 2005. Similarly in the 2005-GBI simulation, maximum velocities were approximately 5 cm/s (63%) faster in both Point aux Chenes and Grand Bay when Grand Batture Island was present. Since 1960, tidal velocities have increased by less than 5 cm/s in the shadow of Petit Bois Pass, with minimal changes in Point aux Chenes Bay and Grand Bay. Velocities also increased from the historic conditions within the dredged shipping channels and the GIWW. Magnitudes of residual currents minimally increased from historic conditions (on the order of millimeters) in the Grand Bay estuary, with slight directional changes from predominately northerly directed currents in the 1848 scenario (and 2005-GBI) to more easterly directed currents in the 2005 scenario.

The flood-ebb ratio (R), the ratio of the magnitude of the maximal flood (U_{flood}) to the maximal ebb (U_{ebb}) currents, indicates if asymmetry exists in the current velocities:

$$R = \frac{U_{flood}}{U_{ebb}} \quad (9)$$

where ratios equal to 1 indicate equal magnitudes of flood and ebb currents (no asymmetry), ratios larger than 1 indicate stronger flood currents than ebb currents (flood dominance), and ratios less than 1 indicate stronger ebb currents than flood currents (ebb dominance). Flood-ebb ratios for 1848, 1917, 1960 and 2005 are summarized in Figure 5.6 as well as percent changes in flood-ebb ratios for 2005 vs. 1848, 2005 vs. 1917 and 2005 vs. 1960 in Figure 5.7. Percent changes equal to 0 indicate no change in the flood-ebb ratio, percent changes greater than 0 indicate currents have become more flood dominant, percent changes less than 0 indicates currents have become more ebb dominant. In the 2005 scenario, the majority of the Sound, Point aux Chenes and Grand Bay had ebb dominant currents. In 1848, portions of the eastern Sound and Grand Bay had flood dominant currents. From 1848 to 2005, the flood-ebb ratio decreased by approximately 9% in Point aux Chenes Bay and 77% in Grand Bay. Since 1917, the flood-ebb ratio remained relatively the same in Point aux Chenes Bay, but decreased by approximately 20% in Grand Bay. In addition, the ratio decreased by approximately 17% landward of Petit Bois Island. Since 1960, the flood-ebb ratio decreased by approximately 10% to 20% throughout most of the Sound. Within the estuary, the ratio decreased by approximately 12% in Point aux Chenes Bay and 23% in Grand Bay. Lastly, the flood-ebb ratio decreased by approximately 20% in Grand Bay in the 2005 vs. 2005-GBI scenario, indicating that currents would be more ebb-dominant if the Grand Batture Island was reconstructed under present day conditions.

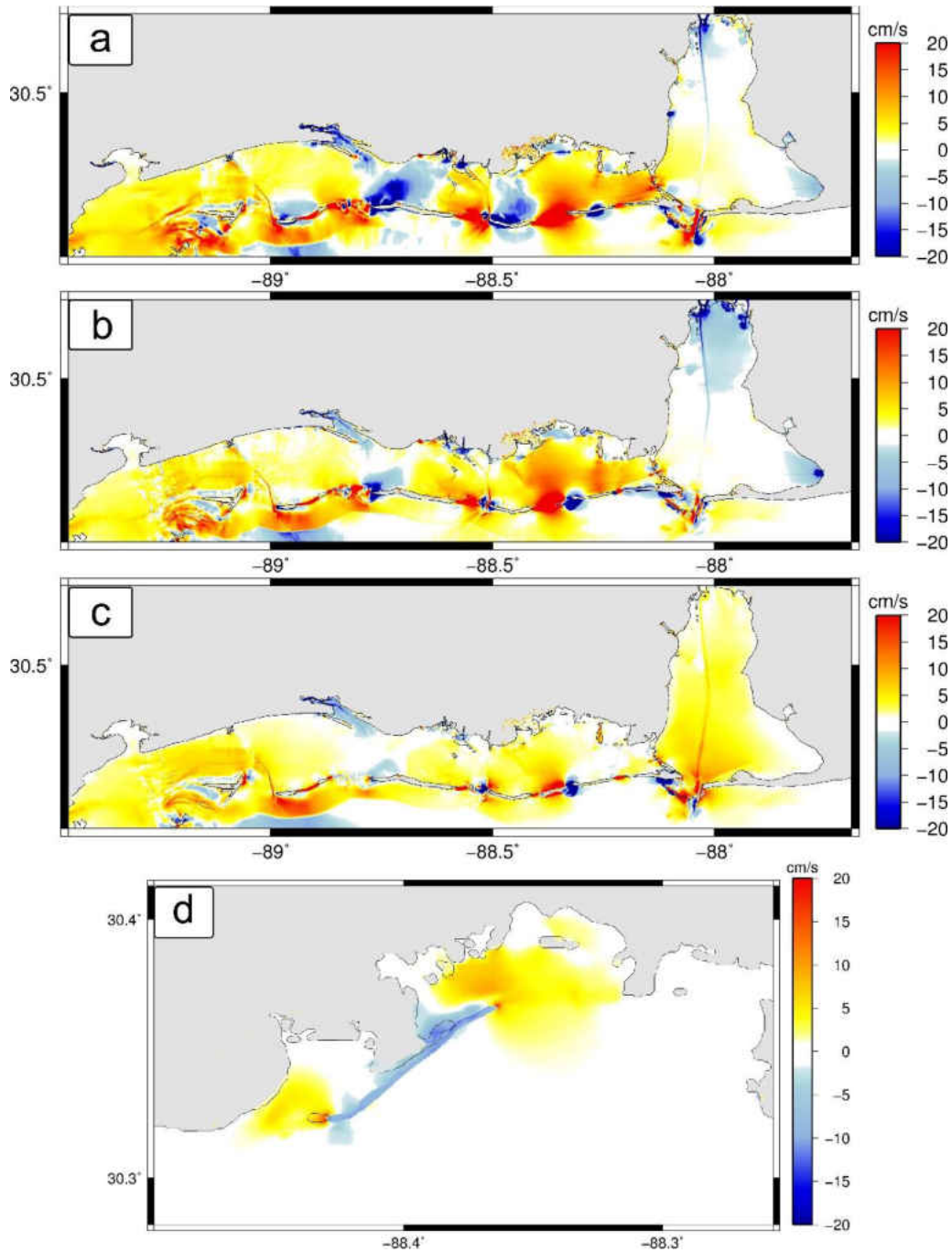


Figure 5.5: Differences in maximum tidal velocities from (a) 1848 to 2005 (b) 1917 to 2005 (c) 1960 to 2005 (d) 2005 to 2005-GBI. The black line represents the 2005 shoreline; differences greater than 0 indicate maximum tidal velocities have increased from the historic condition, differences less than 0 indicate maximum tidal velocities have decreased from the historic condition, differences equal to 0 indicate maximum velocities have not changed.

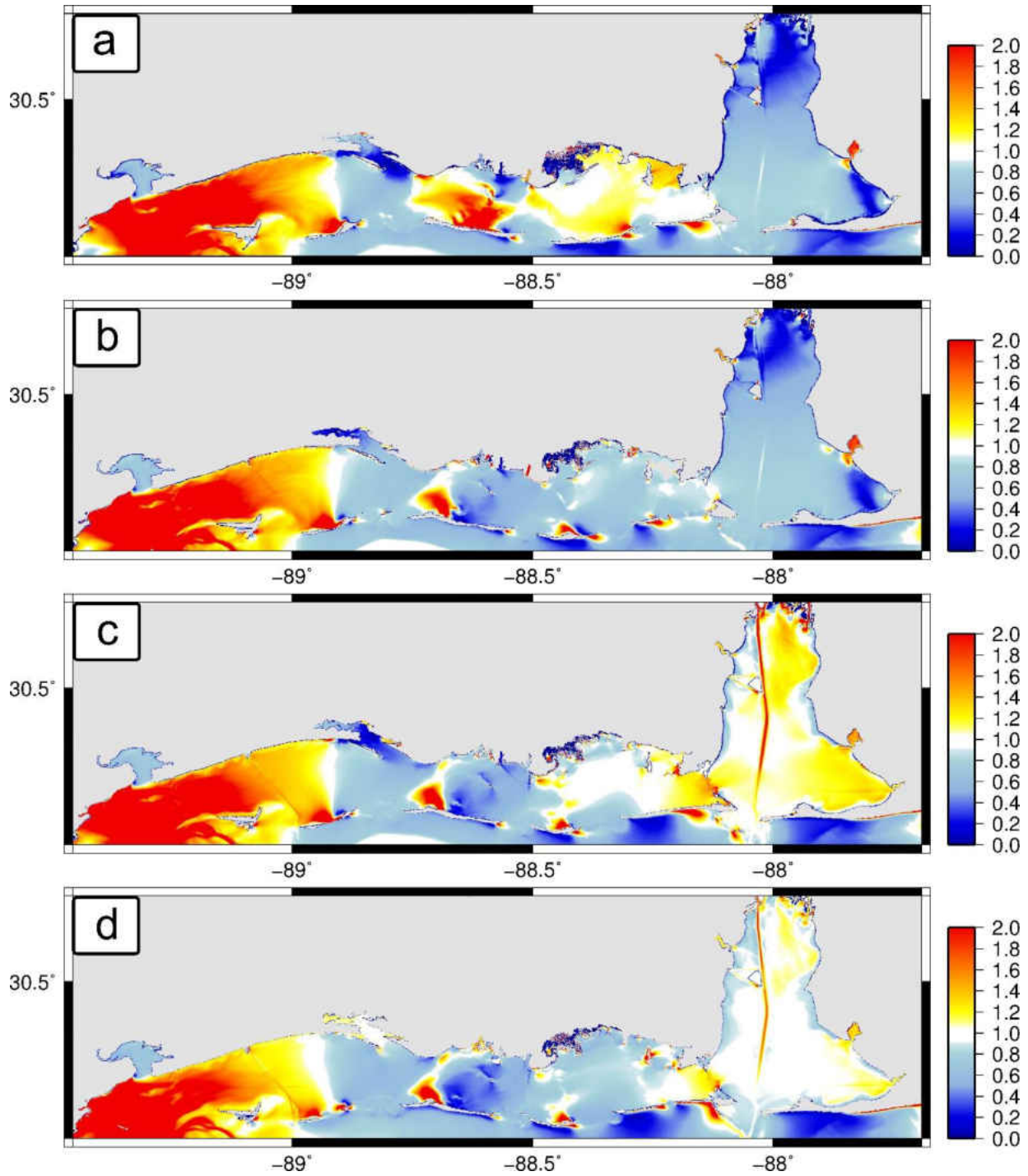


Figure 5.6: Flood-ebb ratios for (a) 1848, (b) 1917, (c) 1960, and (d) 2005. The black line represents the 2005 shoreline; flood-ebb ratios greater than 1 indicate stronger flood currents; ratios less than 1 indicate stronger ebb currents.

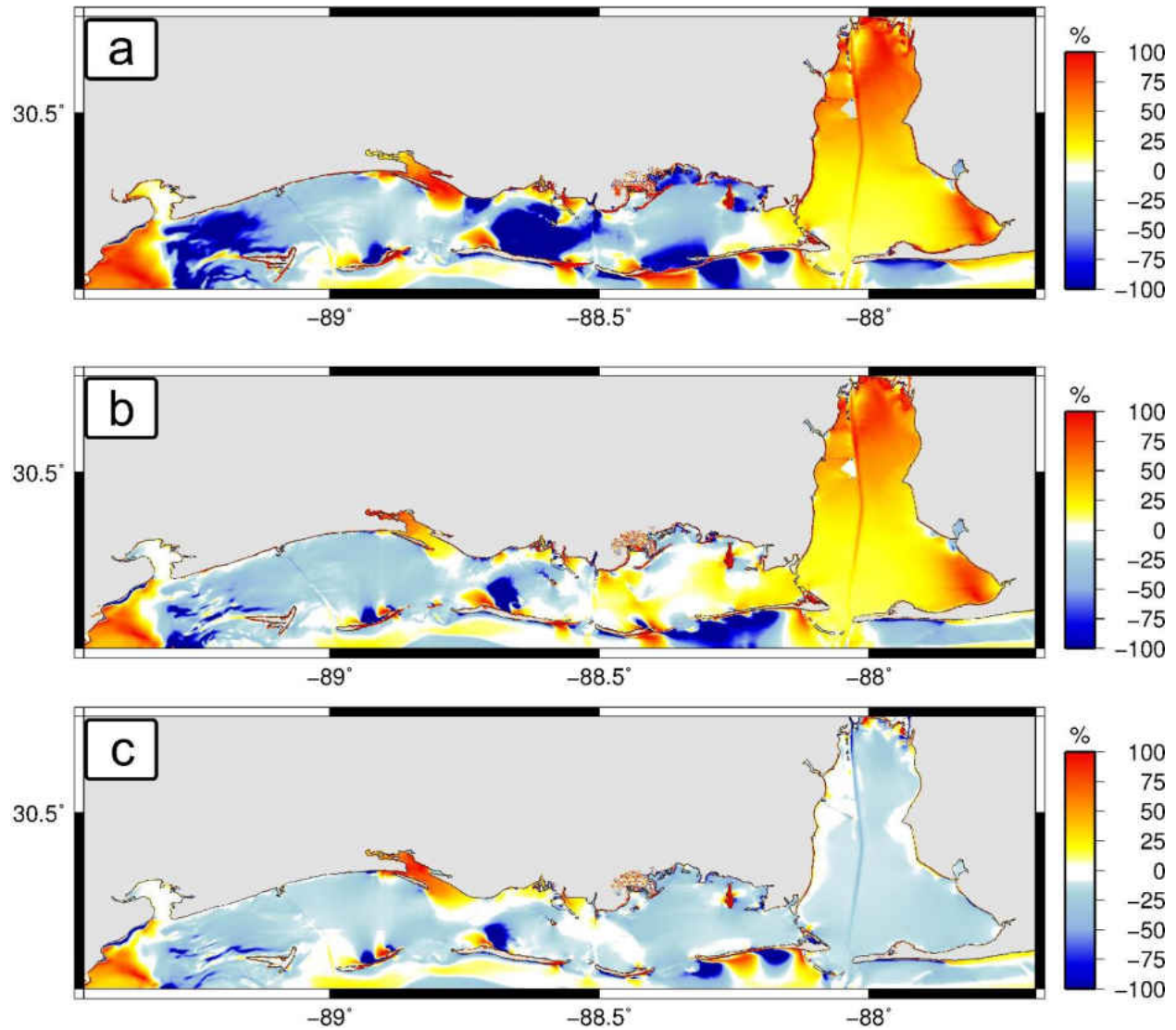


Figure 5.7: Percent change in flood-ebb ratio from (a) 1848 to 2005, (b) 1917 to 2005 and (c) 1960 to 2005.

5.5 Implications

The results of this study reinforce the necessity of considering changes in morphology in SLR assessments, as previous studies have concluded (Bilskie et al., 2014; Passeri et al., 2015); this allows for more comprehensive evaluations. Changes in tidal hydrodynamics are an important consideration for how ecology within the estuary has evolved historically, and how reconstruction

of the Grand Batture Island could affect various species. For example, tidal asymmetries affect sediment transport in marsh tidal creeks, which influences sediment supply. Flood dominant currents in tidal creeks tend to move sediment landward, whereas ebb dominant currents tend to move sediment seaward. Flood dominant currents also increase suspended sediment concentrations at the creek/marsh boundary, which supplies more marine sediment to the marsh and allows for accretion on the marsh platform. Conversely, ebb dominant currents can reduce the sediment supply. As currents within Grand Bay became progressively ebb dominant through time, the sediment transport to the marshes may have been altered. Microtidal marsh systems such as Grand Bay are especially sensitive to changes in suspended sediment concentrations because they are unable to easily adjust their mean platform elevation with respect to the tidal elevation; a relatively small increase in sea level or a decrease in accretion can cause a microtidal marsh to become submerged (Friedrichs and Perry, 2001). Tidal currents also transport nutrients to seagrass beds (Koch et al., 2007). Similar to marshes, seagrass growth is influenced by flood and ebb current strengths (Boer, 2000). Changes in the magnitudes of currents could alter the amount of sediment and nutrients in the water column, thereby affecting seagrass productivity. This is an important consideration for the seagrass beds located in Point aux Chenes and Grand Bay. If the Grand Batture Island was reconstructed, currents would become more ebb dominant which could alter the productivity of these beds. Lastly, increased flow rates can negatively affect oyster recruitment. Flow rates affect larvae delivery and position maintenance during and after settlement (Boudreaux et al., 2009). Again, this is an important consideration if the Grand Batture Island was reconstructed which would increase current velocities by 5 cm/s.

Examining historic changes in tidal hydrodynamics can also provide insight into the effects SLR and future landscape changes. Within 157 years, the Mississippi Sound and Grand Bay experienced significant changes in morphology in conjunction with approximately 47 cm of SLR. As sea level continues to rise and the MSAL islands evolve, tidal hydrodynamics within the Mississippi Sound and the Grand Bay estuary will be further altered. The future of the MSAL barrier islands is dependent on the strength of the islands cores and whether sufficient sand will be available as sea levels rise and storms continue to modify the landscape. The western three fourths of Dauphin Island is presently in a transgressive state; predominant transport is onshore rather than alongshore which allows the barrier to preserve a minimum volume as it migrates landward. Although it is unclear if Petit Bois Island and Horn Island will also enter transgressive phases, it is likely that longshore transport driven by winds, waves and currents will continue in the future. Petit Bois Island is prevented from moving further westward because of the dredged shipping channel at Horn Island Pass. It is expected that Petit Bois Island will continue to erode on the eastern end and narrow under updrift erosion. In addition, it is likely that the island will breach along the narrowest, concave-landward area, where overwash frequently occurs. Horn Island is also expected to narrow, but breaching is unlikely because of the beach-ridge topography that is oriented obliquely to the mainland shoreline (Morton, 2008).

By the year 2100, sea levels are projected to rise between 20 cm to 2 m; the 47 cm of SLR in the study domain between 1848 and 2005 is roughly equivalent to the intermediate-low projection of SLR for the year 2100 (Parris et al., 2012). Under this moderate amount of SLR, it is expected that tidal amplitudes will continue to increase west of Cat Island and Mobile Bay, whereas changes within the Mississippi Sound will be minimal. As Petit Bois Island continues to erode on the

eastern end, the widening of Petit Bois Pass most likely will not affect tidal amplitudes. The phases of the constituents are expected to be altered under future SLR. As seen in the historic scenarios, future SLR may speed up tidal phases within the Sound, Mobile Bay and Grand Bay. Stronger tidal currents in the inlets will continue to shift westward as Petit Bois Pass and Horn Island Pass migrate. Currents within the Grand Bay estuary are likely to become more ebb dominant under future SLR. Under higher rates of SLR, changes in tidal hydrodynamics may be exacerbated and should be evaluated.

5.6 Conclusions

Comparison of past and present tidal hydrodynamics illustrates the response of the system to SLR and the changing landscape. This provides a better understanding of the function of coastal morphology and the role of SLR on hydrodynamics. SLR had more of an impact on tidal amplitudes than the westward migration of the MSAL islands. Tidal amplitudes significantly increased west of Cat Island and in Mobile Bay, although changes within the Sound were minimal. Overall, constituent phases sped up across the study domain from historic conditions as a result of SLR. The position of the MSAL barrier island inlets influenced tidal currents within the Sound; the westward migration of Petit Bois Island allowed stronger tidal velocities to be centered on the Grand Batture Island. Overall, there was a reduction in maximum tidal velocities in Point aux Chenes and Grand bays from the historic conditions. In addition, current velocities in both bays became more ebb dominant since 1848. If the Grand Batture Island was reconstructed under 2005 conditions, tidal amplitudes and phases would not be altered, indicating that the offshore MSAL barrier islands and SLR have a greater influence on the harmonic constituents within the estuary.

However, maximum tidal velocities in Point aux Chenes and Grand Bay would increase by 5 cm/s and the flood-ebb ratio would decrease by 20% in Grand Bay, resulting in currents becoming more ebb dominant.

Ultimately, the results of this study provide insight into potential changes in tidal hydrodynamics under future SLR scenarios and further evolution of the MSAL barrier islands. This study highlights the importance of considering morphological changes in SLR assessments. Investigating historical changes in tidal hydrodynamics provides insight as to how coastal systems may evolve under future scenarios, and which hydrodynamic parameters may be altered. Although simulations of hurricane storm surge were beyond the scope of this study, future work will examine the influence of the dredged shipping channels and barrier island evolution on storm surge. Historical analyses of similar systems will improve the understanding of the effects of SLR and morphological changes on hydrodynamics in estuaries, and aid in coastal management decision making.

5.7 Acknowledgments

This research was funded in part under Award No. NA10NOS4780146 from the National Oceanic and Atmospheric Administration (NOAA) Center for Sponsored Coastal Ocean Research (CSCOR). The STOKES Advanced Research Computing Center (ARCC) (webstokes.ist.ucf.edu) provided computational resources for the simulations. The authors would like to thank W. Underwood from the Grand Bay National Estuarine Research Reserve for providing data used herein, M. Donnelly for providing insight into potential ecological changes, and K. Alizad for his

constructive comments. The statements and conclusions are those of the authors and do not necessary reflect the views of NOAA-CSCOR, STOKES ARCC, or their affiliates.

5.8 References

- Bilskie, M. V., Coggin, D., Hagen, S. C. and Medeiros, S. C. (2015). "Enhancement and application of overland unstructured finite element meshes for shallow water flow models." *Advances in Water Resources* (in revision).
- Bilskie, M. V., Hagen, S. C., Medeiros, S. C. and Passeri, D. L. (2014). "Dynamics of sea level rise and coastal flooding on a changing landscape." *Geophysical Research Letters* 41(3): 927-234.
- Boer, W. F. (2000). "Biomass dynamics of seagrasses and the role of mangrove vegetation as different nutrient sources for an intertidal ecosystem." *Aquatic Botany* 66(3): 225-239.
- Boudreaux, M. L., Walters, L. J. and Rittschoff, D. (2009). "Interactions between native barnacles, non-native barnacles and the easter oyster *crassostrea virginica*." *Bulletin of Marine Science* 84(1): 43-57.
- Buster, N. A. and Morton, R. A. (2011). "Historical bathymetry and bathymetric change in the Mississippi-Alabama coastal region, 1847-2009", U.S. Geological Survey Scientific Investigations Map 3154: 13 p. pamphlet.
- Byrnes, M. R., McBride, R. A., Penland, S., Hiland, M. W. and Westphal, K. A. (1991). "Historical changes in shoreline position along the mississippi sound barrier islands." *12th Annual Research Conference, Gulf Coast Section*.
- Egbert, G. D., Bennett, A. F. and Foreman, M. G. G. (1994). "TOPEX/POSEIDON tides estimated using a global inverse model." *Journal of Geophysical Research: Oceans* 99: 24821-24852.
- Egbert, G. D. and Erofeeva, S. Y. (2002). "Efficient inverse modeling of barotropic ocean tides." *Journal of Atmospheric and Oceanic Technology* 19: 183-204.
- Eleuterius, C. K. and Criss, G. A. (1991). "Point aux Chenes: Past, Present, and Future Perspective of Erosion". Ocean Springs, Mississippi, Physical Oceanography Section Gulf Coast Research Laboratory

- French, J. R. (2008). "Hydrodynamic Modelling of Estuarine Flood Defence Realignment as an Adaptive Management Response to Sea-Level Rise." *Journal of Coastal Research* 24(2B): 1-12.
- Friedrichs, C. T., Aubrey, D. J. and Speer, P. E. (1990). Impacts of relative sea level rise on evolution of shallow estuaries. Residual current and long-term transport. R. T. Cheng. New York, Springer-Verlag.
- Friedrichs, C. T. and Perry, J. E. (2001). "Tidal Salt Marsh Morphodynamics: A Synthesis." *Journal of Coastal Research* SI 27.
- Hall, G. F., Hill, D. F., Horton, B. P., Engelhart, S. E. and Peltier, W. R. (2013). "A high-resolution study of tides in the Delaware Bay: Past conditions and future scenarios." *Geophysical Research Letters* 40: 338-342.
- Koch, E. W., Ackerman, J. D., Verduin, J. and van Keulen, M. (2007). Fluid dynamics in seagrass ecology - from molecules to ecosystems. Seagrasses: biology, ecology and conservation. A. W. D. Larkum, R. J. Orth and C. M. Duarte. Netherlands, Springer: 193-225.
- Leorri, E., Mulligan, R., Mallinson, D. and Cearretta, A. (2011). "Sea-level rise and local tidal range changes in coastal embayments: An added complexity in developing reliable sea-level index points." *Journal of Integrated Coastal Zone Management* 11(3): 307-314.
- Luetlich, R. A., Westerink, J. J. and Scheffner, N. W. (1992). "ADCIRC: An Advanced Three-Dimensional Circulation Model For Shelves, Coasts, and Estuaries, I: Theory and Methodology of ADCIRC-2DDI and ADCIRC-3DL", U.S. Army Corps of Engineers.
- Medeiros, S. C., Hagen, S. C., Weishampel, J. F. and Angelo, J. J. (2015). "Adjusting lidar-derived digital terrain models in coastal marshes based on estimated above ground biomass density." *Remote Sensing* SI (Towards Remote Long-Term Monitoring of Wetland Landscapes): (accepted).
- Morton, R. A. (2008). "Historical Changes in the Mississippi-Alabama Barrier-Island Chain and the Roles of Extreme Storms, Sea Level, and Human Activities." *Journal of Coastal Research* 24(6): 1587-1600.
- Otvos, E. (1979). Barrier Island Evolution and History of Migration, North-Central Gulf Coast. Barrier Islands. S. Leatherman, Academic Press.
- Parris, A., Bromirski, P., Burkett, V., Cayan, D., Culver, M., Hall, J., Horton, R., Knuuti, K., Moss, R., Obeysekera, J., Sallenger, A. and Weiss, J. (2012). "Global Sea Level Rise Scenarios for the United States National Climate Assessment". NOAA Tech Memo OAR CPO-1: 37.

- Passeri, D. L., Hagen, S. C., Bilskie, M. V. and Medeiros, S. C. (2015). "On the significance of incorporating shoreline changes for evaluating coastal hydrodynamics under sea level rise scenarios." *Natural Hazards* 75(2): 1599-1617.
- Peterson, M. S., Waggy, G. L. and Woodrey, M. S. e. (2007). "Grand Bay National Estuarine Research Reserve: An Ecological Characterization", Grand Bay National Estuarine Research Reserve, Moss Point, MS: 268.
- Rosati, J. D. and Stone, G. W. (2009). "Geomorphologic Evolution of Barrier Islands along the Northern U.S. Gulf of Mexico and Implications for Engineering Design in Barrier Restoration." *Journal of Coastal Research* 25(1): 8-22.
- Seim, H. E. and Sneed, J. E. (1988). Enhancement of semidiurnal tidal currents in the tidal inlets of the Mississippi Sound. Hydrodynamics and Sediment Dynamics of Tidal Inlets. D. G. Aubrey and L. Weishar, Springer-Verlag. **29**: 157-163.
- Valentim, J. M., Vaz, L., Vaz, N., Silva, H., Duarte, B., Cacador, I. and Dias, J. (2013). "Sea level rise impact in residual circulation in Tagus estuary and Ria de Aveiro lagoon." *Journal of Coastal Research* Special Issue No. 65: 1981-1986.

CHAPTER 6. TIDAL HYDRODYNAMICS UNDER FUTURE SEA LEVEL RISE AND COASTAL MORPHOLOGY ALONG THE NORTHERN GULF OF MEXICO

The content in this chapter is submitted as: Passeri, D.L., Hagen, S.C., Plant, N.G., Bilskie, M.V., Medeiros, S.C. (2015). "Tidal hydrodynamics under Future Sea Level Rise Scenarios with Coastal Morphology along the Northern Gulf of Mexico." *Earth's Future* (in preparation)

6.1 Introduction

Coasts are dynamic systems that continuously transform over different temporal and spatial scales as a result of geomorphic and oceanographic processes (Cowell et al., 2003a; Cowell et al., 2003b). SLR has the potential to affect coastal environments in a multitude of ways including increased flooding, increased erosion, and ultimately increased submergence. Low-lying coastal environments such as the Northern Gulf of Mexico (NGOM) are particularly vulnerable to the effects of SLR, which may have serious consequences for coastal communities, as well as ecologically and economically significant estuaries. Understanding the future value of these coastal environments relies on the scientific evaluation of risks associated with SLR. This understanding can be used to make informed decisions for managing human and natural communities.

Changes in tidal hydrodynamics under SLR may impact navigation, ecological habitats, infrastructure and the geomorphology of the coastline. Specifically, tidal hydrodynamics influence inundation, circulation and sediment transport processes. Previous studies have found that SLR may cause nonlinear increases in tidal ranges and tidal prisms, and may alter inundation, current velocities and circulation patterns in the nearshore environment (French, 2008; Leorri et al., 2011;

Hall et al., 2013; Valentim et al., 2013). In addition, long-term shoreline erosion rates are expected to increase under future SLR (Gutierrez et al., 2011), which may have consequences for barrier islands and coastal embayments. Despite knowledge of the dynamic nature of the coast, many hydrodynamic assessments of SLR have not accounted for future changes in coastal morphology, which may increase inundation and alter hydrodynamics (Bilskie et al., 2014; Passeri et al., 2015; Passeri et al., 2015). Furthermore, most hydrodynamic assessments have been concentrated on a localized study area (e.g., a single estuary) and have not evaluated the effects of SLR across a broad domain.

This study examines the integrated dynamic effects of SLR and projected morphology on tidal hydrodynamics along the NGOM coast with particular focus on the Apalachicola, Florida, Grand Bay, Mississippi and Weeks Bay, Alabama NERRs. A large-domain hydrodynamic model was used to simulate astronomic tides for present (circa 2005) and future conditions (circa 2050 and 2100). The future conditions included four SLR scenarios and combinations of corresponding changes of shoreline positions and dune elevations. Changes in harmonic constituent amplitudes and phases, current velocities and inundation extents illustrate the tidal hydrodynamic response of the NGOM to SLR under a changing landscape.

6.2 Study Domain

The domain for this study spans the Chandeleur Islands, LA through Apalachicola, FL, including seven embayments (Mississippi Sound, Mobile Bay, Perdido Bay, Pensacola Bay, Choctawhatchee Bay, St. Andrew Bay, and Apalachicola Bay), numerous barrier islands and a stretch of mainland beach (Figure 6.1). This section of the NGOM is a low wave energy, microtidal

environment with an average wave height and tidal range on the order of 0.5 m and less than 1 m, respectively. Astronomic tides change from being mixed semi-diurnal along the west coast of Florida, to mixed diurnal at Apalachicola Bay, to diurnal along the Florida Panhandle through Louisiana (Seim et al., 1987). Shorelines along this stretch of the NGOM coast are currently eroding at rates exceeding 2 m/year (LA) or are nearly stable (FL)(Morton et al., 2004); however, over the past 6000 years, the coast has not experienced the rates of SLR that are projected for the next century (Donoghue, 2011).

Of particular interest are the Apalachicola, FL, Grand Bay, MS, and Weeks Bay, AL NERRs. Each estuary has its own unique morphology and hydrodynamic influences. Therefore, it is likely that each NERR will respond differently to SLR. Apalachicola, FL is a wide, shallow estuary located within the Florida Panhandle. It is the second largest watershed system in the NGOM surpassed only by the Mobile River basin (Isphording, 1985). The estuary is centered on Apalachicola Bay, with East Bay to the northeast. The Apalachicola River discharges into East Bay through a delta and distributary system nearly 3 km wide. The estuary is sheltered from the Gulf of Mexico by a chain of barrier islands. Apalachicola is an ecologically and economically significant estuary that contains oyster reefs, seagrass beds, and salt marshes. Oysters, shrimp, blue crab, and finfish are the most harvested species with a value over \$134 million in economic impact annually. Additionally, Apalachicola Bay provides approximately 90% of Florida's oyster harvest and 10% of the total U.S. harvest (FDEP, 2013).

Grand Bay, MS is located within the Mississippi Sound on the Mississippi-Alabama (MSAL) border. It is comprised of multiple bays, bayous, and salt marshes. Salt marshes provide habitats

for many species, including shrimp, crabs and oysters that are recreationally and commercially fished. The estuary is one of the few remaining extensive coastal marsh environments in Mississippi (O'Sullivan and Criss, 1998) and is being eroded away faster than any other marsh in the state (Mississippi Department of Marine Resources, 1999). Currently, the estuary does not have a fluvial source, and is solely influenced by the hydrodynamics of the Mississippi Sound. The historic breaching and migration of the offshore MSAL barrier islands have altered tidal hydrodynamics within the Mississippi Sound and Grand Bay estuary (Eleuterius and Criss, 1991; Passeri et al., 2015). Lack of a sediment source and reduced protection from wave attack has heightened the susceptibility of the estuary's marsh shorelines to increased erosion under SLR. Additionally, as the offshore barrier islands continue to evolve, tidal hydrodynamic patterns within Grand Bay may be further altered.

Weeks Bay, AL is considered a tributary estuary and is located within the larger estuary system of Mobile Bay, which connects Weeks Bay to marine influences of the Gulf of Mexico. Weeks Bay receives tidal flows from Mobile Bay as well as freshwater discharge from the Fish and Magnolia Rivers. The estuary is a habitat supporting diverse species of flora and fauna, and is a particularly important nursery for commercially significant species including shrimp, bay anchovy, blue crab and shellfish (Miller-Way et al., 1996).

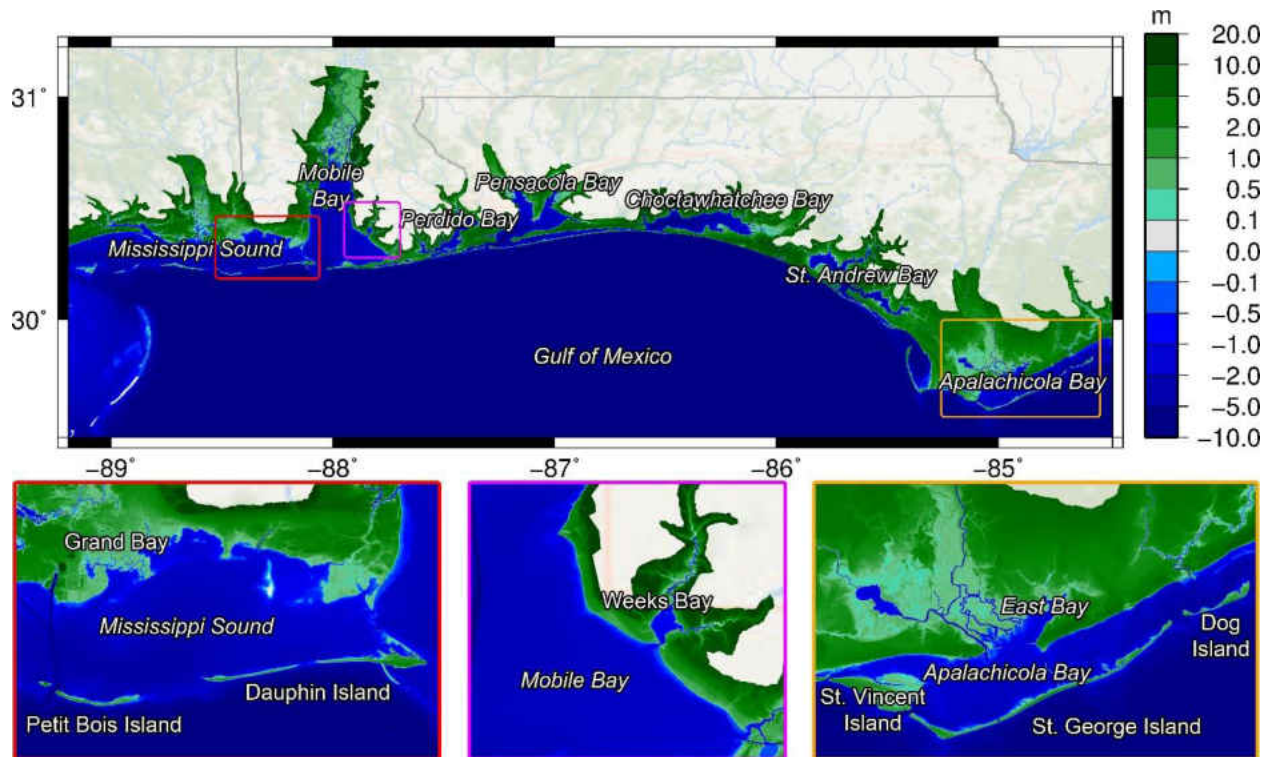


Figure 6.1: Hydrodynamic model elevations of the NGOM study area with insets of the Grand Bay, Weeks Bay and Apalachicola NERRs.

6.3 Methodology

To assess changes in tidal inundation, amplitudes, phases and current velocities due to SLR as well as SLR coupled to morphologic change, a hydrodynamic model was constructed for the study domain. The model construction, forcing, scenarios and analysis are described.

6.3.1 Hydrodynamic Model

To simulate tidal hydrodynamics, this study uses ADCIRC-2DDI, a code that solves the depth-integrated shallow water equations for water surface elevations and currents (Luettich et al., 1992).

The model is a compilation of three previously developed models (Salisbury et al., 2011; University of Central Florida, 2011; Bilskie et al., 2015). The unstructured finite element mesh describes the Western North Atlantic Tidal (WNAT) model domain west of the 60° W meridian (open ocean boundary), including the Caribbean Sea and the Gulf of Mexico. Higher spatial resolution elements (on the order of 20 m to 100 m) are incorporated along the NGOM coast from Louisiana through the Florida panhandle, which permits localized adjustments to be made to support the simulation of future scenarios with changes in shorelines and other morphology. Bathymetric and topographic elevations were derived from a Digital Elevation Model (DEM) constructed with lidar data, as well as NOS (National Ocean Service) hydrographic surveys, U.S. Army Corps of Engineers (USACE) channel surveys and NOAA (National Oceanographic and Atmospheric Administration) nautical charts to represent conditions circa 2005 (post-Katrina) (Coggin, 2011; Bilskie et al., 2015). Within the Apalachicola and Grand Bay marshes, an elevation correction based on biomass density was employed to adjust the lidar-derived elevations. This technique uses ASTER and IfSAR satellite imagery along with lidar-derived canopy heights to classify the above-ground biomass density as high, medium or low. This biomass density class was then used to lower the lidar DEM (Medeiros et al., 2015).

6.3.2 *Future SLR and Morphology*

Future sea levels were obtained from the Parris et al. (2012) scenarios for low, intermediate-low, intermediate-high and high global projections of SLR for the years 2050 (0.11 m, 0.19 m, 0.39 m, 0.62 m of SLR, respectively) and 2100 (0.2 m, 0.5 m, 1.2 m, 2.0 m of SLR, respectively). The low scenario was derived from a linear extrapolation of historical mean SLR using tide gauge records

dating back to 1900. The intermediate-low scenario was determined using the upper end of the IPCC Fourth Assessment Report (AR4) global SLR projections from climate models employing the B1 emissions scenario; the intermediate-high scenario was derived from the average of the high end of semi-empirical global SLR projections, and the highest projection was determined using estimates of maximum possible glacier and ice sheet loss and estimated ocean warming from the IPCC AR4 global SLR projection. These scenarios are considered to be plausible trajectories of global mean SLR for use in assessing vulnerability, impacts and adaptation strategies (Parris et al., 2012).

Projecting long-term changes in coastal morphology is challenging due to the stochastic nature of the processes, particularly tied to uncertainty in frequency and magnitude of storms, as well as a lack of understanding in the dynamic interactions and feedback mechanisms (Sampath et al., 2011). As a result, coastal scientists do not have a reliable, universal model to accurately predict the impacts of SLR along a variety of coastlines (Fitzgerald et al., 2008). Statistical approaches using BNs have been used to make probabilistic predictions of long-term shoreline change that depend on SLR (Hapke and Plant, 2010; Gutierrez et al., 2011; Yates and Le Cozannet, 2012). The BN, based on the application of Bayes' theorem, defines relationships between driving forces, geological constraints and coastal responses (Gutierrez et al., 2011). In this study, an existing BN (Gutierrez et al., 2014) was modified to project future shoreline changes and dune heights along the NGOM coast under each SLR scenario. To do so, the SLR rate variable was constrained in the BN and probabilistic projections of shoreline change and dune heights were output at 4 km sections along the oceanic shorelines of the NGOM coast. The BN was beneficial in this application since it could be applied to a large domain with minimal computational expense because it is trained on

historical data. However, the spatial applicability of the BN was limited to oceanic shorelines due to lack of data in bay and estuarine regions. There was also a limited level of detail in which the BN could make projections; predictions were bound by what the BN had seen historically (e.g., the rate of SLR), and the BN was unable to explicitly represent complex morphological processes such as barrier island translation or overwash (e.g., how the back-barrier shoreline would be altered). The 50th percentile projections of shoreline change and dune heights were selected to represent an “average” projection of future morphology. Since the BN was not trained with SLR rates as large as the high SLR scenario, it was only able to output projections for the low, intermediate-low and intermediate-high scenarios. To obtain projections under the high SLR scenario, the shoreline change and dune elevations predicted by the BN for the low, intermediate-low and intermediate-high projections were linearly extrapolated (Figure 6.2). The majority of the NGOM shoreline was projected to erode, although some areas were projected to accrete especially near inlets. In general, as SLR increased, shoreline erosion increased and dune elevation decreased.

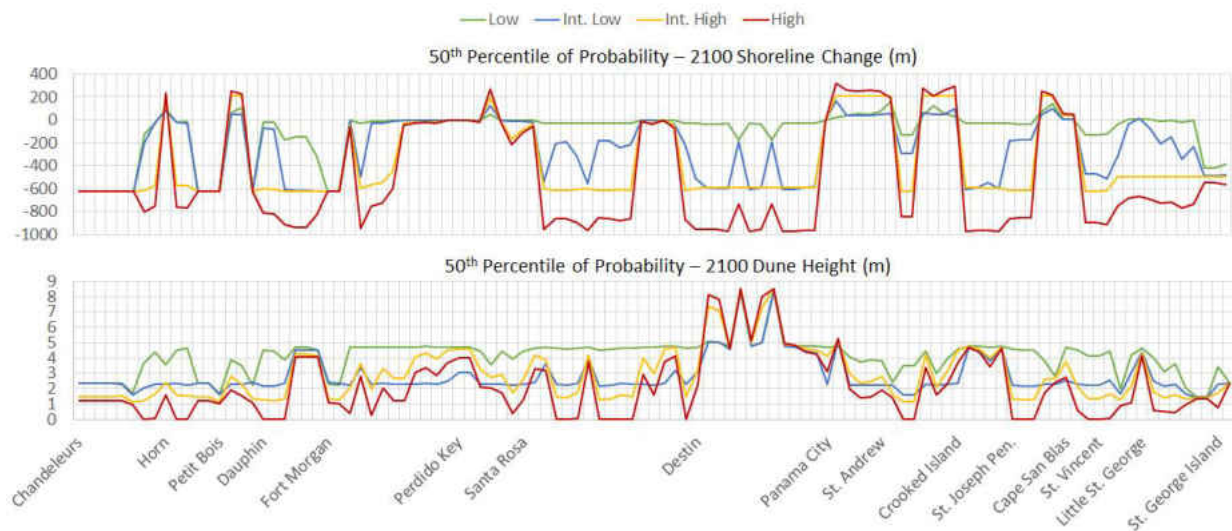


Figure 6.2: 50th percentile of probability projections of shoreline change and dune height for the year 2100 under low, intermediate-low, intermediate-high and high SLR across the NGOM domain. In the plot of shoreline change, positive numbers indicate accretion, negative numbers indicate erosion.

6.3.3 *Modeling Approach*

To examine the effects of SLR on tidal hydrodynamics along the NGOM coast, the hydrodynamic model was altered to reflect future conditions circa 2050 and 2100 (note: morphologic processes were not simulated concurrently with hydrodynamics as the goal is to simulate tidal hydrodynamics in response to SLR and landscape changes). To do so, the DEM was altered using the BN output to represent future elevations. In order to account for the dynamic movement of the shoreface, the beach profile was translated upwards by the amount of SLR, and landwards or seawards by the amount of projected erosion or accretion, while maintaining the profile shape (i.e., equilibrium) (Passeri et al., 2015). The profile translation was implemented for each 4 km section by shifting the active zone portion of the DEM, defined from the shoreline (0 m contour) to the

depth of closure contour (estimated to be approximately 5 m along the coastline (Dean and Grant, 1989)). Bathymetry and topography outside of the active zone remain the same. Dune heights were then modified using the corresponding BN output.

At many locations, the BN-projected shoreline was landward of infrastructure, and/or exceeded the position of the back-barrier shoreline (i.e., the shoreline change exceeded the width of the barrier island). Since the BN was unable to project how the back-barrier shoreline would be altered, it was unable to provide guidance on how the entire barrier island would evolve. To compensate for this short-coming, a decision making flowchart was created to decide how to implement the BN-projected shoreline changes into the hydrodynamic model based on assumptions of whether shorelines would be nourished in the future to prevent barrier island or infrastructure loss (Figure 6.3). A step-by-step explanation of the flowchart follows:

- At accretional sections, the beach profile was translated according to the projection and the dune elevation was altered accordingly.
- At erosional sections, if the projected shoreline position was landward of the back-barrier shoreline and section was urbanized, it was assumed that the shoreline would be nourished in the future. Therefore, the shoreline position was not altered (i.e., horizontal translation was set equal to 0), the profile was shifted vertically by the amount of SLR, and the dune height was changed according to the projection.

- If the projected shoreline position was landward of the back-barrier shoreline and the section was not urbanized, then USGS land use/land cover (LULC) projections for the years 2050 and 2100 using the A2 scenario (<http://landcover-modeling.cr.usgs.gov/projects.php>) were consulted to determine if the area was projected to be developed.
 - If there was projected development, it was assumed the shoreline would be nourished in the future; the shoreline position was not altered and the dune height was changed according to the projection.
 - If there was not projected development but the section was state or government property (e.g., military base, state/national park, etc.), then it was assumed that the shoreline would be nourished in the future; the shoreline position was not altered and the dune height was changed according to the projection.
 - If there was not projected development and the section was not state or government property, then the shoreline position and dune height were altered according to the projections.
- If the projected shoreline position was not landward of the back-barrier shoreline and did not exceed the infrastructure line, then the projected shoreline change and dune height were implemented.

- If the projected shoreline change exceeded the infrastructure line, then the same methodology for if the shoreline projection was landward of the back-barrier shoreline was applied:
 - If there was projected development, it was assumed the shoreline would be nourished in the future; the shoreline position was not altered and the dune height was changed according to the projection.
 - If there was not projected development but the section was state or government property (e.g., military base, state/national park, etc.), then it was assumed that the shoreline would be nourished in the future; the shoreline position was not altered and the dune height was changed according to the projection.
 - If there was not projected development and the section was not state or government property, then the shoreline position and dune height were altered according to the projections.

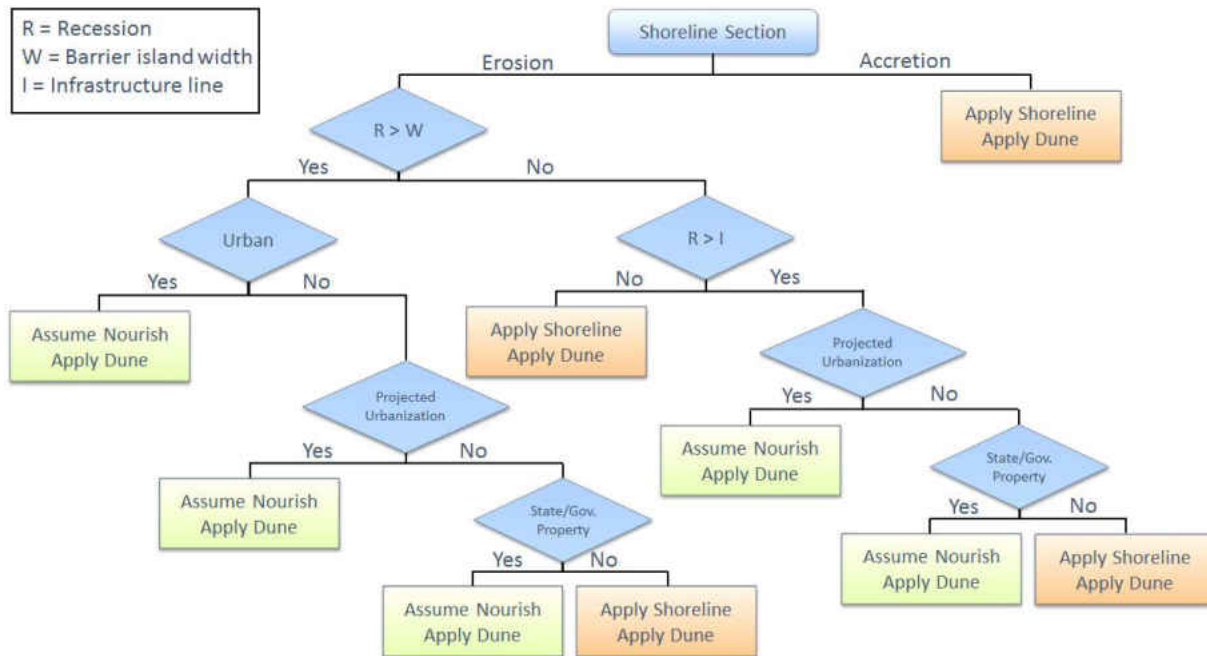


Figure 6.3: Decision making flow chart for how to implement projected shoreline changes and dune heights from BN into hydrodynamic model.

As previously mentioned, the morphology of the MSAL barrier islands influences hydrodynamic patterns within the Mississippi Sound and Grand Bay (Passeri et al., 2015). To account for future lateral migration of the islands, historic migration rates were extrapolated to the years 2050 and 2100, and used to modify elevations in the DEM. The western end of Dauphin Island has grown laterally at an average rate of 45.7 m/year, whereas the eastern end is fixed by its Pleistocene core (Morton, 2008; Rosati and Stone, 2009; Byrnes et al., 2012). Petit Bois Island has migrated westward at an approximate rate of 34.5 m/y with net erosion on the eastern end, that has widened the pass to Dauphin Island. The western end of Petit Bois Island is prevented from migrating further westward due to the maintained shipping channel at Horn Island pass (McBride et al., 1995; Morton, 2008). Horn Island has migrated westward at a rate of approximately 38.7 m/year and

Ship Island has migrated westward at approximately 9 m/year. Cat Island has remained relatively stable historically (Morton, 2008); therefore, the island's morphology was not altered.

Astronomic tides were simulated for nine scenarios in which the sea level, shoreline positions and dune elevations reflect the conditions for time: 2005, 2050-low, 2050-intermediate low, 2050-intermediate high, 2050-high, 2100-low, 2100-intermediate low, 2100-intermediate high, and 2100-high. Astronomic tides were simulated for 45 days beginning from a cold start with a 10-day hyperbolic tangent ramp function. For the 2005 scenario, the model was forced with water surface elevations of eight harmonic constituents (K1, O1, M2, S2, N2, K2, Q1, and P1) along the open ocean boundary (Egbert et al., 1994; Egbert and Erofeeva, 2002). For the future scenarios, a ninth “steady” component with zero-phase and an amplitude equal to the SLR projection for the given scenario was included to increase the sea level. Wind effects were not considered in this study, as preliminary research has shown wind effects average out on an annual scale. Model output consisted of depth-integrated velocities, amplitudes and phases of harmonic constituents, as well as maximum elevations of water and maximum velocities obtained at each node of the mesh for the duration of each simulation.

6.4 Results

6.4.1 Validation

The hydrodynamic model was validated with available astronomic tide data. A tidal validation was performed for the 2005 scenario at 25 NOAA tide gauges located throughout the study domain. Model output consisted of 23 tidal constituents, which were validated against reported tidal

constituents at each of the tidal gauging stations (<http://tidesandcurrents.noaa.gov/>). A comparison of the NOAA-measured and model-computed amplitudes and phases for five dominant constituents (K1, O1, M2, Q1, and S2) is shown in Figure 6.4. Difference bands are plotted at 0.025 m and 0.05 m in the amplitude plots, and 10° and 20° in the phase plots. All of the constituent amplitudes fall within the 0.05 m difference band, and for the most part, the phases of the three most dominant constituents (K1, O1 and M2) fall within the 20° difference band. Although the S2 phases deviate the most, the contribution of this constituent is minimal in comparison with K1, O1 and M2.

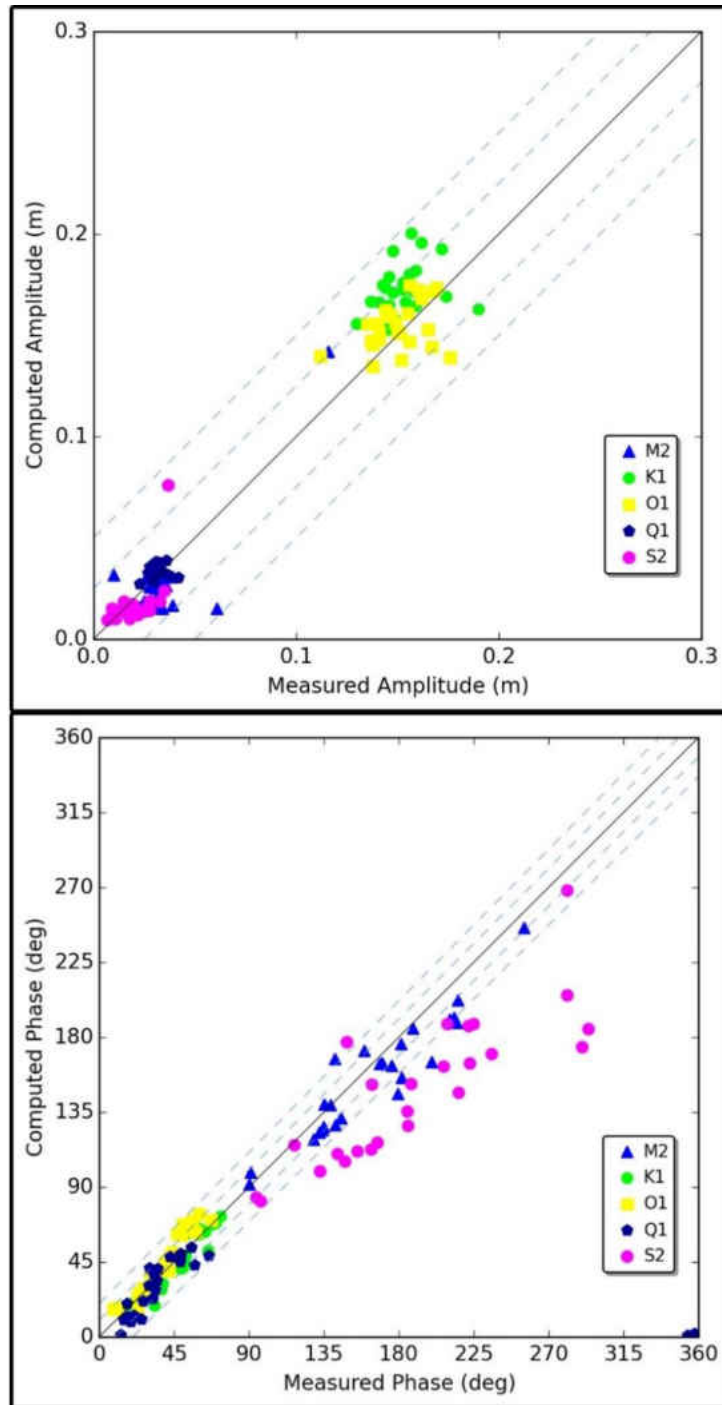


Figure 6.4: Comparison of amplitudes (top) and phases (bottom) measured by NOAA and predicted by the hydrodynamic model. Difference bands are located at 0.025 m and 0.05 m in the amplitude plot, and 10° and 20° in the phase plot.

6.4.2 Water Levels

Tidal amplitudes (i.e., the amplitude of the tide with respect to mean sea level) across the NGOM for the 2005 scenario are summarized in Figure 6.5a. Within the study domain, Apalachicola Bay had the highest tidal amplitudes (on the order of 70 cm) as a result of the strong semidiurnal influence. As the Gulf of Mexico becomes more diurnal westward of Apalachicola, tidal amplitudes generally decrease. Out of all of the embayments, Perdido and Choctawhatchee had the lowest tidal amplitudes (on the order of 21 cm and 15 cm, respectively) due to the bays being connected to the Gulf of Mexico with narrow, shallow inlets that limit tidal exchange.

Changes in tidal amplitudes from the 2005 scenario to the future scenarios were examined; the 2005 vs. 2050-high and 2005 vs. 2100-high comparisons are summarized in Figure 6.5. Differences equal to 0 indicate the tidal amplitude did not change from the 2005 scenario, differences greater than 0 indicate the tidal amplitude increased from the 2005 scenario; differences less than 0 indicate the tidal amplitude decreased from the 2005 scenario. In all of the scenarios, the offshore tidal amplitudes were unaltered, illustrating the nonlinear effects of SLR within semi-enclosed embayments. In the 2005 vs. 2050-low scenario, no changes occurred within any of the bays. Similarly, changes were minimal in the 2100-low scenario with increases only in Perdido Bay and Choctawhatchee Bay of approximately 9% (1.9 cm), and 8% (1.2 cm), respectively. In the 2050-high scenario, tidal amplitudes increased from the 2005 scenario by approximately 9% (3.5 cm), 23% (4.8 cm) and 26% (11.9 cm) in Mobile Bay, Perdido Bay and Choctawhatchee Bay, respectively. The most substantial changes occurred in the 2100-high scenario with increases of 15% (6.5 cm), 35% (7.3 cm), 67% (10.0 cm) and 8% (5.5 cm) in Mobile

Bay, Perdido Bay, Choctawhatchee Bay and Apalachicola Bay, respectively. Pensacola Bay and St. Andrew Bay had negligible changes (less than 2%).

Previous research has illustrated the relationship between inlet cross-sectional area (i.e., the cross-sectional area of the inlet at high tide) and tidal prisms (i.e., the amount of water flowing into a bay during high tide) (Jarrett, 1976). As sea level rises, the inlet cross-sectional area is altered. Under the 2100-high scenario, Choctawhatchee Bay had the largest relative increase in the inlet cross-sectional area by approximately 78%, whereas St. Andrew Bay had the smallest by approximately 20%. The relative change in the inlet cross-sectional area versus SLR is plotted in Figure 6.6 for each bay that is connected to the Gulf of Mexico with a single inlet (i.e., Mobile, Perdido, Pensacola, Choctawhatchee and St. Andrew). Trendlines fitted to the data can be used to project the relative change in the inlet cross-sectional area in each bay under various SLR scenarios that are less than or equal to 2 m. As the inlet geometry changes under SLR, the tidal hydrodynamic behavior within the bay is altered. The correlation between the ratio of the future to present tidal amplitude ($\text{Amplitude}_{\text{future}}/\text{Amplitude}_{\text{present}}$) and the ratio of the future to present inlet cross-sectional area ($\text{Area}_{\text{future}}/\text{Area}_{\text{present}}$) for each SLR scenario is summarized in Table 6.1. As evident by the high correlation coefficients (R), there is a strong linear correlation between the change in the inlet cross-sectional area and the change in the bay's tidal amplitude for each SLR scenario. The larger the increase in the inlet cross-sectional area, the larger the increase in the tidal amplitude within the bay.

Unlike the semi-enclosed embayments in the study domain, changes in tidal amplitudes within the Mississippi Sound and Grand Bay were negligible in all future scenarios due to the Sound's open

exposure to the Gulf of Mexico. As a result, SLR did not alter the tidal amplitude response. Tidal amplitudes in the embayment west of the Chandeleur Islands decreased by approximately 11% (5.7 cm) in the 2100-high scenario as a result of the islands being overtopped, which created direct exposure to the Gulf of Mexico. This dampened the tidal response and caused the tidal hydrodynamic behavior in the embayment to be more similar to the open ocean.

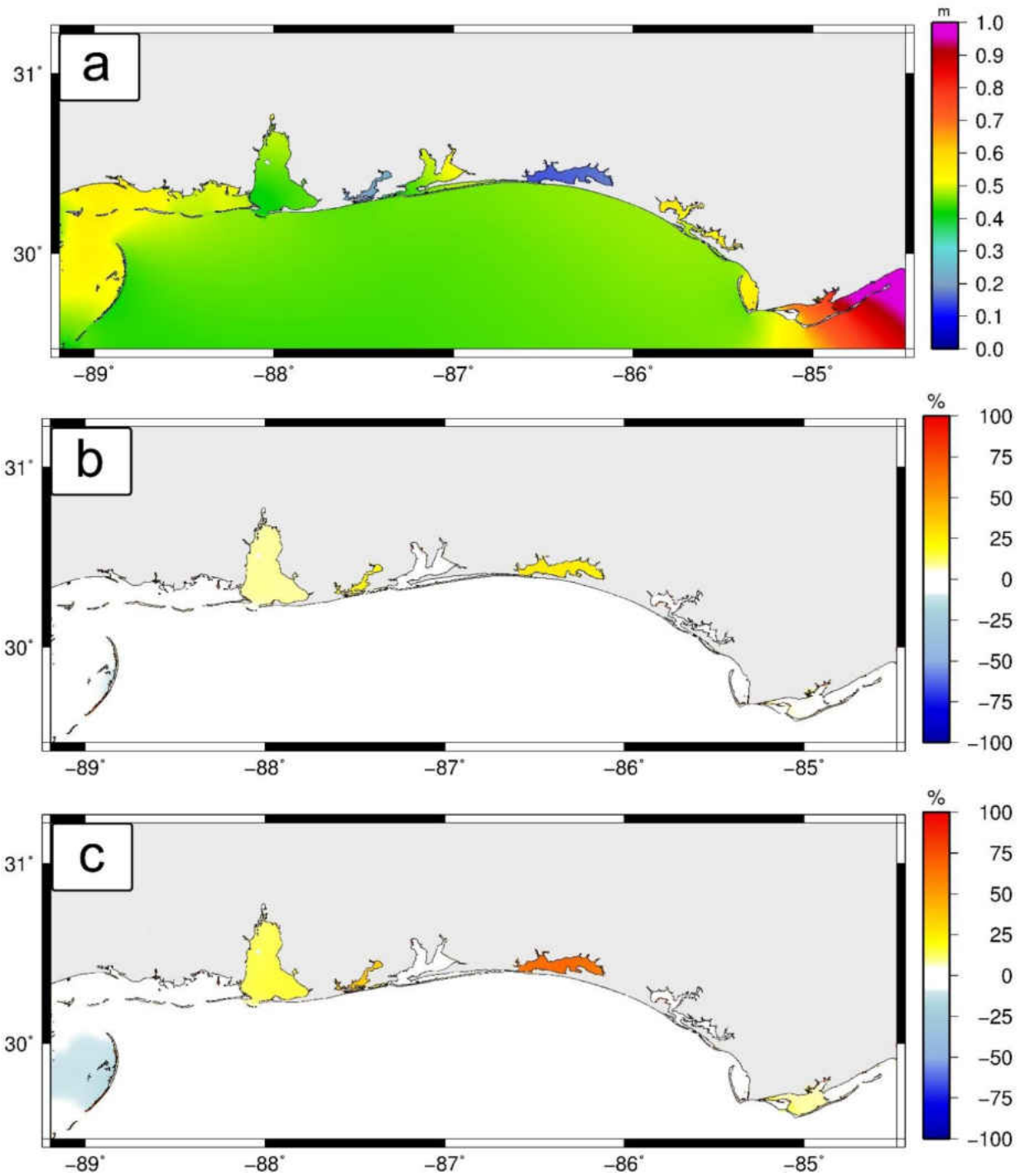


Figure 6.5: (a) Total tidal amplitudes across the NGOM for the 2005 scenario; (b) percent change in tidal amplitude from 2005 to 2050-high scenario; (c) percent change in tidal amplitude from 2005 to 2100-high scenario.

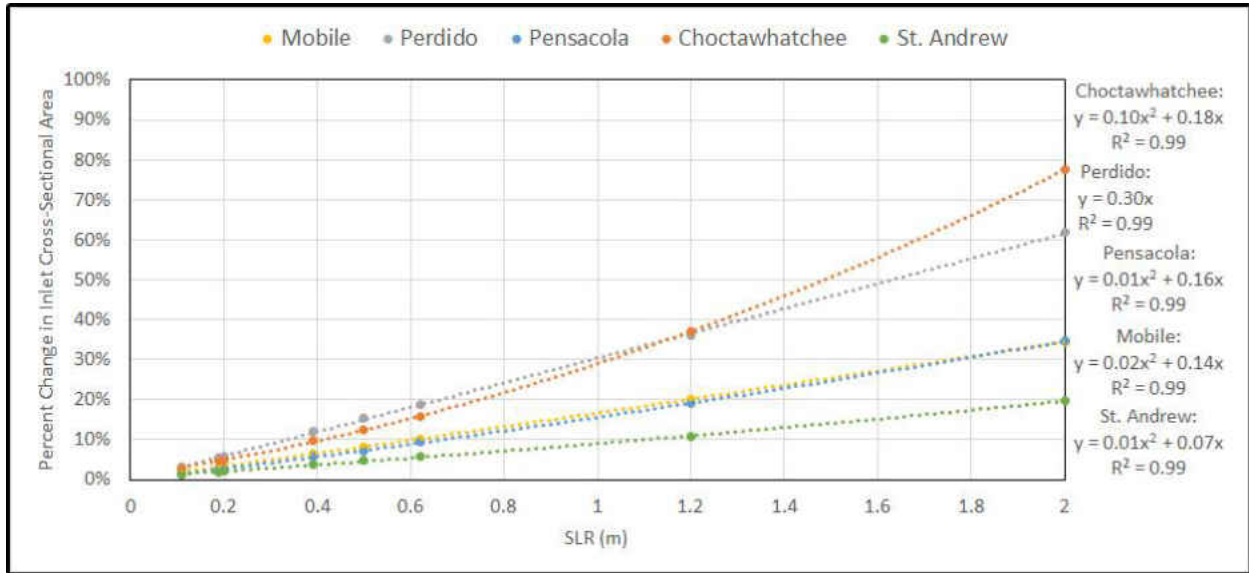


Figure 6.6: Percent change in inlet cross-sectional area versus SLR for each bay; data is fitted with trend equations.

Table 6.1: Trend equations, correlation coefficient (R) and coefficient of determination (R^2) between the ratio of the future to present tidal amplitude ($\text{Amplitude}_{\text{future}}/\text{Amplitude}_{\text{present}}$) versus the ratio of the future to present inlet cross-sectional area ($\text{Area}_{\text{future}}/\text{Area}_{\text{present}}$) for each future scenario.

<i>Scenario</i>	<i>Trendline</i>	<i>R</i>	<i>R²</i>
2050 Low	$y = 2.66x - 1.69$	0.99	0.99
2050 Int. Low	$y = 2.55x - 1.60$	0.99	0.99
2050 Int. High	$y = 2.21x - 1.29$	0.97	0.93
2050 High	$y = 2.16x - 1.30$	0.93	0.86
2100 Low	$y = 2.50x - 1.55$	0.99	0.99
2100 Int. Low	$y = 2.19x - 1.30$	0.96	0.92
2100 Int. High	$y = 1.43x - 0.62$	0.94	0.89
2100 High	$y = 1.15 - 0.42$	0.97	0.97

To further examine the influence of SLR and morphology on tidal amplitudes, changes in the dominant tidal constituents were examined. The 2005 dominant tidal constituent amplitudes as well as changes in constituent amplitudes and phases from 2005 to the 2100-high scenario are summarized in Table 6.2. The dominant tidal constituents within the NGOM are the diurnal K1 and O1, as well as the semidiurnal M2. K1 and O1 dominate in the diurnal section of the NGOM, including the Mississippi Sound, Grand Bay, Mobile Bay, Weeks Bay, Perdido Bay, Pensacola Bay, Choctawhatchee Bay and St. Andrew Bay. K1, O1 and M2 dominate in Apalachicola Bay as a result of the strong semidiurnal influence. In the diurnal bays, large increases in the K1 and O1 amplitudes contributed to the total increase in the tidal amplitude; although the M2 amplitudes also changed, the change was small relative to the total tidal amplitude. As expected, Choctawhatchee and Perdido bays had the largest increases in the K1 and O1 amplitudes. In Apalachicola Bay, the O1 and K1 constituents increased minimally, whereas the M2 constituent increased by 31.2% (3.7 cm), further illustrating the semidiurnal character of the tides in Apalachicola.

The phases of the dominant constituents (i.e., the phase lag) also changed from the 2005 scenario to the 2100-high scenario. In all of the bays except St. Andrew Bay, constituent phases were faster in the 2100-high scenario than in the 2005 scenario, meaning that high tide would occur earlier than in 2005. The largest phase differences occurred in Weeks Bay, with the K1 and O1 phases being 116 min and 134 min faster in the 2100-high scenario, respectively. In St. Andrew Bay, the K1 and O1 phases were slower in the 2100-high scenario by approximately 14.7 min and 14.1 min, respectively. St. Andrew Bay had the smallest relative increase in the cross-sectional area of the inlet under the 2100-high scenario and experienced slower tidal propagation in the future scenario

than in 2005. On the contrary, bays with larger relative increases in the cross-sectional area of the inlets experienced faster tidal propagation in the future scenario than in 2005. Similar to the tidal amplitudes, no differences in the constituent phases occurred offshore.

Table 6.2: Dominant harmonic constituent amplitudes for the 2005 scenario and changes in constituent amplitudes and phases from the 2005 scenario to the 2100-high scenario within each bay system in the NGOM.

<i>Location</i>	2005 Amplitude (cm)			% Change in Amplitude from 2005 to 2100-high			Difference in Phase from 2005 to 2100-high (min)		
	<i>K1</i>	<i>O1</i>	<i>M2</i>	<i>K1</i>	<i>O1</i>	<i>M2</i>	<i>K1</i>	<i>O1</i>	<i>M2</i>
Mississippi Sound	17.8	16.2	2.5	-4.4%	-3.8%	5.8%	19.9	23.7	11.3
Grand Bay	17.0	15.8	2.4	-2.4%	-2.1%	10.5%	23.1	27.3	15.2
Mobile Bay	16.2	14.3	1.4	7.4%	9.5%	87.6%	90.4	102.3	22.1
Weeks Bay	16.4	14.5	1.4	9.7%	11.6%	88.6%	116.8	134.6	-9.2
Perdido Bay	7.9	7.0	0.6	37.1%	39.2%	12.5%	76.1	86.7	14.8
Pensacola Bay	17.3	15.5	2.0	0.0%	1.0%	-6.9%	44.2	54.4	88.4
Choctawhatchee Bay	5.7	5.0	0.4	70.7%	73.6%	35.8%	86.3	92.8	22.8
St. Andrew Bay	16.4	15.3	2.8	0.9%	-0.7%	-25.2%	-14.7	-14.6	-44.7
Apalachicola Bay	15.5	14.2	12.0	1.2%	0.4%	31.2%	58.5	68.9	35.7

6.4.3 Currents

The 2005 maximum tidal current velocities varied across the domain with faster velocities in the semidiurnal region as well as within the inlets to the embayments; within the Mississippi Sound, tidal velocities were faster within the inlets of the barrier islands (up to 30 cm/s). Within the three NERRs, the 2005 maximum tidal velocities at the locations specified in Figure 6.8 were 6.1 cm/s, 4.1 cm/s, and 17.4 cm/s in Grand Bay, Weeks Bay and East Bay (Apalachicola), respectively.

Changes in maximum tidal current velocities from the 2005 scenario to the future scenarios were compared; the changes from the 2005 scenario to the 2050-high and 2100-high scenarios are summarized in Figure 6.7. Differences equal to 0 indicate the maximum velocity did not change from the 2005 scenario; differences greater than 0 indicate the maximum velocity increased from the 2005 scenario; differences less than 0 indicate the maximum velocity decreased from the 2005 scenario. In the 2050-low scenario and the 2100-low scenarios, the only notable changes occurred in the Mississippi Sound within the present and future locations of the inlets of the offshore barrier islands. The westward migration of the barrier islands shifted the location of the strong velocities within the inlets. In the 2050-high scenario, velocities minimally increased in Grand Bay and Apalachicola Bay. Westward of the Chandeleur Islands, velocities decreased along the northern end as a result of the barrier islands being overtopped and hydrodynamics within the embayment becoming more like the open ocean. Within the rest of the domain, changes were negligible except offshore of Pensacola Bay where velocities increased by approximately 3 cm/s (88%) along the continental shelf break. In the 2100-high scenario, larger changes occurred across the domain and within the embayments. Westward of the northern Chandeleur Islands, tidal velocities decreased by approximately 16 cm/s; this also occurred north of Dauphin Island in the Mississippi Sound as a result of the barrier island being overtopped. Tidal velocities increased within all of the bays; within the NERRs, velocities increased by approximately 6.1 cm/s (102%) in Grand Bay, 1.7 cm/s (39%) in Weeks Bay and 10.8 cm/s (63%) in East Bay (Apalachicola). Additionally, velocities increased offshore along the continental shelf break. The largest increase (approximately 18 cm/s) occurred offshore of Pensacola Bay where the slope of the shelf break is steep (i.e., greater depths,

faster) whereas smaller increases (of approximately 6 cm/s) occurred where the slope is more gradual.

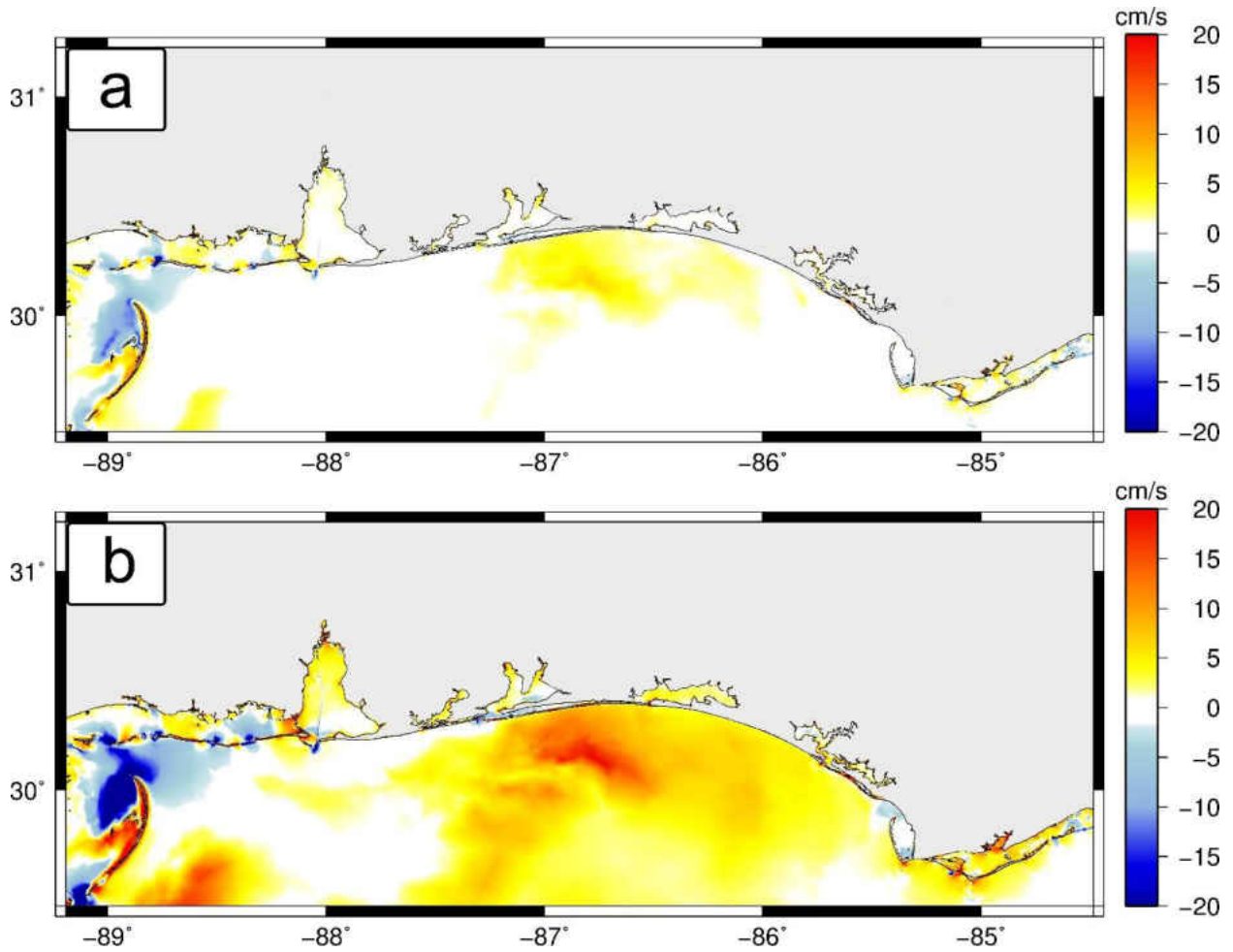


Figure 6.7: Changes in tidal velocities from the 2005 scenario for (a) the 2050-high scenario and (b) the 2100-high scenario; warm colors indicate tidal velocities have increased from the 2005 scenario, cool colors indicate tidal velocities have decreased from the 2005 scenario.

The flood-ebb ratio (R), the ratio of the magnitude of the maximal flood (U_{flood}) to the maximal ebb (U_{ebb}) currents, indicates if asymmetry exists in the current velocities:

$$R = \frac{U_{flood}}{U_{ebb}} \quad (10)$$

Ratios equal to 1 indicate equal magnitudes of flood and ebb currents (no asymmetry), ratios larger than 1 indicate stronger flood currents than ebb currents (flood dominance), and ratios less than 1 indicate stronger ebb currents than flood currents (ebb dominance). The flood-ebb ratios for the 2005 scenario for Grand Bay, Weeks Bay and Apalachicola are illustrated in Figure 6.8. Tidal currents in the 2005 scenario within Grand Bay were ebb-dominant (ratio of 0.75), whereas currents in Weeks Bay and Apalachicola were flood-dominant (ratios of 1.10 and 1.35, respectively).

The flood-ebb ratio under the future scenarios as well as the percent change in the flood-ebb ratio are summarized in Table 6.3. In all of the future scenarios, ebb current strengths within Weeks Bay and Apalachicola increased more than flood current strengths, resulting in a decrease in flood-dominance. In the 2050-intermediate high, 2050-high, 2100-intermediate low, 2100-intermediate high and 2100-high scenarios, the flood-ebb ratio reversed from flood dominant to ebb dominant. SLR can change flood dominant currents to ebb dominant currents depending on the geometry of the basin and the tidal conditions (Friedrichs et al., 1990; van Maanen et al., 2013). In flood dominant systems, this is because the ratio of the tidal amplitude to the water depth typically decreases with SLR (Friedrichs et al., 1990). Weeks Bay and Apalachicola had small increases in tidal amplitudes under SLR relative to the increase in water depth. In addition, the amount of

intertidal area in both estuaries increased. In Grand Bay, the flood-ebb ratio increased (currents became less ebb dominant) under the lower SLR scenarios due to larger increases in the flood current velocities than the ebb current velocities. However, in the 2100-intermediate high and 2100-high scenarios, ebb current velocities increased more than flood current velocities, which resulted in currents becoming more ebb dominant. This is a result of Dauphin Island and Petit Bois Island being extensively overtopped, which increased the tidal prism and altered current strengths within the Mississippi Sound.

The magnitudes of the 2005 residual current velocities were approximately two orders smaller than tidal current velocities in the NGOM. Similar to the increases in maximum tidal velocities, Grand Bay experienced the largest relative increase in residual current velocities from the 2005 scenario to the 2100-high scenario, whereas Weeks Bay had the smallest relative increase. At the locations specified in Figure 6.8, residual current velocities increased by 531% (0.7 mm/s) in Grand Bay, 75% (0.1 mm/s) in Weeks Bay and 300% (1.0 mm/s) in Apalachicola. There were no significant changes in residual current directions, although currents tended to be directed more northward.

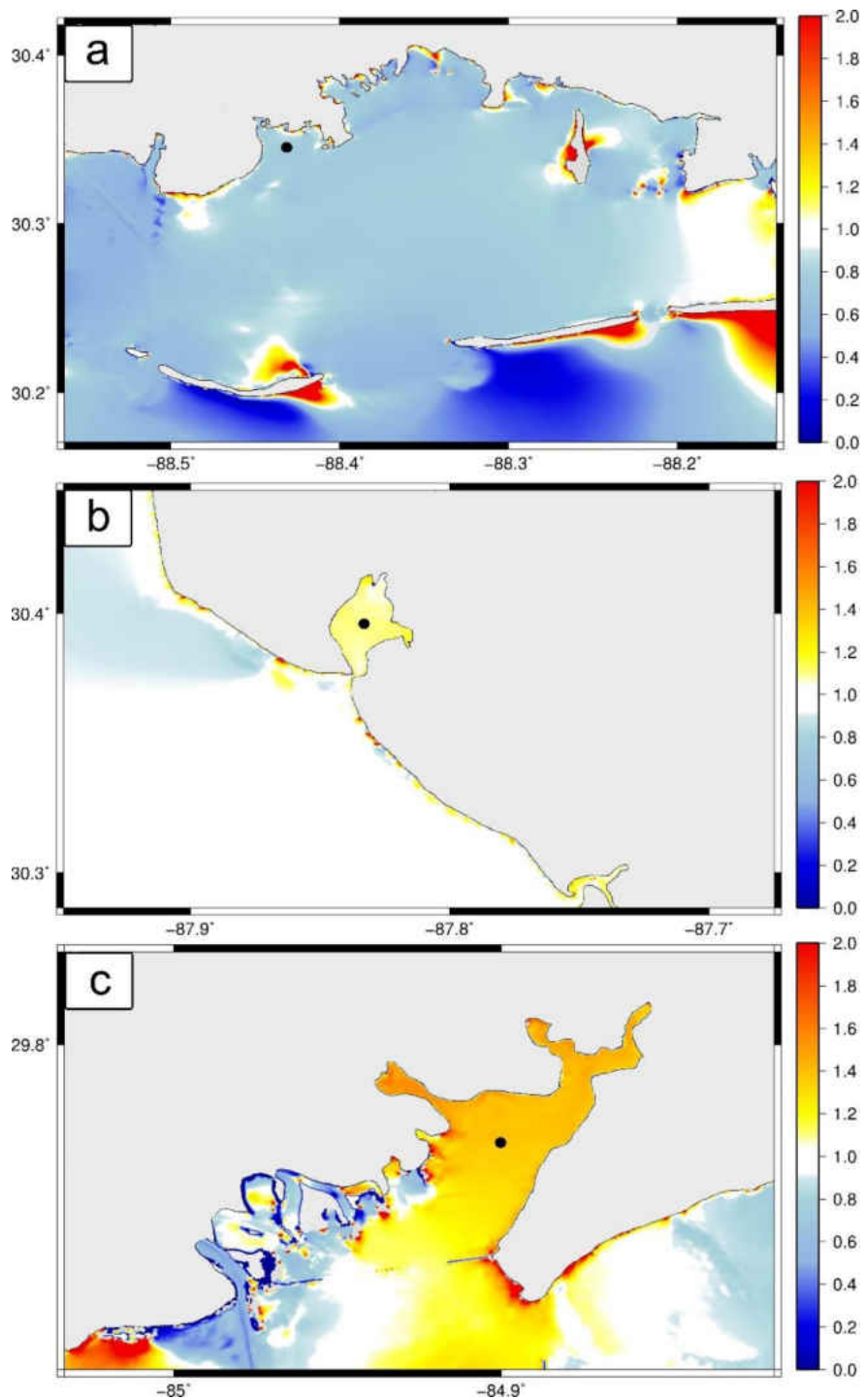


Figure 6.8: Flood-ebb ratios for the 2005 scenario in (a) Grand Bay, (b) Weeks Bay and (c) Apalachicola; at the locations marked with the black dot, flood-ebb ratios are (a) 0.75, (b) 1.10 and (c) 1.35.

Table 6.3: Change in flood-ebb ratio from 2005 to future scenarios in the three NERRs. The top number is the flood-ebb ratio for the given scenario, the number in parentheses is the percent change in the flood-ebb ratio from the 2005 scenario to the given future scenario.

<i>Location</i>	<i>2050 low</i>	<i>2050 int. low</i>	<i>2050 int. high</i>	<i>2050 high</i>	<i>2100 low</i>	<i>2100 int. low</i>	<i>2100 int. high</i>	<i>2100 high</i>
Grand Bay	0.82 (9.5%)	0.88 (17.1%)	0.90 (19.4%)	0.91 (20.9%)	0.89 (19.1%)	0.93 (24.6%)	0.63 (-16.4%)	0.63 (-15.4%)
Weeks Bay	1.03 (-6.2%)	1.02 (-7.3%)	0.93 (-15.8%)	0.87 (-20.9%)	1.03 (-6.8%)	0.90 (-18.5%)	0.89 (-19.5%)	0.81 (-26.0%)
Apalachicola	1.23 (-8.7%)	1.18 (-12.6%)	0.96 (-29.1%)	0.86 (-36.1%)	1.17 (-13.4%)	0.89 (-34.4%)	0.93 (-31.4%)	0.82 (-39.6%)

6.4.4 *Inundation*

Tidal inundation across the barrier islands and within the floodplain increased under all of the future scenarios. Floodplain inundation increased by 78.7 km², 881.7 km², 157.7 km², and 1472.2 km² in the 2050-low, 2050-high, 2100-low and 2100-high scenarios, respectively. Apalachicola had the largest increase in inundation in the low-lying areas surrounding the Apalachicola River and East Bay; this is the largest estuary and contains more low-lying land than Weeks Bay and Grand Bay. Additionally, portions of eastern St. Joseph's Island were overtopped in the 2100-high scenario as a result of the island's projected low dune elevations. Inundation within Grand Bay also increased within the marsh. Offshore, Petit Bois Island and Dauphin Island were significantly overtopped in the 2100-high scenario as a result of the low dune elevations in the future scenario. Weeks Bay had the least amount of increased inundation due to the estuary having less low-lying marsh area and being more developed than Apalachicola and Grand Bay.

6.5 Implications

This research improves the overall understanding of the dynamic effects of SLR on tidal hydrodynamics in microtidal environments. It is likely that other microtidal regions with low wave energy will experience similar changes in tidal hydrodynamics under SLR. Additionally, this research supports a paradigm shift in the way coastal scientists and engineers model the effects of SLR (Bilskie et al., 2014). Accounting for the co-evolution of morphology in conjunction with SLR allows for more comprehensive evaluations of hydrodynamics.

Findings can be used to inform various coastal assessments of SLR. The decision-making flow chart (Figure 6.3) can provide direction for future hydrodynamic assessments of SLR implementing projections of morphology. Outputs in the form of future scenarios (sea levels and projections of morphology) enable storm surge assessments of SLR across the NGOM to aid in infrastructure planning. In addition, findings can provide insight for ecological assessments. Changes in tidal amplitudes are an important consideration for salt marshes; the governing parameters for biomass productivity are the elevation of the marsh table and the tidal range, which also dictates the marsh hydroperiod (Morris et al., 2002). The marsh hydroperiod is expected to increase with SLR, which can allow for either more deposition on the marsh platform (therefore increasing productivity) or more erosion and drowning of vegetation. Microtidal marsh systems are especially sensitive to SLR because they cannot quickly adjust their mean platform elevation with respect to the tidal elevation; a relatively small increase in sea level can cause a microtidal marsh to become submerged (Friedrichs and Perry, 2001).

From a biological and ecological standpoint, increased flow rates can negatively affect oyster recruitment; flow rates affect larvae delivery and position maintenance during and after settlement (Boudreaux et al., 2009). This is especially important for the economy of Apalachicola Bay. Tidal asymmetries affect sediment transport in marsh tidal creeks, which can also dictate marsh sediment supply. Flood dominant tides in salt marsh creeks tend to move sediment landward, whereas ebb dominant tides tend to move sediment seaward. Flood dominant currents increase suspended sediment concentration at the creek/marsh boundary, which supplies more marine sediment to the marsh and allows for accretion on the marsh platform. Conversely, ebb dominant currents reduce the sediment supply to the marsh (Friedrichs and Perry, 2001). The marshes in Grand Bay have significantly eroded historically; if the system becomes more ebb dominant under extreme SLR, marsh erosion may be exacerbated. Seagrass growth is also influenced by flood and ebb current direction (Boer, 2000), as tidal currents transport nutrients to seagrass beds (Koch et al., 2007). Changes in flood and ebb currents may alter the amount of sediment and nutrients in the water column, thereby affecting seagrass productivity. Projections of future shoreline positions can be used in biological studies assessing future impacts to nesting species such as sea turtles, beach mice and shore birds.

Projected inundation areas, tidal amplitudes and changes in tidal propagation can advise future navigational studies; traffic patterns may be altered due to changes in shallow areas and the timing of high and low tide. In addition, if the changes in tidal hydrodynamics increase sediment deposition in the bays, the navigational channels will require more frequent maintenance dredging.

Changes in tidal hydrodynamics are an important consideration for how natural and built communities along the NGOM may be altered in the future. It is important to recognize that SLR is the primary driver of the changes in the tidal hydrodynamics, rather than morphology. This complicates adaptation strategies if the rate of SLR cannot be mitigated. Results from this research can be used in management decision making and adaptation planning. Quantifying future shoreline positions and dune heights can aid in identifying erosion risks to establish monitoring, stabilization and nourishment projects. Projections of changes in tidal amplitudes under SLR within each of the bays can assist in designing mitigation strategies, such as inlet stabilization. Areas prone to increased tidal inundation may be prohibited from future development or modification and designated as protected habitats. Overall, this leads to improved coastal management decision making.

6.6 Conclusions

This research evaluated the integrated dynamic effects of future SLR and morphology on tidal hydrodynamics along the NGOM, with particular focus on the Grand Bay, Weeks Bay and Apalachicola NERRs. A large-domain hydrodynamic model modified with future SLR scenarios and projections of future morphology provided by a BN was used to simulate tidal hydrodynamics under present and future scenarios. Tidal amplitudes significantly increased under the 2100-high scenario in some of the bays by as much as 67% (10.0 cm). There was a high correlation between the change in the inlet cross-sectional area and the change in the tidal amplitude in the bay. Changes in harmonic constituent phases indicated faster tidal propagation in the future scenarios in most of the bays. Tidal velocities increased in all of the NERRs under the 2100-high scenario,

especially in Grand Bay where current velocities doubled. The flood-ebb velocity ratio decreased (i.e., currents became less flood dominant) by as much as 26% and 39% in all of the future scenarios within Weeks Bay and Apalachicola, respectively. Under the higher SLR scenarios, currents within both estuaries reversed from being flood dominant to ebb dominant. In Grand Bay, the flood-ebb ratio increased (i.e., currents became less ebb dominant) by as much as 25% under the lower SLR scenarios, but decreased (i.e., currents became more ebb dominant) by as much as 16% under the higher SLR as a result of the offshore barrier islands being overtopped which increased the tidal prism in the Mississippi Sound. The tidal inundation extent increased along the NGOM study area, especially along low-lying marsh areas and barrier islands with low dune elevations. Overall, this research improves the understanding of the effects of SLR on tidal hydrodynamics in microtidal environments and reinforces taking a dynamic approach and considering estimates of future morphology when modeling the effects of SLR. Results can be used in a variety of coastal studies including storm surge and ecological assessments of SLR. Ultimately, the outcomes of this research will allow coastal managers and policy makers to make more informed decisions that address specific needs and vulnerabilities of each particular estuary, the NGOM coastal system, and estuaries elsewhere with similar conditions.

6.7 Acknowledgments

The authors wish to thank Christine Szpilka for providing post-processing resources for the simulations. This research was funded in part under Award No. NA10NOS4780146 from the National Oceanic and Atmospheric Administration (NOAA) Center for Sponsored Coastal Ocean Research (CSCOR) and the Louisiana Sea Grant Laborde Chair endowment. This work used the

Extreme Science and Engineering Discover Environment (XSEDE), which is supported by the National Science Foundation grant number ACI-1053575. The statements and conclusions are those of the authors and do not necessary reflect the views of NOAA-CSCOR, Louisiana Sea Grant, XSEDE, or their affiliates.

6.8 References

- Bilskie, M. V., Coggin, D., Hagen, S. C. and Medeiros, S. C. (2015). "Enhancement and application of overland unstructured finite element meshes for shallow water flow models." *Advances in Water Resources* (in revision).
- Bilskie, M. V., Hagen, S. C., Medeiros, S. C. and Passeri, D. L. (2014). "Dynamics of sea level rise and coastal flooding on a changing landscape." *Geophysical Research Letters* 41(3): 927-234.
- Boer, W. F. (2000). "Biomass dynamics of seagrasses and the role of mangrove vegetation as different nutrient sources for an intertidal ecosystem." *Aquatic Botany* 66(3): 225-239.
- Boudreaux, M. L., Walters, L. J. and Rittschoff, D. (2009). "Interactions between native barnacles, non-native barnacles and the easter oyster *crassostrea virginica*." *Bulletin of Marine Science* 84(1): 43-57.
- Byrnes, M. R., Rosati, J. D., Griffee, S. F. and Berlinghoff, J. L. (2012). "Sediment Budget: Mississippi Sound Barrier Islands". Vicksburg, Mississippi, U.S. Army Corps of Engineers: 171p.
- Coggin, D. (2011). "A digital elevation model for Franklin, Wakulla, and Jefferson Counties." *Florida Watershed Journal* 4(2): 5-10.
- Cowell, P. J., Stive, M. J. F., Niedoroda, A. W., De Vriend, H. J., Swift, D. J. P., Kaminsky, G. M. and Capobianco, M. (2003a). "The coastal tract: Part 1: A conceptual approach to aggregated modelling of low-order coastal change." *Journal of Coastal Research* 19: 812-827.
- Cowell, P. J., Stive, M. J. F., Niedoroda, A. W., Swift, D. J. P., De Vriend, H. J., Buisjman, M. C., Nicholls, R. J., Roy, P. S. and Co-authors (2003b). "The coastal tract. Part 2: Applications of aggregated modelling of lower-order coastal change." *Journal of Coastal Research* 19: 828-848.

- Dean, R. G. and Grant, J. (1989). "Development of Methodology for Thirty-Year Shoreline Projections in the Vicinity of Beach Nourishment Projects". Tallahassee, FL, Division of Beaches and Shores, Florida Department of Natural Resources.
- Donoghue, J. F. (2011). "Sea level history of the northern Gulf of Mexico coast and sea level rise scenarios for the near future." *Climatic Change* 107(1-2): 17-33.
- Egbert, G. D., Bennett, A. F. and Foreman, M. G. G. (1994). "TOPEX/POSEIDON tides estimated using a global inverse model." *Journal of Geophysical Research: Oceans* 99: 24821-24852.
- Egbert, G. D. and Erofeeva, S. Y. (2002). "Efficient inverse modeling of barotropic ocean tides." *Journal of Atmospheric and Oceanic Technology* 19: 183-204.
- Eleuterius, C. K. and Criss, G. A. (1991). "Point aux Chenes: Past, Present, and Future Perspective of Erosion". Ocean Springs, Mississippi, Physical Oceanography Section Gulf Coast Research Laboratory
- FDEP (2013). "Apalachicola National Estuarine Research Reserve Management Plan, June 2013". Tallahassee, FL, Florida Department of Environmental Protection.
- Fitzgerald, D. M., Fenster, M. S., Argow, B. A. and Buynevich, I. V. (2008). "Coastal Impacts Due to Sea Level Rise." *Annual Review Earth Planet Science* 36: 601-647.
- French, J. R. (2008). "Hydrodynamic Modelling of Estuarine Flood Defence Realignment as an Adaptive Management Response to Sea-Level Rise." *Journal of Coastal Research* 24(2B): 1-12.
- Friedrichs, C. T., Aubrey, D. J. and Speer, P. E. (1990). Impacts of relative sea level rise on evolution of shallow estuaries. Residual current and long-term transport. R. T. Cheng. New York, Springer-Verlag.
- Friedrichs, C. T. and Perry, J. E. (2001). "Tidal Salt Marsh Morphodynamics: A Synthesis." *Journal of Coastal Research* SI 27.
- Gutierrez, B. T., Plant, N. G., Pendleton, E. A. and Thieler, E. R. (2014). "Using a Bayesian Network to predict shoreline change vulnerability to sea level rise for the coasts of the United States", U.S. Geological Survey Open-File Report 2014-1083: 26.
- Gutierrez, B. T., Plant, N. G. and Thieler, E. R. (2011). "A Bayesian network to predict coastal vulnerability to sea level rise." *Journal of Geophysical Research* 116(FO2009).

- Hall, G. F., Hill, D. F., Horton, B. P., Engelhart, S. E. and Peltier, W. R. (2013). "A high-resolution study of tides in the Delaware Bay: Past conditions and future scenarios." *Geophysical Research Letters* 40: 338-342.
- Hapke, C. and Plant, N. (2010). "Predicting coastal cliff erosion using a Bayesian probabilistic model." *Marine Geology* 278: 140-149.
- Isphording, W. C. (1985). "Sedimentological Investigation of the Apalachicola Bay, Florida Estuarine System: prepared for the Mobile District, Corps of Engineers", University of Alabama.
- Jarrett, J. T. (1976). "General Investigation of Tidal Inlets Report 3", U.S. Army Engineer Waterways Experiment Station, Vicksburg, Mississippi.
- Koch, E. W., Ackerman, J. D., Verduin, J. and van Keulen, M. (2007). Fluid dynamics in seagrass ecology - from molecules to ecosystems. Seagrasses: biology, ecology and conservation. A. W. D. Larkum, R. J. Orth and C. M. Duarte. Netherlands, Springer: 193-225.
- Leorri, E., Mulligan, R., Mallinson, D. and Cearretta, A. (2011). "Sea-level rise and local tidal range changes in coastal embayments: An added complexity in developing reliable sea-level index points." *Journal of Integrated Coastal Zone Management* 11(3): 307-314.
- Luetlich, R. A., Westerink, J. J. and Scheffner, N. W. (1992). "ADCIRC: An Advanced Three-Dimensional Circulation Model For Shelves, Coasts, and Estuaries, I: Theory and Methodology of ADCIRC-2DDI and ADCIRC-3DL", U.S. Army Corps of Engineers.
- McBride, R. A., Byrnes, M. R. and Hiland, M. W. (1995). "Geomorphic response-type model for barrier coastlines: a regional perspective." *Marine Geology* 126: 143-159.
- Medeiros, S. C., Hagen, S. C., Weishampel, J. F. and Angelo, J. J. (2015). "Adjusting lidar-derived digital terrain models in coastal marshes based on estimated above ground biomass density." *Remote Sensing SI (Towards Remote Long-Term Monitoring of Wetland Landscapes)*: (accepted).
- Miller-Way, T. L., Dardeau, M. and Crozier, G. (1996). "Weeks Bay National Estuarine Research Reserve: An Estuarine Profile and Bibliography", Dauphin Island Sea Lab.
- Mississippi Department of Marine Resources (1999). "Mississippi's Coastal Wetlands". Biloxi, MS, Coastal Preserves Program.
- Morris, J. T., Sundareshwar, P. V., Nietch, C. T., Kjerfve, B. and Cahoon, D. R. (2002). "Responses of Coastal Wetlands to Rising Sea Level." *Ecology* 83(10): 2869-2877.

- Morton, R. A. (2008). "Historical Changes in the Mississippi-Alabama Barrier-Island Chain and the Roles of Extreme Storms, Sea Level, and Human Activities." *Journal of Coastal Research* 24(6): 1587-1600.
- Morton, R. A., Miller, T. L. and Moore, L. J. (2004). "National assessment of shoreline change: Part 1: Historical shoreline changes and associated coastal land loss along the U.S. Gulf of Mexico". Open-file Report 2004-1043. St. Petersburg, Florida, U.S. Geological Survey: 45p.
- O'Sullivan, W. T. and Criss, G. A. (1998). "Continuing Erosion in Southeastern Coastal Mississippi-Point aux Chenes Bay, West Grand Bay, Middle Bay, Grande Batture Islands: 1995-1997". Sixty-Second Annual Meeting of the Mississippi Academy of Sciences. Biloxi Mississippi.
- Parris, A., Bromirski, P., Burkett, V., Cayan, D., Culver, M., Hall, J., Horton, R., Knuuti, K., Moss, R., Obeysekera, J., Sallenger, A. and Weiss, J. (2012). "Global Sea Level Rise Scenarios for the United States National Climate Assessment". NOAA Tech Memo OAR CPO-1: 37.
- Passeri, D. L., Hagen, S. C., Bilskie, M. V. and Medeiros, S. C. (2015). "On the significance of incorporating shoreline changes for evaluating coastal hydrodynamics under sea level rise scenarios." *Natural Hazards* 75(2): 1599-1617.
- Passeri, D. L., Hagen, S. C., Medeiros, S. C. and Bilskie, M. V. (2015). "Impacts of historic morphological changes and sea level rise on tidal hydrodynamics in a microtidal estuary (Grand Bay, MS)." *Continental Shelf Research* (submitted).
- Rosati, J. D. and Stone, G. W. (2009). "Geomorphologic Evolution of Barrier Islands along the Northern U.S. Gulf of Mexico and Implications for Engineering Design in Barrier Restoration." *Journal of Coastal Research* 25(1): 8-22.
- Salisbury, M. B., Hagen, S. C., Coggin, D., Bacopoulos, P., Atkinson, J. H. and Roberts, H. J. (2011). "Unstructured mesh development for the Big Bend Region (Florida)." *Florida Watershed Journal* 4(2): 11-14.
- Sampath, D. M. R., Boski, T., Silva, P. and Martins, F. A. (2011). "Morphological evolution of the Guadiana estuary and intertidal zone in response to projected sea level rise and sediment supply scenarios." *Journal of Quaternary Science* 26(2): 156-170.
- Seim, H. E., Kjerfve, B. and Sneed, J. E. (1987). "Tides of Mississippi Sound and the Adjacent Continental Shelf." *Estuarine, Coastal and Shelf Science* 25: 143-156.
- University of Central Florida (2011). "Flood Insurance Study: Florida Panhandle and Alabama, Model Validation". Technical Study Documentation Notebook, FEMA.

- Valentim, J. M., Vaz, L., Vaz, N., Silva, H., Duarte, B., Cacador, I. and Dias, J. (2013). "Sea level rise impact in residual circulation in Tagus estuary and Ria de Aveiro lagoon." *Journal of Coastal Research* Special Issue No. 65: 1981-1986.
- van Maanen, B., Coco, G., Bryan, K. R. and Friedrichs, C. T. (2013). "Modeling the morphodynamic response of tidal embayments to sea-level rise." *Ocean Dynamics* 63(11-12): 1249-1262.
- Yates, M. L. and Le Cozannet, G. (2012). "Evaluating European coastal evolution using Bayesian Networks." *Natural Hazards Earth System Sciences* 12: 1173-1177.

CHAPTER 7. CONCLUSION

The objective of this research was to evaluate the integrated influences of SLR and coastal morphology on tidal hydrodynamics along the NGOM, with particular focus on three NERRs. The research began with a thorough literature review of the integrated, dynamic effects of SLR on hydrodynamics, coastal morphology and marsh ecology. Many studies neglect to consider the nonlinear effects of SLR, despite knowledge of the dynamic nature of coastal systems. More recent efforts have considered the dynamic effects of SLR (e.g., the nonlinear response of hydrodynamics under SLR); however, little research has considered the integrated feedback mechanisms and co-evolution of multiple interdependent systems (e.g., the nonlinear responses and interactions of hydrodynamics and coastal morphology under SLR). It was recommended that future assessments of SLR implement a synergistic approach that integrates the dynamic interactions between physical and ecological environments.

Projecting future morphology for SLR assessments is a difficult task; various models and methodologies have been implemented to provide insight as to how shoreline positions may change in the future. Shoreline change rates established by two USGS databases were compared with erosion rates estimated using a conceptual model along the South Atlantic Bight and NGOM coasts. The intent was not to regard one method as superior to another, but rather to explore similarities and differences between the methods. Based on the comparison, the following recommendations were offered for quantifying future shoreline positions under SLR. In areas where long term erosion rates correspond well with rates predicted by the Bruun Rule, shoreline retreat can be completely attributed to forces related to SLR and the Bruun Rule can be applied to

estimate future shoreline positions under sea level rise scenarios. If long term erosion rates are higher than the rates predicted by the Bruun Rule, a hybrid approach can be taken to include a factor for background erosion. Lastly, care should be taken when extrapolating change rates determined by the CVI or National Assessment of Shoreline Change to project future shoreline positions. CVI rates may be projected when considering extreme shoreline change, as they are typically larger than long term historic rates.

A sensitivity analysis examining the incorporation of future shoreline changes into hydrodynamic modeling assessments of SLR was conducted along the NGOM coast. A large-domain hydrodynamic model was used to simulate astronomic tides and hurricane storm surge under present conditions, the 2050 sea level, and the 2050 sea level with projections of shoreline changes. Incorporating the projected shoreline position had variable effects on the hydrodynamics. Tidal ranges were not altered, although some bays experienced changes in tidal prisms depending on whether the planform area of the bay increased or decreased. Barrier islands with projected erosion were vulnerable to increased overtopping from storm surge (as much as a 75% increase when projected shoreline changes were included), which impelled more water into the back-bays and increased the inland inundation extent. Inundation along barrier islands with projected accretion remained relatively the same as inundation under present day shorelines. It was recommended that future hydrodynamic studies should not only consider modeling SLR as a dynamic processes, but also at a minimum, should include an assessment of related dynamic shoreline changes.

Evaluating how hydrodynamics have been altered historically under a changing landscape in conjunction with SLR can provide insight into to how water levels and currents may change in the

future. Of the three NERRs, Grand Bay has undergone the most significant landscape changes. Using historic shoreline positions, bathymetric data and sea level trends dating back to 1848, historic tidal hydrodynamics were simulated and compared with present day hydrodynamics. Changes in tidal amplitudes from the historic conditions varied; there were no changes in the Mississippi Sound although within Mobile Bay tidal amplitudes increased by as much as 20%. Tidal phases in the Sound were slower by as much as 40 minutes in 1848. The position of the offshore barrier island inlets influenced tidal currents; as the islands migrated westward, stronger tidal velocities were centered on the Grand Batture Island. Within Grand Bay, maximum tidal velocities were 5 cm/s higher in 1848 than in 2005. Additionally, currents were flood dominant in 1848 and reversed to being ebb dominant sometime after. If the Grand Batture Island was reconstructed under 2005 conditions, tidal amplitudes and phases would not be altered, although maximum tidal velocities would increase by 5 cm/s and the flood-ebb ratio would decrease by 20% in Grand Bay, resulting in currents becoming more ebb dominant. This could negatively impact oyster and seagrass productivity within the estuary. The results illustrate the hydrodynamic response of the system to SLR and the changing landscape. This provides insight into tidal parameters that may be altered under future SLR and evolution of the barrier islands.

Lastly, the integrated dynamic effects of future SLR and morphology on tidal hydrodynamics were evaluated along the NGOM system, with particular focus on the Grand Bay, Weeks Bay and Apalachicola NERRs. A large-domain hydrodynamic model modified with future SLR scenarios and projections of future morphology provided by a Bayesian Network. The model was used to simulate tidal hydrodynamics under present (circa 2005) and future (circa 2050 and 2100) conditions. Tidal amplitudes increased by as much as 68% in the embayments; there was a high

correlation between the change in the bay's inlet cross-sectional area and the change in the bay's tidal amplitude under SLR. In most of the bays, tidal phases were faster in the future scenarios than in the present scenario. Tidal velocities increased in all of the NERRs under the 2100-high scenario, especially in Grand Bay where current velocities doubled. The flood-ebb velocity ratio decreased in all of the future scenarios within Weeks Bay and Apalachicola by as much as 26% and 39%, respectively. Under the higher SLR scenarios, currents within the bays reversed from flood-dominant to ebb-dominant. In Grand Bay, the flood-ebb ratio increased by as much as 25% under the lower SLR scenarios, but decreased by as much as 16% under the higher SLR as a result of the offshore barrier islands being overtopped which increased the tidal prism and altered tidal current strengths.

7.1 Implications

This dissertation improves the understanding of the response of tidal hydrodynamics to morphology and SLR. A major outcome of this research is a paradigm shift in the way coastal scientists and engineers model the effects of SLR; this dissertation acts as an agent of change for this paradigm shift, promoting a transition from the simplistic bathtub approach towards consideration of the integrated coastal dynamics of SLR. This is beneficial not only to the scientific community, but also to the management and policy community. Synergistic studies that integrate the dynamic interactions between physical and ecological environments will aid in adaptation planning, permitting coastal managers to make more informed decisions regarding the impacts of SLR.

These findings will have synergistic effects with a variety of coastal studies. The decision-making flow chart on how to implement projected morphology into hydrodynamic assessments of SLR will provide direction for future studies in other regions. Outputs in the form of boundary conditions (i.e., harmonic constituents) and future scenarios (i.e., coastal morphology and SLR) enable storm surge and biological assessments of SLR to be fulfilled by other Civil Engineering and Biology PhD students. Storm surge assessments of SLR will aid in infrastructure planning and design, managing flood control, and land acquisition to mitigate storm damage. Projections of future tidal parameters (e.g., tidal amplitudes and velocities) can be used as inputs to biological models examining marsh, oyster and SAV productivity. Changes in tidal amplitudes are an important consideration for salt marsh productivity, increased tidal velocities may negatively affect oyster recruitment, and changes in flood and ebb dominance can alter the sediment supply to marshes and seagrass beds. Projections of future shoreline positions can be used in biological studies assessing future impacts to nesting species such as sea turtles, beach mice and shore birds. Overall, this will benefit established monitoring and restoration activities in the NERRs.

Quantifying changes in tidal hydrodynamics and coastal morphology under SLR will also aid in developing management strategies to reduce future risk within built and natural environments. Projections of shoreline positions and dune heights can aid in identifying vulnerable areas for monitoring, stabilization and nourishment projects to reduce erosion. This is imperative for socioeconomic assessments estimating future damages and adaptation costs when designing mitigation or adaptation strategies. Additionally, examining the influence of the Grand Batture Island on tidal hydrodynamics within Grand Bay can inform nourishment studies exploring barrier island reconstruction. Changes in tidal parameters such as water levels, phases and currents can

also be used in navigational studies. Areas vulnerable to increased tidal inundation may be prohibited from future development or modification and designated as protected lands. Ultimately, the outcomes of this research will allow coastal managers and policy makers to make more informed decisions that address specific needs and vulnerabilities of each particular estuary, the NGOM coastal system, and estuaries elsewhere with similar conditions.